COMPOUND STRIP METHOD FOR THE ANALYSIS OF CONTINUOUS ELASTIC PLATES

Jay A. Puckett

Richard M. Gutkowski

Structural Research Report No. 48
Civil Engineering Department
Colorado State University
Fort Collins, Colorado 80523

October 1983

COMPOUND STRIP METHOD FOR THE ANALYSIS OF CONTINUOUS ELASTIC PLATES

Jay A. Puckett

Richard M. Gutkowski

Structural Research Report No. 48
Civil Engineering Department
Colorado State University
Fort Collins, Colorado 80523

October 1983

ABSTRACT

COMPOUND STRIP METHOD FOR THE
ANALYSIS OF CONTINUOUS ELASTIC PLATES

A finite strip method (FSM) is developed for the analysis of linear elastic flat plate systems which are continuous over deflecting supports. The approach presented incorporates the effect of the support elements in a direct stiffness methodology. The stiffness contribution of the support elements have been derived and are given in the form of strip matrices which are directly added to the plate strip stiffness matrix at the element level. This summation of plate and support stiffness contributions constitutes a substructure which is termed a compound strip.

The validity of the compound strip method is demonstrated in several illustrative problems which include single and multipanel plates continuous over flexible and rigid beams and columns. The FSM and finite element method (FEM) compare favorably for displacement and moment.

The rate of convergence of the compound strip method was studied and results are given for a continuous multipanel system. The FSM is shown to be computationally more efficient than the FEM when maximum values for moment or deflection are required. The FEM exhibits favorable convergence characteristics in locations where the magnitudes of displacement and moment are relatively small.

ACKNOWLEDGEMENTS

The writer expresses his deepest appreciation to Professor R. M. Gutkowski for his constant encouragement, guidance and insightful advice concerning this research. Professor Gutkowski, through his sincere dedication, has provided this investigator with a creative and rewarding experience which forms the foundation of a hopefully productive engineering career. The author also thanks Professor Gutkowski for his helpful advice and comments concerning engineering education which has greatly aided this young instructor.

The author also acknowledges the University Computer Center for its financial support of his computer time.

TABLE OF CONTENTS

TABLE OF CONTENTS (continued)

LIST OF TABLES

LIST OF FIGURES

LIST OF FIGURES (continued)

LIST OF FIGURES (continued)

Figure | Page

CHAPTER I

1. INTRODUCTION

1.1. Theory of Plates

A thin plate is an initially flat structural element for which the thickness is much smaller than the plan dimensions. Many practical engineering problems are in the category of "thin plates in flexure due to transverse load." Familiar examples of plates are the walls and bottom of tanks, bulkheads, side panels and roofs of buildings, and floor slabs. The transverse loads act perpendicular to the plane of the plate surfaces. Rectangular plates composed of an isotropic linear elastic material are governed by the differential equation

$$\frac{\partial^4 w(x,y)}{\partial x^4} + 2\,\frac{\partial^4 w(x,y)}{\partial x^2 \partial y^2} + \frac{\partial^4 w(x,y)}{\partial y^4} = \frac{q(x,y)}{D} \qquad [1]$$

in which x and y are coordinates and $w(x,y)$ is the deflection of the midplane of the plate, $q(x,y)$ is the transverse loading and D is the flexural rigidity. For orthotropic plates the governing differential equation is

$$D_x\,\frac{\partial^4 w(x,y)}{\partial x^4} + 2(D_1 + D_{xy})\,\frac{\partial^4 w(x,y)}{\partial x^2 \partial y^2} + D_y\,\frac{\partial^4 w(x,y)}{\partial y^4} = q(x,y) \qquad [2]$$

in which D_x and D_y are the flexural rigidities in the x and y directions, respectively, D_1 is the rigidity due to Poisson's effect and D_{xy} is the twisting rigidity. The various plate rigidities are related to the material properties and the plate thickness. Equations 1 and 2 are based upon the fundamental Kirchoff hypotheses (1,2,3)

Direct mathematical solution of Eqs. 1 and 2, incorporating boundary conditions, is possible and several methods are available (principally developed by Navier, Kirchoff and Levy) and described in familiar textbooks (1,2,3). Numerical solution techniques (developed by Galerkin, Ritz, Wahl, and others) are also described in the same references. However, for irregular loading and complex geometrical shapes such techniques are usually intractable.

1.2. The Finite Strip Method--An Alternative to the Finite Element Method

A contemporary approach to solving such problems by computer analysis is the finite element method (FEM) (4). The FEM is a powerful method for analysis of complex plate problems which may have highly irregular plan geometry. However, the necessity of employing a relatively fine mesh to obtain an accurate model can lead to a large number of simultaneous structural equations. Design engineers may find the FEM to be prohibitive for continuous plate systems of reasonable size. The costs involved can be high, particularly for dynamic analysis. Further, the core storage and execution time requirements for an accurate FEM analysis of a large plate system can exceed the capacity of the available hardware (particular desktop models). This may be true even when efficient equation solving techniques are employed. Additionally, analyst time required for model development , mesh generation and interpretation of results can be considerable and often more costly than computing time. In particular, practicing engineers who are inexperienced in the application of the FEM can have difficulty selecting appropriate finite elements and determining an efficient, accurate mesh layout.

Several numerical techniques are available to reduce core storage and computational time, e.g., use of higher order finite element models to improve convergence and/or reduce the mesh size, or use of macroelements which, by themselves, can represent full size structural components. Alternatively, for plate continua with regular geometry and boundary conditions, the power and versatility of the conventional FEM is not required. For such continua Cheung (5,6) has developed a specialized plate element which offers a powerful alternative to conventional finite elements. Because the plan geometry of plate is discretized in one principal direction only, Cheung's methodology is termed the "finite strip method" (FSM). By avoiding a two-way geometric discretization, the FSM considerably shortens and simplifies the analyst input and output effort, reduces computer memory capacity and time requirements, and offers greater computational efficiency than the FEM for those types of problems geometrically suited to both methods. In effect, the FSM reduces a two dimensional analysis to a series of one dimensional analyses, which results in fewer equations with a small half band width. In references 5 and 6, Cheung reports excellent comparison with classical solutions and significant reduction in computational effort vis-a-vis several FEM models.

Many common flat and folded plate systems have characteristics that are amenable to the FSM. Thus considerable research was conducted from 1968 to the present (a review of the pertinent literature is presented in a subsequent chapter) to advance Cheung's original work. The FSM has been successfully applied to a variety of plate systems including flat plates, folded plates, and box girders. Despite this work an impasse has apparently been reached in attempting to apply the FSM method to one important category of plate problems, namely any system which is continuous over flexible beams and columns. Indeed, prior to this work the simple problem of a single plate supported by a column at each of its corners is intractable by any FSM techniques presently available. Some progress was made by researchers using a flexibility formulation, but the efficiency of the FSM relative to the FEM has been compromised in those approaches.

1.3. Objective

The objective of the study reported herein was to extend the capability of the finite strip method to permit a direct stiffness analysis of rectangular two-way, beam and column-supported plate systems. Previous researchers have addressed some aspects of the incorporation of beam and column supports in a finite strip formulation. Most of the past work has been based upon use of a flexibility approach. Employing a flexibility method of analysis is computationally cumbersome, inefficient, and generally requires considerable judgment. Further, the treatment of supporting beams is presently limited to the case of unidirectional support. In this study the significant limitations of the <u>flexibility</u> approach have been overcome by the development of a finite strip formulation in which supporting beams and columns can be readily incorporated in a <u>stiffness</u> methodology. The incorporation of these supports in the FSM required the development of new strip elements termed "compound finite strips."

CHAPTER II

2. FINITE STRIP METHOD - BASIC CONCEPTS

2.1. Definition of a Finite Strip

Cheung has applied the finite strip modeling to a variety of continuum problems, e.g., the flat plate structure shown in Figure 2.1.

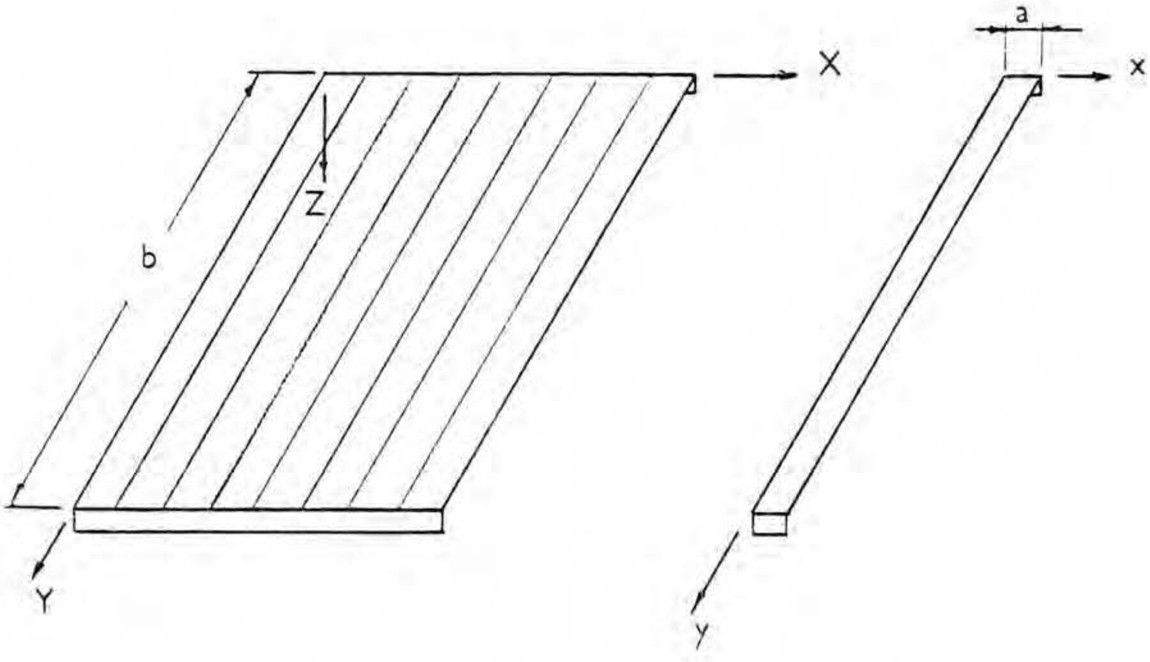

Figure 2.1. Finite Strip Modeling of a Continuous Plate.

Basically, the continuum is divided into a number of "finite strips" each having a finite width (dimension "a") and length equal to the full distance between the discontinuous edges (dimension "b").

The flat plate in Figure 2.1 has been divided into five finite strips. The two opposite ends of dimension "b" coincide with the boundaries of the structure.

2.2. Mathematical Formulation

The principle of stationary potential energy is a fundamental approach used to develop stiffness models. Briefly, the principle can be stated "Of all compatible displacements satisfying given boundary conditions, those which satisfy equilibrium make the total potential energy a stationary value." Mathematically stated

$$\left(\frac{\partial \phi}{\partial \delta_{kn}}\right) = 0 \qquad [3]$$

where ϕ is the total potential energy of the system. The δ_{kn} refers to an individual displacement parameter or state variable.

For the finite strip method ϕ is based upon an approximate displacement function, $w_s(x,y)$ used for each strip. Commonly, the assumed displacement function combines a polynomial function in the direction transverse to the strip and a series expression in the direction along the strip. The δ_{kn} values are the four (k=1 to 4) unknown displacement parameters in the nth term of $w_s(x,y)$. The outer subscript n refers to an arbitrary mode as defined below in Eq. 4. (Described in more detail in subsequent text.) Minimizing the total potential energy with respect to each unknown displacement parameter yields a set of simultaneous linear algebraic equations which may be solved for the δ_{kn} values.

For two dimensional structures such as the flat plate shown in Figure 2.1, the finite strip displacement function is

$$w_s(x,y) = \sum_{m=1}^{r} X_m(x)\, Y_m(y) \qquad [4]$$

$X_m(x)$ is an approximate "shape function" involving the unknown displacements at the transverse (continuous) edges (i and j in Figure 2.1), $Y_m(y)$ is a "boundary function" chosen to satisfy the specified boundary conditions at the opposite ends of dimension b, and r is the highest term considered in the series. Each term, m, of the series is referred to as a "mode." The subscript s in subsequent text refers to the individual element or strip.

Commonly the boundary functions, $Y_m(y)$ are functions which are derived from the solution of the governing equation for beam vibration,

$$\frac{d^4 Y(y)}{dx^4} = \frac{\mu^4}{b^4}\, Y(y) \qquad [5]$$

where b is the length of beam (strip) and μ is a parameter. The resulting expressions are commonly referred to as basic functions or eigenfunctions.

The general form of the solution to Eq. 5 is:

$$\begin{aligned} Y(y) &= B_1 \sin\left(\frac{\mu y}{b}\right) + B_2 \cos\left(\frac{\mu y}{b}\right) \\ &+ B_3 \sinh\left(\frac{\mu y}{b}\right) + B_4 \cosh\left(\frac{\mu y}{b}\right) \end{aligned} \qquad [6]$$

where B_1, etc. are determined from the boundary conditions at the discontinuous ends of the strip. For example, $Y_m(y)$ for a plate bending strip with simply supported boundaries on the strip ends is

$$Y_m(y) = \sin\left(\frac{\mu_m y}{b}\right) \quad \mu_m = \pi,\ 2\pi,\ 3\pi, \ldots m\pi \qquad [7]$$

Other boundary conditions yield series forms more complex than Eq. 7 (37,38).

Similar to the FEM, the FSM requires integration of the displacement function and its derivatives over the domain of the strip. Because eigenfunctions are mathematically orthogonal, the integration is readily executed. The significance of this aspect is shown later.

The shape function, $X_m(x)$, contains four unknown modal displacement parameters. A commonly used plate bending element polynomial function adopted for this study is

$$X_m(x) = [C_1, C_2, C_3, C_4] \begin{Bmatrix} \delta_{1m} \\ \delta_{2m} \\ \delta_{3m} \\ \delta_{4m} \end{Bmatrix} = [C]\{\Delta\}_m \qquad [8]$$

where
$$C_1 = 1 - 3\bar{x}^2 + 2\bar{x}^3$$
$$C_2 = x(1 - 2\bar{x} + \bar{x}^2)$$
$$C_3 = 3\bar{x}^2 - 2\bar{x}^3$$
$$C_4 = x(\bar{x}^2 - \bar{x})$$
$$\bar{x} = x/a$$

and $\{\Delta\}_m^T = \{\delta_{1m}, \delta_{2m}, \delta_{3m}, \delta_{4m}\}$ contains the four displacement parameters for mode m. Determination of these parameters for an appropriate number of modes establishes the displaced shape of the finite strip.

2.3. Matrix Formulation

The matrix form of the displacement function [4] is

$$w_s(x,y) = Y_m \left[[C][C]\ldots[C]\right] \begin{Bmatrix} \{\Delta\}_1 \\ \{\Delta\}_2 \\ \cdot \\ \cdot \\ \cdot \\ \{\Delta\}_r \end{Bmatrix} = \sum_{m=1}^{r} [N]_m \{\Delta\}_m \qquad [9]$$

where $[N]_m = Y_m$ [C]; [C] contains the polynomials given in Eq. 8; $\{\Delta\}_m$, are modal displacement parameters or state variables; Y_m is the orthogonal boundary function; and r is the highest mode considered.

The curvatures of the plate for mode m are given by

$$\{X\}_m = \begin{Bmatrix} X_x \\ X_y \\ X_{xy} \end{Bmatrix} = \begin{Bmatrix} -\dfrac{\partial^2 w}{\partial x^2} \\ -\dfrac{\partial^2 w}{\partial y^2} \\ 2\dfrac{\partial^2 w}{\partial x \partial y} \end{Bmatrix} = [B]_m \{\Delta\}_m \qquad [10]$$

The flexural and twisting moments for mode m may be related to the curvatures for mode m by

$$\{M\}_m = [D]\ \{X\}_m \qquad [11]$$

or in expanded form

$$\begin{Bmatrix} M_x \\ M_y \\ M_{xy} \end{Bmatrix} = \begin{bmatrix} D_x & D_1 & 0 \\ D_1 & D_y & 0 \\ 0 & 0 & D_{xy} \end{bmatrix} \begin{Bmatrix} X_x \\ X_y \\ X_{xy} \end{Bmatrix} \qquad [12]$$

where D_x, D_1, D_y, and D_{xy} are defined in Eq. 2.

The total potential energy for any statically loaded body is composed of two parts, the internal strain energy and the potential energy due to external surface loads. The internal flexural strain energy of a finite strip is

$$U_p = \frac{1}{2} \sum_{m=1}^{r} \int_{Vol} \{M\}_m^T \{X\}_m \, dV_s \qquad [13]$$

and substituting Eqs. 10 and 11 into Eq. 13 gives

$$U_p = \sum_{m=1}^{r} \sum_{n=1}^{r} \frac{1}{2} \{\Delta\}_n^T \int_{Vol} [B]_n^T [D] [B]_m \, dV_s \{\Delta\}_m \qquad [14]$$

The potential energy due to external surface load $q(x,y)$ is

$$W = - \int_{Area} w_s(x,y) \, q(x,y) \, dA_s = - \sum_{n=1}^{r} \{\Delta\}_n^T \int_{Area} [N]_n^T q(x,y) \, dA_s \qquad [15]$$

The total potential energy of the entire plate, ϕ, is the sum of U_p and W contributions from all the strips. Thus

$$\phi = \sum_{s=1}^{NS} \phi_s = \sum_{s=1}^{NS} \{ [\frac{1}{2} \{\Delta\}_n^T \int_{Vol} [B]_n^T [D] [B]_m \, dV_s \{\Delta\}_m$$
$$- \{\Delta\}_n^T \int_{Area} [N]_n^T q(x,y) \, dA_s \} \qquad [16]$$

where NS is the number of strips. Note the m and n summation symbols are omitted for brevity. Substituting Eq. 16 into Eq. 3 gives a set of simultaneous equations which is solved to establish displaced state of the system. This set of equations is written in the matrix format

$$[K] \{\Delta\} - \{F\} = \{0\} \qquad [17]$$

where [K] the structure stiffness matrix, the assemblage of the stiffness matrices for the strips comprising the plate system, and {F} is the corresponding assemblage of element load matrices. The element stiffness matrix, [S], of a single strip is identified as

$$[S] = \sum_{m=1}^{r} \sum_{n=1}^{r} \int_{Vol} [B]_n^T \, [D] \, [B]_m \, dV_s \qquad [18]$$

The expanded element stiffness and load matrices are given below.

$$[S] = \int_{Vol} \begin{bmatrix} [B]_1^T[D][B]_1 & [B]_1^T[D][B]_2 & \cdots & [B]_1^T[D][B]_r \\ [B]_2^T[D][B]_1 & [B]_2^T[D][B]_2 & \cdots & [B]_2^T[D][B]_r \\ \cdots & \cdots & \cdots & \cdots \\ \cdots & \cdots & \cdots & \cdots \\ [B]_r^T[D][B]_1 & [B]_r^T[D][B]_2 & \cdots & [B]_r^T[B][B]_r \end{bmatrix} dV_s \qquad [19]$$

and

$$\{F\}_s = \int_{Area} \begin{Bmatrix} [N]_1^T \\ [N]_2^T \\ \cdot \\ \cdot \\ \cdot \\ [N]_r^T \end{Bmatrix} q(x,y) \, dA_s \qquad [20]$$

For a prismatic strip with a uniform load q_o Eqs. 19 simplifies to

$$[S] = \int_{Vol} \begin{bmatrix} [S]_{11} & [S]_{12} & \cdots & [S]_{1r} \\ [S]_{21} & [S]_{22} & \cdots & [S]_{2r} \\ \vdots & & & \\ [S]_{r1} & [S]_{r2} & \cdots & [S]_{rr} \end{bmatrix} dV_s \qquad [21]$$

where the results of the integration are given in Figure 2.2, and Eq. 20 reduces to

$$\{F\} = \begin{Bmatrix} \{F\}_1 \\ \{F\}_2 \\ \vdots \\ \{F\}_r \end{Bmatrix} \qquad [22]$$

where

$$\{F\}_m = q_o \begin{Bmatrix} b/2 \\ b^2/12 \\ b/2 \\ -b^2/12 \end{Bmatrix} \int_o^b Y_m \, dy \qquad [23]$$

2.4. Commentary

A judicious choice of a displacement function can greatly simplify Eq. 19. As previously mentioned, the series expression is a basic function which possesses the valuable property of orthogonality. Mathematically stated for $m \neq n$,

$$\int_o^b Y_m Y_n \, dy = \int_o^b \left(\frac{d^2 Y_m}{dy^2}\right) \left(\frac{d^2 Y_n}{dy^2}\right) dy = 0 \qquad [24]$$

This greatly reduces the effort involved in determining the strip stiffness matrix.

$$[S]_{mn} = \frac{1}{420a^3} \begin{bmatrix} S_{11} & S_{12} & S_{13} & S_{14} \\ & S_{22} & S_{23} & S_{24} \\ (\mathrm{sym}) & & S_{33} & S_{34} \\ & & & S_{44} \end{bmatrix}$$

$$S_{11} = S_{33} = -S_{13} = 5040\ D_x I_1 - 504a^2 D_1 I_2 - 504a^2 D_1 I_3 + 156a^4 D_y I_4 + 2016a^2 D_{xy} I_5$$

$$S_{22} = S_{44} = 1680\ a^2 D_x I_1 - 56a^4 D_1 I_2 - 56a^4 D_1 I_3 + 4a^6 D_y I_4 + 224a^4 D_{xy} I_5$$

$$S_{12} = -S_{34} = 2520aD_x I_1 - 462a^3 D_1 I_2 - 42a^3 D_1 I_3 + 22a^5 D_y I_4 + 168a^3 D_{xy} I_5$$

$$S_{23} = 1680a^2 D_x I_i - 56a^4 D_1 I_2 - 56a^4 D_1 I_3 + 4a^6 D_y I_4 + 224a^4 D_{xy} I_5$$

$$S_{24} = 840a^2 D_x I_1 + 14a^4 D_1 I_2 + 14a^4 D_1 I_3 - 3a^6 D_y I_4 - 56a^4 D_{xy} I_5$$

$$I_1 = \int_o^b Y_m Y_n d_y;\quad I_2 = \int_o^b Y_m'' Y_n d_y;\quad I_3 = \int_o^b Y_m Y_n'' d_y;$$

$$I_4 = \int_o^b Y_m'' Y_n'' d_y;\quad I_5 = \int_o^b Y_m' Y_n'' d_y \qquad (\text{for } m \neq n,\ I_1 = I_4 = 0)$$

Figure 2.2. Strip Stiffness Matrix.

Further, for systems which are simply supported, the eigenfunction is the sine series given in Eq. 7. For this function

$$\int_o^b Y_m Y_n \, dy = \int_o^b Y_m Y_n'' \, dy \quad [25]$$

$$= \int_o^b Y_m'' Y_n \, dy = \int_o^b Y_m' Y_n' \, dy = \int_o^b Y_m'' Y_n'' \, dy = 0 \quad [26]$$

These integrations reduce Eq. 21 to a matrix with submatrices along the diagonal. This uncouples the equations allowing independent analyses for each term of the series and superposition of the results after convergence has been achieved. For other support conditions the basic FSM method is unchanged but the uncoupling does not occur. Thus, all r terms must be solved simultaneously.

CHAPTER III

3. STATE-OF-THE-ART

3.1. Literature Review

The finite strip concept just described was introduced by Cheung in two papers (5,6). A review of pertinent subsequent developments is necessary to put the research described in subsequent sections in perspective. Powell and Oden (7) working independently of Cheung, developed a similar element for application to orthotropic steel plate bridge decks. Later, Cheung (8) extended the FSM to the analysis of folded plate structures. Two new concepts were introduced: (1) treatment of in-plane stresses and (2) rotation of the strip stiffness matrix to account for the various orientations of the plate elements. Analytical results compared favorably with the solutions obtained by DeFries-Skene and Scordelis using classical analysis and a direct stiffness matrix method (9).

Cheung (10,11,12) also applied the techniques developed for the analysis of folded plate systems orthotropic right bridges, and box girders. Applicability of the method was limited to single-span structures with end diaphragms. End diaphragms were assumed to be infinitely rigid in-plane and infinitely flexible out-of-plane. The plates did not have intermediate supports or diaphragms.

Soon after the development of the techniques for folded plate and box-girder analysis, Cheung extended the FSM to the analysis of cylindrical orthotropic curved bridge decks (13). Fundamentally, the finite strip displacement function, Eq. 4, was expressed in polar coordinates but the fundamental theory was unchanged. The results compared closely with FEM solutions obtained by Coull and Das (14) and test results performed by Cheung on a scale model.

The work just described was limited to systems with clear spans, i.e., no intermediate beam or column supports. M. S. Cheung et al. developed a beam stiffness matrix compatible with the finite strip plate element (15). However, the method was restricted to beams oriented <u>parallel</u> to the longitudinal direction (y-direction) of the strip. Cheung also described a flexibility analysis which could be used to incorporate column supports.

Gutkowski successfully extended the finite strip concept to a "finite panel" model which accommodated interior beams (16,17,18). In this model the rectangular plate was incorporated by a macro-element using a displacement function of the form

$$w(x,y) = \sum_{m=1}^{\infty} [Y_m(y)\sin\frac{m\pi x}{a} + X_m(x)\sin\frac{m\pi y}{b}] \qquad [27]$$

Both isotropic and orthotropic systems were treated (17,18) but applications were limited to two-way plates continuous over pinned supports.

Cheung (19) applied the FSM to the analysis of freely vibrating polygonal plates. In two papers (20,21), Cheung and Cheung treated free vibration of curved and straight beam-slab and box girder bridges with clear spans (20) and introduced higher order polynomial displacement functions (21). These functions require more unknown displacement parameters per strip than the previously used lower order strips. This results in fewer structural equations but increases the bandwidth of the corresponding stiffness matrix.

The literature cited thus far is restricted to static analyses. In all cases, the referenced authors have cited the minimal computation and storage requirements as strong points of the FSM method.

A contribution to the FSM was made by Wu (22) in a paper on frequency analysis of rectangular plates continuous over pinned supports in either one or two directions. The important aspect of this work is the formulation of a strip displacement function which is the product of the eigenfunction for a continuous beam and a polynomial function which contains the displacement parameters. This was the first application of the FSM to plate systems continuous over non-deflecting supports without the use of the flexibility method. This is advantageous because a flexibility approach requires numerous FSM analyses prior to invoking conditions of compatibility. Although this method is a significant advancement over the flexibility approach the requirement of non-deflecting beams limits its use. Delcourt and Cheung (23) later extended the multi-span FSM to folded plate systems. The technique was used to analyze a continuous folded plate previously studied by Beaufait (24), and Scordelis and Lo (25) using other methods. The results compared closely with finite element, classical elasticity, and empirical methods.

Cheung and Chan contributed a paper on the analysis of continuous curved box girder bridges (26). Example bridges with intermediate columns were analyzed with the flexibility analysis. Cheung also studied a flexibility analysis for box girder bridges with intermediate flexible diaphragms. He employed a technique developed by Rao (27) for the analysis of a folded plate continuous over flexible diagrams. Compatibility of deflection is enforced at several locations along the plate diaphragm interface. A finite strip analysis must be performed for each point where compatibility is invoked.

Dynamic analysis and buckling of plate systems are not included in work described herein. However, a number of contributions in this area have been made by other researchers (28-32) using the FSM. Also thick plates have been investigated by Cheung (33), and Mawenya and Davies (34). Recently, Brown and Ghali (35) extended the FSM to quadrilateral plates. Sisodiya et al. (36) have analyzed single- and double-celled box girder bridges.

In summary, the FSM is an efficient structural analysis tool which may be used to analyze a wide range of practical problems. It should be emphasized that the FSM is applicable only when certain boundary and geometric conditions are met. The FSM is efficient for single-span structures and may also be applied to continuous systems but requires involved repetitive analyses using flexibility techniques or specialized eigenfunction analyses to generate the basic functions required for the displacement function. In either case, these techniques lack generality. Extending either of these techniques to more complex systems would be a difficult if not impossible task.

3.2. Extension of the Finite Strip Stiffness Formulation

Efficient techniques such as the FSM are advantageous because of the limited computer input required, small storage requirements and computational efficiency. Many FSM models could be used on a microcomputer for the static and dynamic analysis of plate systems traditionally analyzed with less rigorous approaches. As indicated in the preceding section, the state-of-the-art of static analysis of plate systems continuous over flexible beams and columns is a flexibility approach. This approach has been successfully applied to bridge systems with small number of redundants, such as a bridge with a few column supports in the interior. The flexibility approach has also been applied to plate systems with flexible beam or diaphragm supports. This approach requires enforcement of compatibility of displacements at a sufficient number of points along the beam or diaphragm to insure accuracy. For each chosen point a redundant force is created along each interface. Separate finite strip analyses are required for each redundant. Because the number of redundants is usually large the efficiency of the flexibility technique is often compromised. A need exists to incorporate these features in a direct, computationally efficient manner. A stiffness formulation to accomplish this is described in remaining sections of this manuscript.

The versatility of the stiffness approach for the analysis of continuous plate systems has been overlooked in past research. Using concepts developed herein, beam and column stiffness may be incorporated directly into the system equations. The advantages of the stiffness method to be described are:

1. Repetitive FSM analyses, inherent in any flexibility method, is not be required, thus computational efficiency will be improved.
2. The analyst does not have to determine the number of points for which to invoke displacement compatibility. This important task (which requires a great degree of judgment) is not a feature of the method described herein.

3. The stiffness method is well suited to dynamic and stability analyses, the flexibility technique is not.

CHAPTER IV

4. MODELING SUPPORT ELEMENTS

4.1. Scope

At present the FSM lacks a general and direct technique for the analysis of flat plates continuous over supporting beams and columns. The primary objective of the study reported herein is to provide the capability to include beams oriented transverse to the strip (transverse beam), beams oriented parallel to the strip (longitudinal beams), and columns in the FSM by use of a stiffness method. Key features are the inclusion of (1) flexural stiffness of beams, (2) torsional stiffness of beams, (3) axial stiffness of columns, and (4) flexural stiffness of columns. These are necessary advancements which will simplify the analysis of continuous systems by overcoming the cumbersome features embodied in the approaches previously discussed. The versatility and capability of the FSM is particularly enhanced by incorporating the second and fourth features cited above. Neither torsional stiffness of transverse beams nor flexural stiffness of columns have been considered in any past research reported in the literature.

The stiffness formulation is based upon use of the finite strip displacement function, $w_s(x,y)$ presented in Eqs. 4, 6 and 8. Supporting beams and columns are incorporated in a manner mathematically consistent with this displacement function and is described in Section 4.3. The scope will include isotropic and orthotropic flat plate systems subjected to static loads.

4.2. Addition of the Support Elements

4.2.1. Finite element method

In the conventional FEM the structure stiffness matrix is assembled in a direct manner. At the various nodes of the mesh discrete degrees-of-freedom are designated as the unknown nodal displacements. The element stiffness matrix for each individual structural component is added to the structure stiffness matrix by accounting for its connectivity to these nodes. The important points are (1) an element stiffness matrix is developed for each component, whether it be a plate, column, beam, or any other type of structural element, and (2) the contents of displacement vector are the independent displacements at the node points to which the particular component is attached. This feature renders the conventional finite element analysis of structures composed of a combination of different types of elements to a process of directly adding the contents of individual element stiffness matrices to appropriate locations of the structure stiffness matrix and execution of the subsequent matrix operations of the FEM. The inability to employ this assembly process to incorporate supporting beams and columns has been the primary drawback of the FSM. This difficulty and a method that overcomes it are described in the following sections.

4.2.2. Finite strip method

In the FSM discrete nodal degrees-of-freedom do not exist. For example, consider the example finite strip model presented earlier in Figure 2.1. Attachment of any finite strip to adjacent strips is only possible at the continuous (transverse) edges i and j. Mathematically, the contents of {Δ} in Eq. 17 in a finite strip formulation are modal displacement parameters and these do not constitute nodal degrees-of-freedom. Thus, to date the only type of supporting component successfully treated by the FSM in a stiffness formulation has been a beam placed coincident with either edge i or j. A beam stiffness matrix in series form consistent with Eq. 7 was used. To date no stiffness method has been developed which accommodates either transverse beams or columns.

A proper FSM formulation must produce compatibility of the displaced support components with the interior displaced shape of the plate strip in a manner consistent with superposed edge modal displacement parameters. In the FEM the connectivity to the displacements degrees-of-freedom accomplishes this requirement. In the FSM the <u>direct connectivity</u> to modal displacement edge functions is not possible except for beams coincident with the longitudinal edges. In subsequent sections, a method to achieve proper compatibility of supporting beams and columns with the plate strip, regardless of location, and orientation, by the development and use of "compound strip" elements is described. Further, this approach will enable the use of conventional direct assembly processes for incorporating element stiffness matrices into the structure stiffness matrix.

For reference, consider the compound finite strip shown in Figure 4.1. In the compound strip formulation developed in this work, the supporting elements are embodied at the outset of the derivation, i.e., the total strain energy of the compound strip is expressed in the form

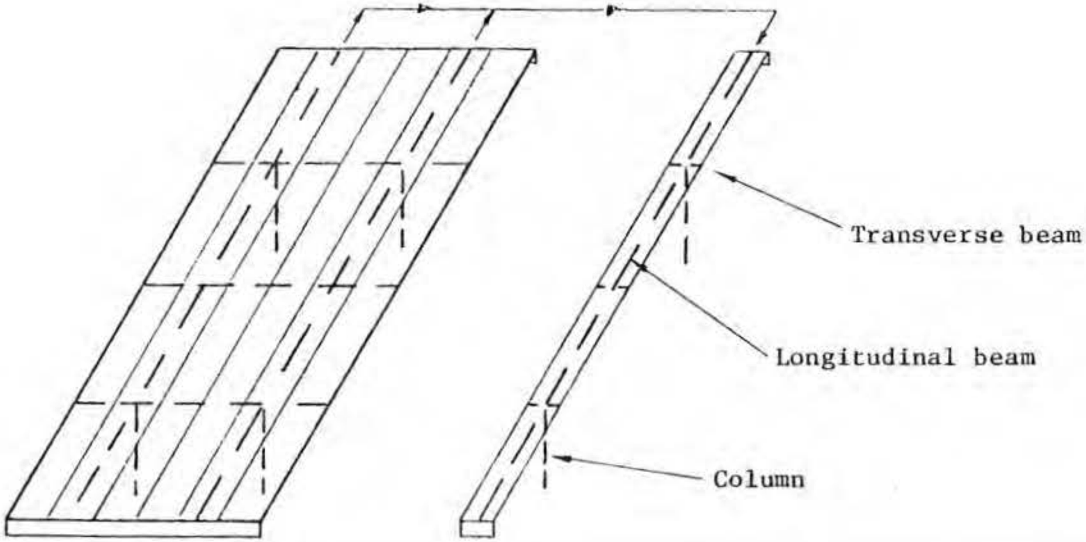

Figure 4.1. Division into Compound Strips.

$$U = U_{fl} + U_{ft} + U_{tl} + U_{tt} + U_{ac} + U_{cx} + U_{cy} + U_p \qquad [28]$$

U_{fl} and U_{tl} are the flexural and torsional strain energy of the longitudinal support beams, respectively, U_{ft} and U_{tt} are the flexural and torsional strain energy of the transverse support beams, respectively, U_{ac} is the axial strain energy of the columns, U_{cx} and U_{cy} are the flexural strain energy of the column and U_p is the flexural strain energy in the plate. Each of the strain energy terms in Eq. 28 is developed in a manner consistent with the assumed strip displacement function, Eq. 4, repeated below as Eq. 29. The derivation is presented in the following sections.

$$w_s(x,y) = \sum_{m=1}^{r} X_m(x)\, Y_m(y) \qquad [29]$$

4.3. Mathematical Formulation of Compound Strip Stiffness Matrices

Each term in Eq. 28 is examined individually in the following sections.

4.3.1. Flexural stiffness-longitudinal beam

The flexural strain energy for a beam is

$$U_{fl} = \frac{EI}{2} \int_{o}^{b} \left(\frac{\partial^2 w}{\partial y^2}\right)^2 dy \qquad [30]$$

where EI is the flexural rigidity of the beam and w is its displacement function.

To incorporate the beam in the FSM the displacement function is

$$w = \sum_{m=1}^{r} X_m(X)\, Y_{m(y)} = \sum_{m=1}^{r} [N]_m \{\Delta\}_m \qquad [31]$$

Taking the derivative of U_{fl} with respect to δ_{kn} gives

$$\frac{\partial U_{f1}}{\partial \delta_{kn}} = EI \int_o^b (\frac{\partial^2 w}{\partial y^2}) \frac{\partial}{\partial \delta_{kn}} (\frac{\partial^2 w}{\partial y^2}) \, dy \quad [32]$$

where δ_{kn} is a displacement parameter in mode n. Substituting the displacement function of Eq. 31 into Eq. 32 gives

$$\frac{\partial U_{b1}}{\partial \delta_{kn}} = EI \sum_{m=1}^{r} \int_o^b \left[[\frac{\partial^2 [N]_m}{\partial y^2}] \{\Delta\}_m \right] \frac{\partial}{\partial \delta_{kn}} (\frac{\partial^2 w}{\partial y^2}) \, dy \quad [33]$$

where all functions are evaluated at the local x coordinate of the beam.

Letting k=1, the first row of the stiffness matrix is determined for mode n. Accordingly, Eq. 33 simplifies to

$$\frac{\partial U_{f1}}{\partial \delta_{1n}} = EI \sum_{m=1}^{r} \int_o^b \left[\frac{\partial^2 [N]_m}{\partial y^2} \right] \{\Delta\}_m (\frac{\partial^2 N_{1n}}{\partial y^2}) \quad [34]$$

where N_{1n} is the first term of the matrix $[N]_n$. Using Eq. 8,

$$\frac{\partial^2 N_{1n}}{\partial y^2} = (1 - 3\bar{x}^2 + 2\bar{x}^3) \frac{\partial^2 Y_n}{\partial y^2} = C_1 \frac{\partial^2 Y_n}{\partial y^2}$$

where $\bar{x}$ is the normalized x coordinate of the beam. Eq. 34 simplifies to

$$\frac{\partial U_{f1}}{\partial \delta_{1n}} = EI \; C_1 \left[[C_1 \; C_2 \; C_3 \; C_4] \{\Delta\}_n \right] \int_o^b \frac{\partial^2 Y_m}{\partial y^2} \frac{\partial^2 Y_n}{\partial y^2} \, dy \quad [35]$$

where C_1–C_4 are the polynomials in x given in Eq. 8 evaluated at the local x coordinate of the beam and the summation in Eq. 34 is implied.

Similar expressions have been developed for the other rows. The only change from Eq. 35 is that the first C_1 increments to C_2, C_3, and C_4, accordingly. The element stiffness matrix associated with the displacement parameters $\{\Delta\}_n$ is

$[S]_{mn}$ (flexural-longitudinal) =

$$EI(I_4)\begin{bmatrix} C_1C_1 & C_1C_2 & C_1C_3 & C_1C_4 \\ C_2C_1 & C_2C_2 & C_2C_3 & C_2C_4 \\ C_3C_1 & C_3C_2 & C_3C_3 & C_3C_4 \\ C_4C_1 & C_4C_2 & C_4C_3 & C_4C_4 \end{bmatrix} \quad [36]$$

where $C_1 = 1 - 3\bar{x}^2 + 2\bar{x}^3$

$C_2 = x - 2\bar{x}x + \bar{x}^2x$

$C_3 = 3\bar{x}^2 - 2\bar{x}^3$

$C_4 = x(\bar{x}^2 - x)$

are evaluated at the local x coordinates of the beam. Due to the use of orthogonal boundary functions

$$I_4 = \int_o^b \frac{\partial^2 Y_m}{\partial y^2}\frac{\partial^2 Y_n}{\partial y^2}\,dy \qquad m=n$$

$$I_4 = 0 \qquad m\neq n$$

To illustrate the use of Eq. 36 an example is given. Let x=0 and the boundary function be $Y_m = \sin\frac{m\pi y}{b.}$ Thus $I_4 = \int_o^b Y_mY_n dy = m^4\pi^4/2b^3$ and at $x=\bar{x}=0$, $C_1=1$ and $C_2=C_3=C_4=0$. $S_{mn}(1,1) = m^4\pi^4EI/2b^3$ and all other entries are zero.

4.3.2. Torsional stiffness-longitudinal beam

The torsional strain energy is

$$U_{t1} = \frac{GJ}{2} \int_o^b \left(\frac{\partial^2 w}{\partial x \partial y}\right)^2 dy \qquad [37]$$

where GJ is the torsional rigidity of the beam.

Substituting Eq. 31 into 37 gives

$$U_{t1} = \frac{GJ}{2} \int_o^b \left[\sum_{m=1}^{r} [\frac{\partial^2 [N]_m}{\partial x \partial y}] \{\Delta\}_m \right]^2 dy \qquad [38]$$

which may be minimized with respect to each displacement parameter in the displacement vector. Taking the derivative with respect to δ_{kn} gives

$$\frac{\partial U_{t1}}{\partial \delta_{kn}} = GJ \sum_{m=1}^{r} \left[[\frac{\partial^2 [N]_m}{\partial x \partial y}] \{\Delta\}_m \right] \frac{\partial}{\partial \delta_{kn}} \left(\frac{\partial^2 w}{\partial x \partial y}\right) dy \qquad [39]$$

where all functions are evaluated at the local x coordinate of the beam. Similar to Sec. 4.3.1, let k range from 1 to 4 to give the four rows of element stiffness matrix $[S]_{mn}$. The boundary functions are available in the literature in closed form (37,38), but are not, in general, orthogonal for the integral in Eq. 38. Performing the required differentiation and integration gives the strip stiffness matrix.

$[S]_{mn}$ (torsional - longitudinal) =

$$GJI_5 \begin{bmatrix} C_1'C_1' & C_1'C_2' & C_1'C_3' & C_1'C_4' \\ & C_2'C_2' & C_2'C_3' & C_2'C_4' \\ & & C_3'C_3' & C_3'C_4' \\ (sym) & & & C_4'C_4' \end{bmatrix} \qquad [40]$$

where the prime denotes the first derivative with respect to x and

$$I_5 = \int_o^b \left(\frac{\partial Y_m}{\partial y}\right) \left(\frac{\partial Y_n}{\partial y}\right) dy$$

Also

$$C_1' = -6\bar{x}/a + 6\bar{x}^2/a$$

$$C_2' = 1 - 4\bar{x} + 3\bar{x}^2$$

$$C_3' = 6\bar{x}/a - 6\bar{x}^2/a$$

$$C_4' = 3\bar{x} - 2\bar{x}$$

are evaluated at the local x coordinate of the beam. As an example consider a simply supported beam located at local x coordinate of zero. It follows $C_2' = 1$ and $C_1' = C_3' = C_4' = 0$. Assume $Y_m = \sin m\pi y/b$ thus $I_5 = m^2\pi^2/2b$. The stiffness matrix contains one nonzero entry per mode, $S_{mn}(2,2) = m^2\pi^2/2b$. Similarly, if the local x is equal to a, the strip width, this stiffness matrix also contains one nonzero entry per mode, $S_{mn}(4,4) = m^2\pi^2/2b$.

4.3.3. Flexural stiffness - transverse beam

The flexural strain energy for the beam is

$$U_{ft} = \frac{EI}{2} \int_{o}^{a} (\frac{\partial^2 w}{\partial x^2})^2 \, dx \qquad [41]$$

Again minimizing with respect to the displacement parameters gives

$$\frac{\partial U_{ft}}{\partial \delta_{kn}} = EI \int_{o}^{a} (\frac{\partial^2 w}{\partial x^2}) \frac{\partial}{\partial \delta_{kn}} (\frac{\partial^2 w}{\partial x^2}) \, dx \qquad [42]$$

Substituting Eq. 31 into 42 and performing the differentiation gives

$$\frac{\partial U_{ft}}{\partial \delta_{kn}} = EI \sum_{m=1}^{r} \int_{o}^{a} \left[[\frac{\partial^2 [N]_m}{\partial x^2}] \{\Delta\}_m \right] \frac{\partial^2 [N_{kn}]}{\partial x^2} \qquad [43]$$

where all functions are evaluated at local y coordinate of the beam. As before, k ranges from 1 to 4 giving the four rows of the stiffness matrix per mode. Substituting Eq. 8 into 43, performing the differentiation and integration yields

$[S]_{mn}$ (flexural-transverse) =

$$EI \, Y_m \, Y_n \begin{bmatrix} 12/a^3 & 6/a^2 & -12/a^3 & 6/a^2 \\ & 4/a & -6/a^2 & 2/a \\ (sym) & & 12/a^3 & -6/a^2 \\ & & & 4/a \end{bmatrix} \qquad [44]$$

where Y_n and Y_m are evaluated at the local y coordinate of the beam.

4.3.4. Torsional stiffness - transverse beam

The torsional strain of a transverse beam is

$$U_{tt} = \frac{GJ}{2} \int_{o}^{a} (\frac{\partial^2 w}{\partial x \partial y})^2 \, dx \qquad [45]$$

where GJ is the torsional rigidity and y is evaluated at the local y coordinate of the beam. Minimizing with respect to δ_{kn} gives

$$\frac{\partial U_{tt}}{\partial \delta_{kn}} = GJ \int_o^a \left(\frac{\partial^2 w}{\partial x \partial y}\right) \frac{\partial}{\partial \delta_{kn}} \left(\frac{\partial^2 w}{\partial x \partial y}\right) dx \qquad [46]$$

and substituting Eq. 8 into 46 and differentiating gives

$$\frac{\partial U_{tt}}{\partial \delta_{kn}} = GJ \sum_{m=1}^{r} \int_o^a \left[[\frac{\partial^2}{\partial x \partial y} [N]_m] \{\Delta\}_m \right] \frac{\partial^2 N_{kn}}{\partial x \partial y} dx \qquad [47]$$

Performing the differentiation and integration yields

$[S]_{mn}$ (torsional-transverse) =

$$\frac{GJ}{30a} \left(\frac{\partial Y_n}{\partial y}\right) \left(\frac{\partial Y_m}{\partial y}\right) \begin{bmatrix} 36 & 3a & -36 & 3a \\ & 4a^2 & -3a & a^2 \\ (sym) & & 36 & -3a \\ & & & 4a^2 \end{bmatrix} \qquad [48]$$

4.3.5. Column stiffness - axial

The axial strain energy in a support column attached to a strip is

$$U_c = \frac{1}{2} K_A \left[w(x_c, y_c)\right]^2 = \frac{1}{2} K_A w_c^2 \qquad [49]$$

where K_A is the axial stiffness of the column and w_c, the axial deformation is obtained by evaluating the displacement function w at the local coordinates, x_c, y_c, corresponding to its location in the strip. Minimizing with respect to the displacement parameter δ_{kn} gives

$$\frac{\partial U_c}{\partial \delta_{kn}} = K_A \left[w_c\right] \frac{\partial}{\partial \delta_{kn}} \left[w_c\right] \qquad [50]$$

Substituting Eq. 8 into 50 gives

$$\frac{\partial U_c}{\partial \delta_{kn}} = K_A \sum_{m=1}^{r} \left[[N]_m \{\Delta\}_m\right] \frac{\partial}{\partial \delta_{kn}} \left[[N]_m \{\Delta\}_m\right] \qquad [51]$$

which after differentiation simplifies to

$$\frac{\partial U_c}{\partial \delta_{kn}} = K_A \sum_{m=1}^{r} \left[[N]_m \; \{\Delta\}_m \right] N_{kn} \qquad [52]$$

where N_{kn} is defined in Eq. 34 and k ranges from 1 to 4 to give the four rows of the stiffness matrix for mode n. Thus

$$[S]_{mn}(\text{Axial}) = K_A Y_m Y_n \begin{bmatrix} C_1C_1 & C_1C_2 & C_1C_3 & C_1C_4 \\ & C_2C_2 & C_2C_3 & C_2C_4 \\ (\text{sym}) & & C_3C_3 & C_3C_4 \\ & & & C_4C_4 \end{bmatrix} \qquad [53]$$

where C_1-C_4 are the polynomials given in Eq. 8 evaluated at x_c and Y_m, Y_n are the boundary functions evaluated at y_c.

4.3.6. Flexural stiffness - column

The flexural strain energy in the columns has two components, bending transverse and parallel to the strip. The "bending transverse" is associated with a rotation in the local y direction using the right hand rule. This action will be examined first followed by the orthogonal rotation to be termed "bending longitudinal."

The strain energy for the "bending transverse" state is

$$U_{cx} = \frac{1}{2} K_{cx} \left[\frac{\partial w(x_c, y_c)}{\partial x}\right]^2 = \frac{1}{2} K_{cx} \left[\frac{\partial w_c}{\partial x}\right]^2 \qquad [54]$$

where K_{cx} is the flexural stiffness of the column. Minimizing with respect to the displacement parameter δ_{kn} gives

$$\frac{\partial U_{cx}}{\partial \delta_{kn}} = K_{cx} \left[\frac{\partial w_c}{\partial x}\right] \frac{\partial}{\partial \delta_{kn}} \left[\frac{\partial w_c}{\partial x}\right] \qquad [55]$$

Substituting Eq. 8 into 55 gives

$$\frac{\partial U_{cx}}{\partial \delta_{kn}} = K_{cx} \sum_{m=1}^{r} \left[\frac{\partial [N]_m}{\partial x}\{\Delta\}_m\right] \frac{\partial}{\partial \delta_{kn}} \left[\frac{\partial [N]_m}{\partial x}\{\Delta\}_m\right] \tag{56}$$

which simplifies to

$$\frac{\partial U_{cx}}{\partial \delta_{kn}} = K_{cx} \sum_{m=1}^{r} \left[\frac{\partial}{\partial x}[N]_m\{\Delta\}_m\right] \frac{\partial N_{kn}}{\partial x} \tag{57}$$

where k ranges from 1 to 4 to give the four rows of the stiffness matrix shown below.

$[S]_{mn}$ (column flexural-transverse) =

$$K_{cx} Y_m Y_n \begin{bmatrix} C_1'C_1' & C_1'C_2' & C_1'C_3' & C_1'C_4' \\ & C_2'C_2' & C_2'C_3' & C_2'C_4' \\ (\text{sym}) & & C_3'C_3' & C_3'C_4' \\ & & & C_4'C_4' \end{bmatrix} \tag{58}$$

The strain energy in the column bent orthogonal to the case just described is given by

$$U_{cy} = \frac{1}{2} K_{cy} \left[\frac{\partial w_c}{\partial y}\right]^2 \tag{59}$$

A procedure similar to that described by Eqs. 54-58 may be employed to yield the stiffness matrix given below.

$[S]_{mn}$ (column flexural-longitudinal) =

$$K_{cy} \left(\frac{\partial Y_m}{\partial y}\right) \left(\frac{\partial Y_n}{\partial y}\right) \begin{bmatrix} C_1C_1 & C_1C_2 & C_1C_3 & C_1C_4 \\ & C_2C_2 & C_2C_3 & C_2C_4 \\ & & C_3C_3 & C_3C_4 \\ & & & C_4C_4 \end{bmatrix} \tag{60}$$

where C_1-C_4 are polynomials given in Eq. 8. The polynomials and their first derivatives are evaluated at x_c. Y_m and Y_n are the boundary function evaluated at y_c.

4.4. Summary

Several strip stiffness matrices have been derived for attached beams or columns. Each $[S]_{mn}$ matrix has dimensions 4x4 and will add directly at the element level to the strip matrix described in chapter two.

CHAPTER V

5. PROGRAM STRIP

5.1. Introduction

The theory presented in chapter four has been incorporated in a computer code which is described herein and is entitled Program STRIP. A general discussion of the program capabilities and features is followed by a more extensive discussion of the program algorithm. Mathematical and coding details are omitted to present a clear view of the important steps of the algorithm. The reader familiar with conventional finite element analysis will observe several similarities between the finite element and finite strip methods. Major distinctions between the methods are noted and issues relevant to this research are emphasized.

STRIP has the capability for static, linear elastic analysis of beam and column supported rectangular orthotropic flat plates. The Kirchoff assumptions (1,2,3) are used throughout. Each beam may be oriented either parallel or perpendicular to the longitudinal direction of the strip. Each column can be located anywhere in plan but must be perpendicular to the plate surface. In-plane plate deformations are neglected. STRIP is restricted to straight, prismatic beams, and rectangular strip elements. Any strip may be loaded with uniformly distributed load and/or multiple concentrated loads.

Program STRIP requires minimal input data thus economizing analyst preparation time and avoiding the laborious input often required of finite element codes. This feature frees the designer/analyst to investigate many alternative systems at the preliminary stages of design with the same degree of rigor as typically applied only to the final system configuration. In addition, the displacements and internal actions may be calculated and output at any location in the system. Often cumbersome hand calculations or a post-processor routine must be used with conventional finite element codes to obtain displacements or actions at chosen points.

Although the input is minimal and straightforward, the reader is cautioned that the FSM is an approximate method and, as such, its use is somewhat an art. Proper use requires judgment based on the experience of the analyst. Similar to the FEM, the analyst must insure that convergence of the quantities of interest (deflections, etc.) has been achieved. Illustrative examples in the subsequent chapter give the reader an insight into the convergence characteristics compound strip method.

5.2. Computer Algorithm

Program STRIP was written in Fortran IV using a macro programming technique which employs an "executive program" to control the algorithm flow via calls to appropriate subroutines. The algorithm used in STRIP is illustrated in Figure 5.1. Each segment of this flow chart, which corresponds to a subroutine in STRIP, is described in the following sections.

The algorithm is composed of the ten parts given in Fig. 5.1.

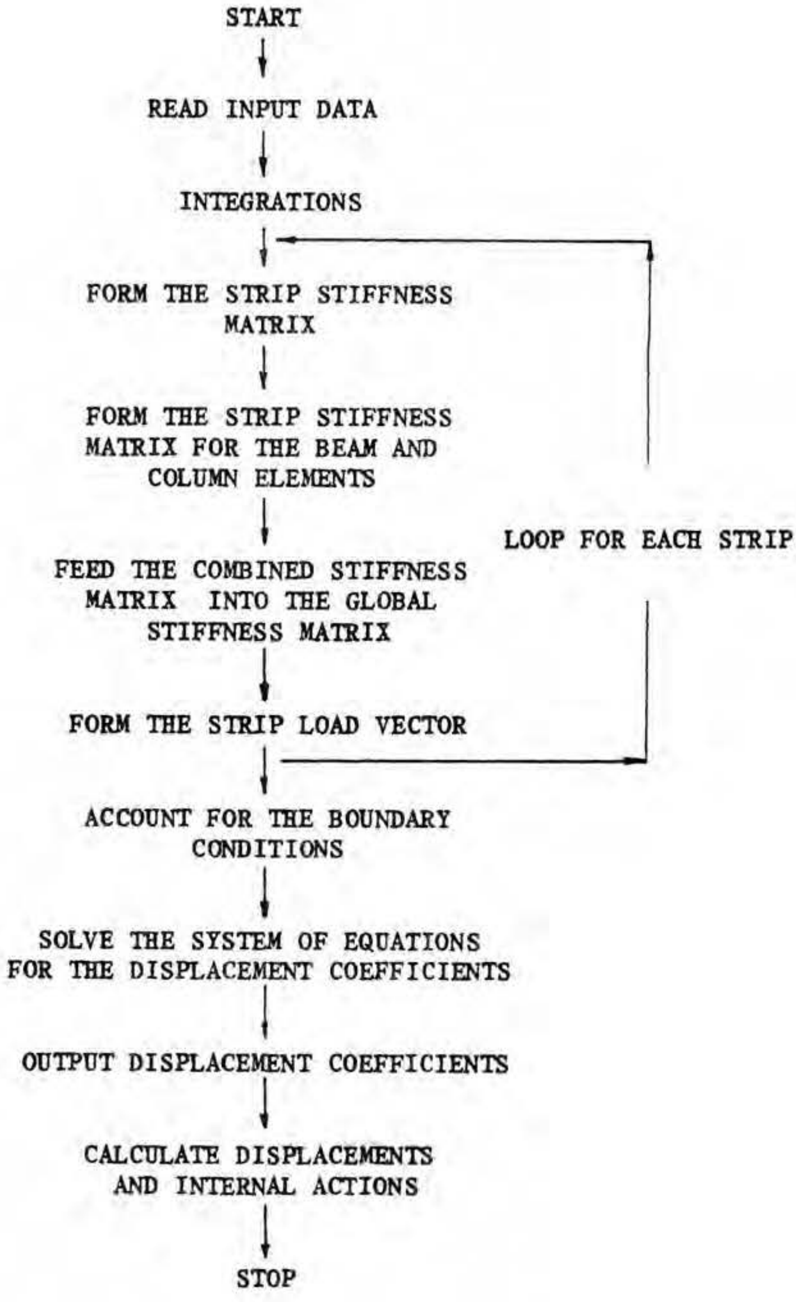

Figure 5.1. Flow Chart for STRIP

The first two parts are performed once for each analysis while parts three through seven are repeated for each strip and for each non-zero harmonic considered. Nodal line boundary conditions are invoked after the assembly of the global stiffness matrix and load vectors are completed. The displacement coefficients are determined using Gauss elimination to solve the set of linear simultaneous equations which result. The displacement coefficients establish the displaced shape of the middle surface of the plate allowing the moments to be calculated in the final routine. Although possible, shears are not calculated.

5.2.1. Read input data

Subroutine INPUT reads and echos all input data. Presently no data checks are made imposing the responsibility of logical data input on the analyst. As previously mentioned much of the laborious input data required of many finite element codes is not necessary in the FSM. Further, any tedious input has been omitted in STRIP by employing coordinate and strip element generation routines. This latter step is comparable to "automated mesh generation" in the finite element method.

5.2.2. Integrations

The formation of the element load and stiffness matrices involve the integrations given in Figure 2.1. The integrals are evaluated for each non-zero harmonic considered and stored for later use. STRIP has two integration options, sixteen point Gaussian quadrature and closed-form formulae. Sixteen point quadrature is required to accurately integrate the displacement function of the higher harmonics. The closed-form formulae were generated by Felgar in 1950 (37,38). To the author's knowledge, the availability of these formulae has not been reported in the finite strip literature. Employment of these formulae allows the analyst to consider as many non-zero harmonics as necessary whereas common numerical integration techniques can produce inaccuracies at the higher modes.

5.2.3. Formulation of the strip compound stiffness matrices

Each strip stiffness matrix (Figure 2.1) is created for all non-zero harmonic and is fed into the global stiffness matrix. This formation routine is nested in a double loop executing the double summation as shown in Eq. 16. If beam and/or columns are attached to the strip, the beam and/or column strip stiffness contribution are assembled in the same manner as the plate stiffness matrix. The assembling procedure is a matrix addition performed at the element level thus producing the "compound strip" stiffness matrix for subsequent assembling of the structure stiffness matrix.

In general, the beam and column stiffnesses effect every entry in the strip stiffness matrix and this can have important implications. A support element could dominate the strip stiffness matrix making all of the terms large and a strip with excessive stiffness results. For example, consider a plate supported by a column somewhere in its plan. Columns usually have a very large axial stiffness relative to the stiffness of the attached elements in flexure. This large stiffness, K_A in Eq. 57, could "overshadow" the entire strip causing the strip to behave as if it were rigid. As illustrated in the subsequent chapter, proper modeling of rigid supports can be achieved by using elements with moderate stiffness.

5.2.4. Form and assemble the strip load vectors

The strip load vector is created for each non-zero harmonic and fed into the global load vector. Contributions of uniform and concentrated loads are combined at the element level.

5.2.5. Boundary conditions

Unlike the finite element method, the global stiffness matrix of a structure generated in the FSM is non-singular and can be inverted without the introduction of the boundary constraints. Boundary constraints, either due to a real boundary or introduced to take advantage of symmetry, are imposed by a numerical technique called the "big number method". For each constraint this involves scaling the appropriate diagonal term of the stiffness matrix by a large number, say 10^{50}. In effect, this row is decoupled from the rest of the matrix. Solving the equation produces zero value for the displacement coefficient associated with that equation to be zero. If more than one harmonic is considered, several diagonal terms must be multiplied by the large number for each individual constraint.

STRIP has the capability to model knife edge, clamped, and guided support conditions in addition to the free edge. Beams can be placed at an edge and columns can be placed at an edge or corner by simply specifying appropriate coordinates for the structural component. This is done without recourse to the features just described for explicit support conditions.

5.2.6. Solution of simultaneous equations

The system of simultaneous structural equations which results is solved to determine the displacement coefficients. These coefficients should not be confused with nodal displacements in the FEM. The coefficients must be substituted into the assumed displacement function to determine the desired displacements. In general, this involves a summation of each harmonic's contribution to the displacement.

The finite strip model produces a system of equations whose coefficient matrices exhibits symmetry about the major diagonal and is tightly banded. The number of equations, NUMEQ, and the half-bandwidth, IB can be determined as follows:

$$\text{NUMEQ} = (\text{NST} + 1) * \text{NT} * 2 \qquad [60]$$

$$\text{IB} = 4 * \text{NT}$$

where NT is the number of non-zero harmonics considered and

NST is the number of strip elements.

Note the half-bandwidth is not a function of the number of strips. Thus the mesh may be very fine and only a few harmonics required resulting in a system of equations with a narrow bandwidth. In general the bandwidth is filled with nonzero entries, no "skyline" or "sparse" effects exist. The equation solver employed operates on the stiffness matrix stored in an array dimensioned NUMEQ x IB in order to economize on execution time and storage required. Gauss elimination is used to triangularize the stiffness matrix from which the displacement parameters may be determined.

5.2.7. Displacements and internal actions

The displacement coefficients are substituted into the assumed displacement functions to arrive at the displacement at a given location.

Similarly, to determine internal actions these displacement coefficients are substituted into the appropriate derivatives of the displacement functions and scaled by the elastic constants. For example, the moments can be found by substituting the displacement coefficients into the functions for curvatures and multiplying the curvatures by the compliance matrix, Eq. 12, to arrive at moments.

STRIP calculates deflections, rotations, and moments along any prescribed line at specified intervals. Thus displacements and moments at any point in the continuum may be determined.

5.3. Summary

A brief general description of STRIP has been given. Mathematical and programming details have been omitted to allow the reader to develop a clear understanding of the important steps in the FSM.

The beam and/or column stiffness contribution add directly to the strip stiffness matrix. Thus the stiffness of these elements is in effect "smeared out" over the entire strip effecting each entry in the strip stiffness matrix. This limits the range of values for the ratio of the beam and/or column stiffness to the plate stiffness which may be successfully modeled with STRIP. As illustrated in the next chapter, this is not a severe limitation but must be considered when modeling rigid support elements.

CHAPTER VI

6. ILLUSTRATIVE EXAMPLES

6.1. Introduction

Several plate solutions are presented as verification of the correctness of the theory. First, a single panel plate was analyzed with various support conditions which were chosen to exemplify the use of the compound strip matrices presented in chapter four. Each extension of the FSM is illustrated separately and then a comprehensive example is given which incorporates most of the new elements in a single panel plate problem. Second, a multi-panel plate system which incorporates many of the compound strip elements is given. This problem exemplifies the capabilities of the compound strip elements with a practical problem previously studied by other researchers using other methods (16,17,40). The example presented is also compared to the results from several finite element analyses.

This chapter concludes with a rate of convergence study. The FSM and FEM are compared on the basis of accuracy and computation effort required.

6.2. Single Panel Systems

6.2.1. General description

The single panel plate systems shown in Figure 6.1 have been analyzed with the finite strip and finite element methods. This set of plates incorporates a variety of boundary conditions including a clamped

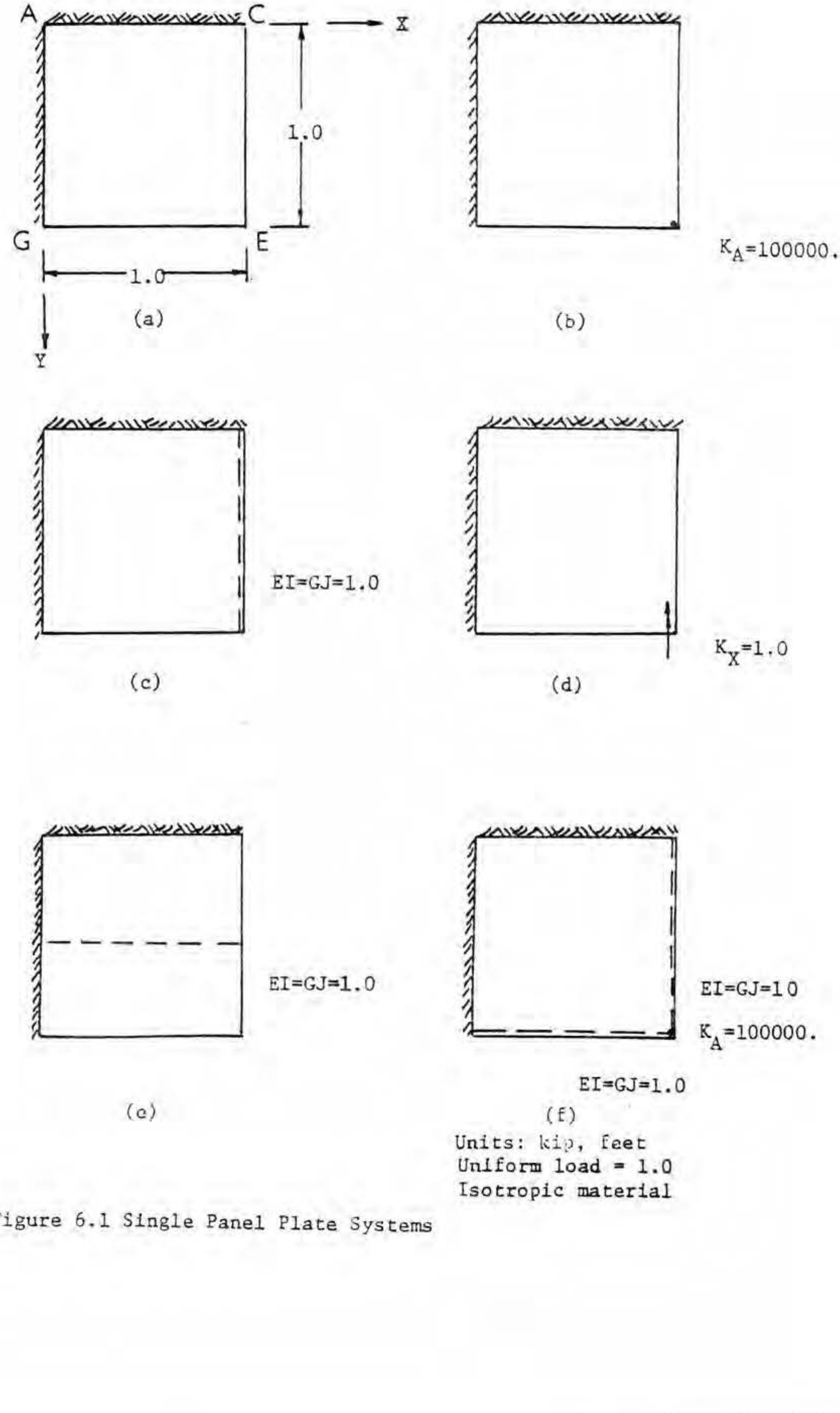

Figure 6.1 Single Panel Plate Systems

support along AC, a knife edge or pinned support along AG, and two adjacent free edges along CE and EG. The finite strips are oriented in the y-direction in all cases, thus the eigenfunction which corresponds to a cantilever beam was used. The plates are square with sides of unit length and have isotropic rigidities D_x, D_y, D_1, D_{xy} of 1.0, 1.0, 0.30, 0.35, respectively. The beams' flexural and torsional rigidities EI and GJ were assigned values of unity. The column axial stiffness was given a large value (100000 k/ft.) to limit the deflection at E to a small fraction of the unsupported case. Columns usually have a large axial stiffness as compared to the stiffness of a beam or plate, thus this was deemed reasonable. The loading was uniform for all cases.

6.2.2. Modeling

The finite element and finite strip methods were used to analyze the plate systems described in the previous section. The structural analysis program SAP IV was used for the finite element analyses. This program uses a quadrilateral plate bending element composed of four triangular elements (39) with the common degrees of freedom condensed out at the element level. SAP IV was chosen on the basis of availability to the author and familiarity to the engineering community. The single panel systems were modeled with five by five and nine by nine meshes with nodal lines equally spaced resulting in square elements for all analyses. Beam elements were employed to model the beams and columns.

A nine strip model was used for the finite strip analysis of the single panel systems. The number of harmonics was varied. The intent was not to show convergence but rather to illustrate the FSM with a constant number of strips. Consequently, it cannot be expected that

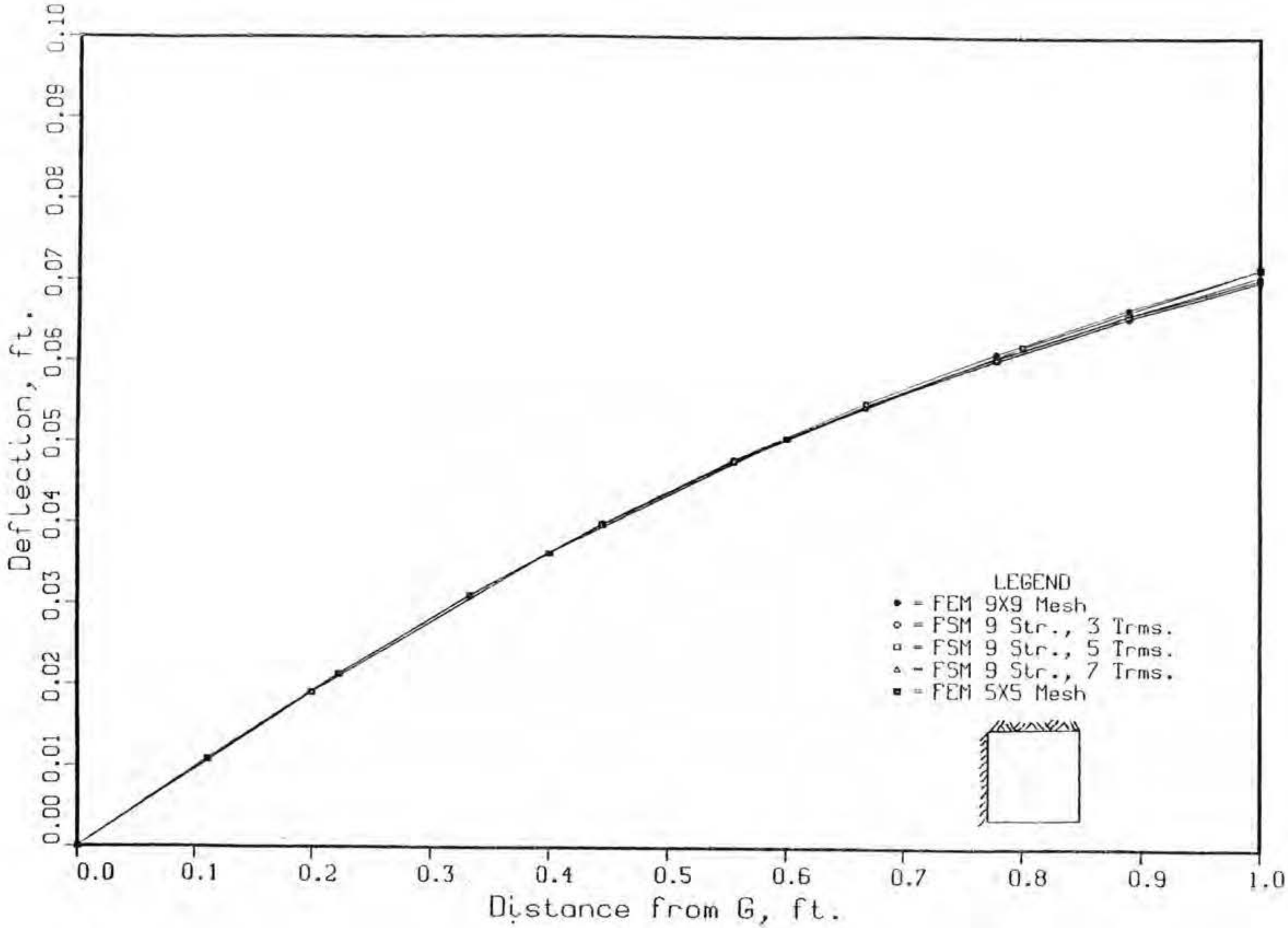

Fig. 6.3 Deflection along G-E

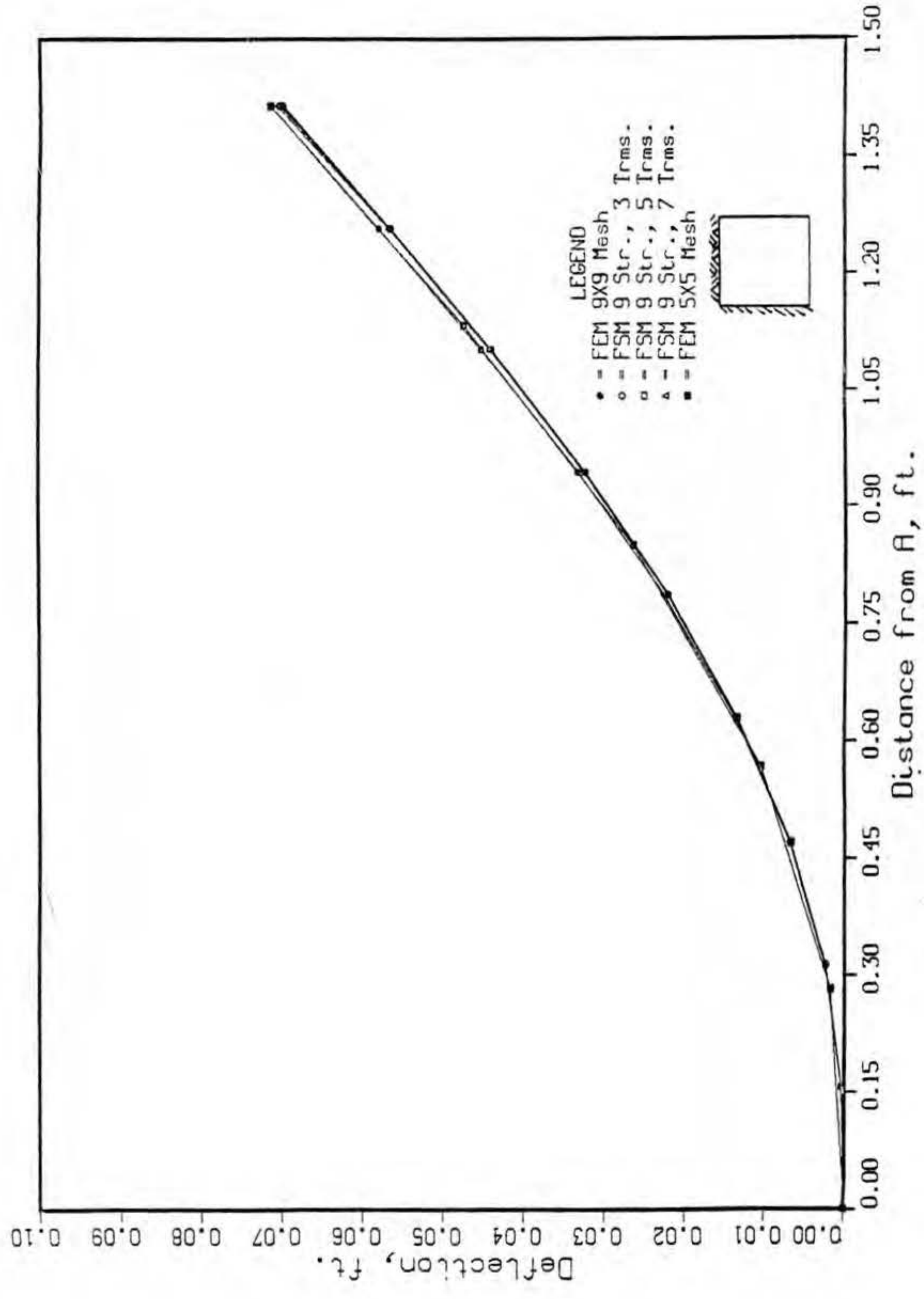

Fig. 6.4 Deflection along A-E

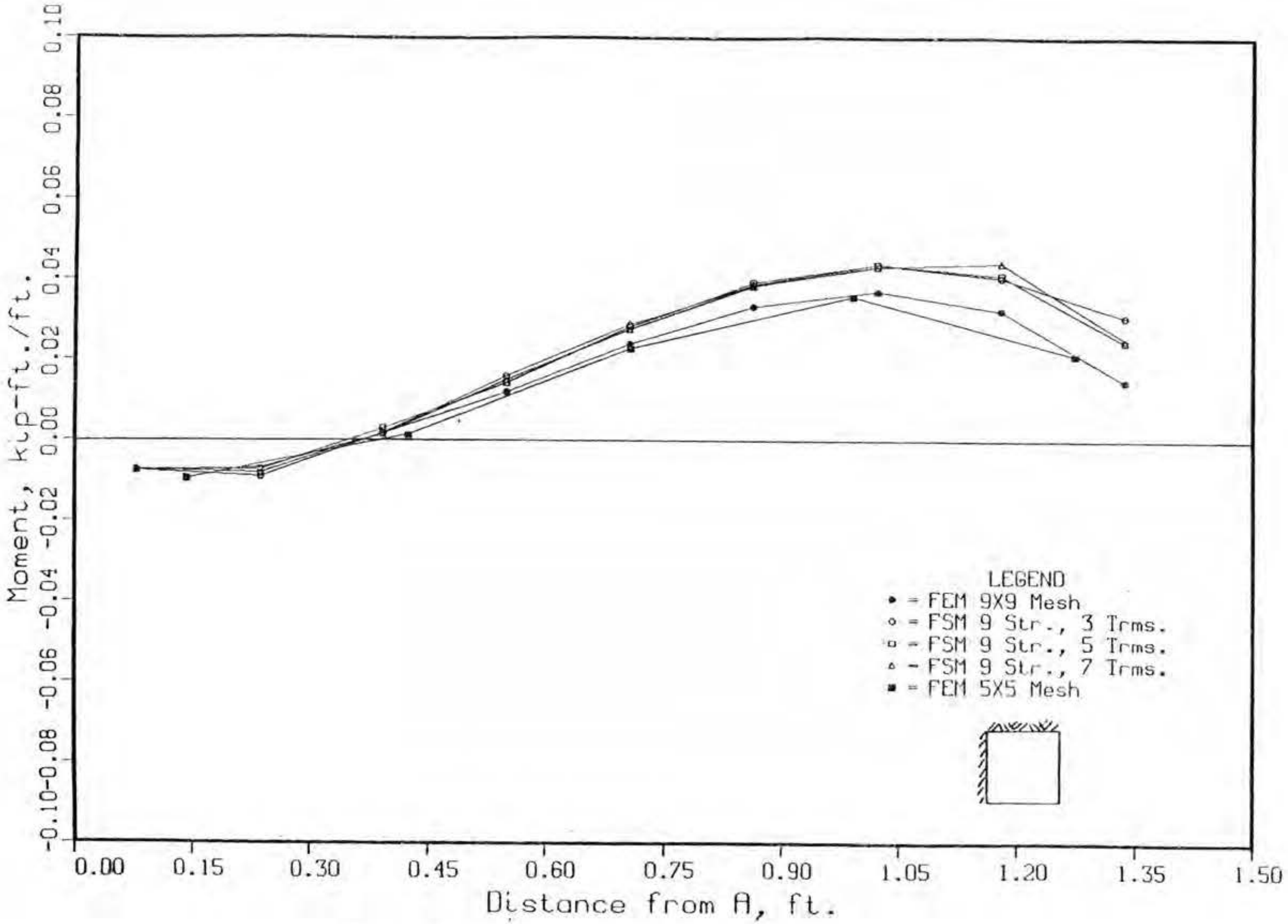

Fig. 6.5 Moment-X along A-E

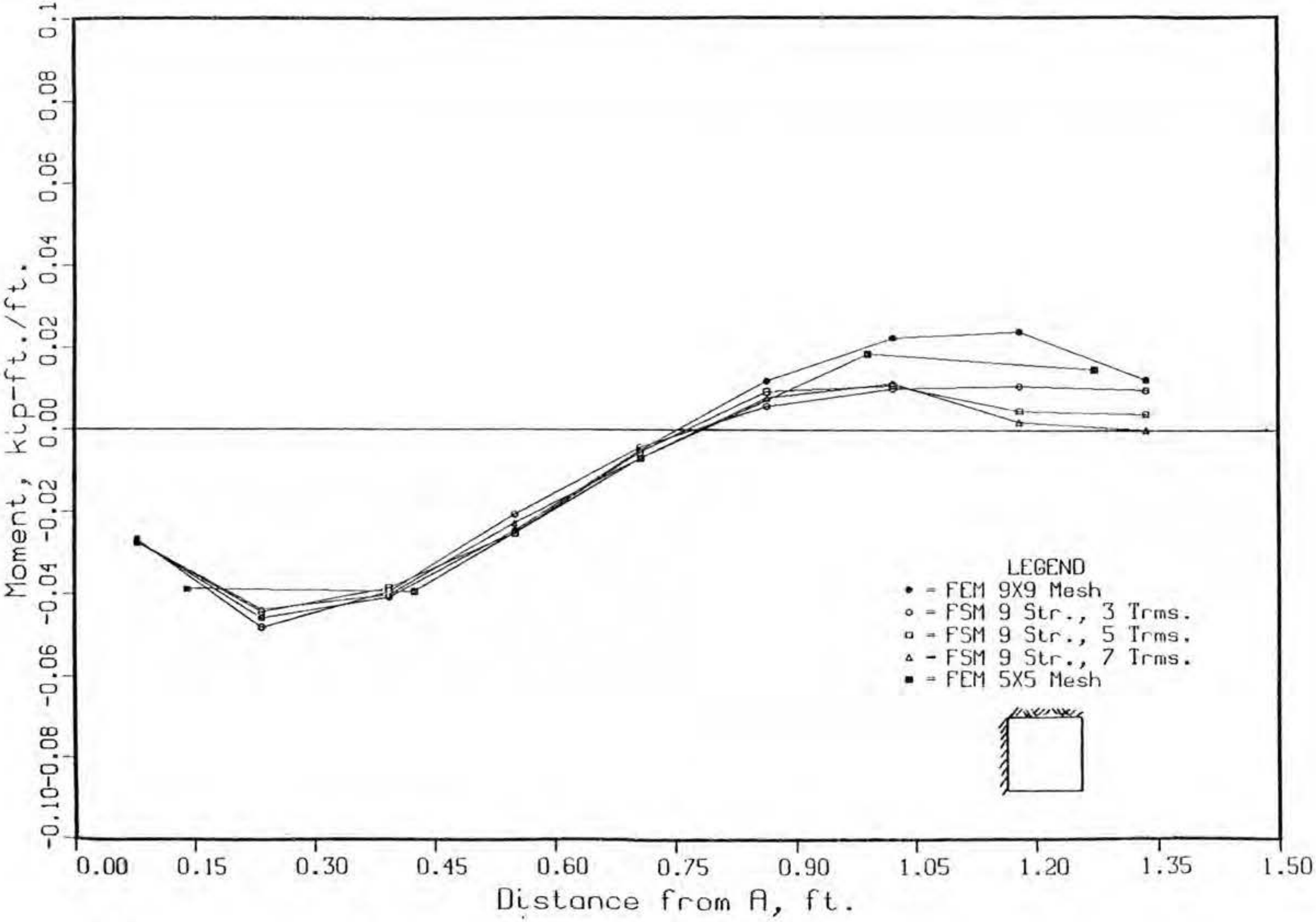

Fig. 6.6 Moment-Y along A-E

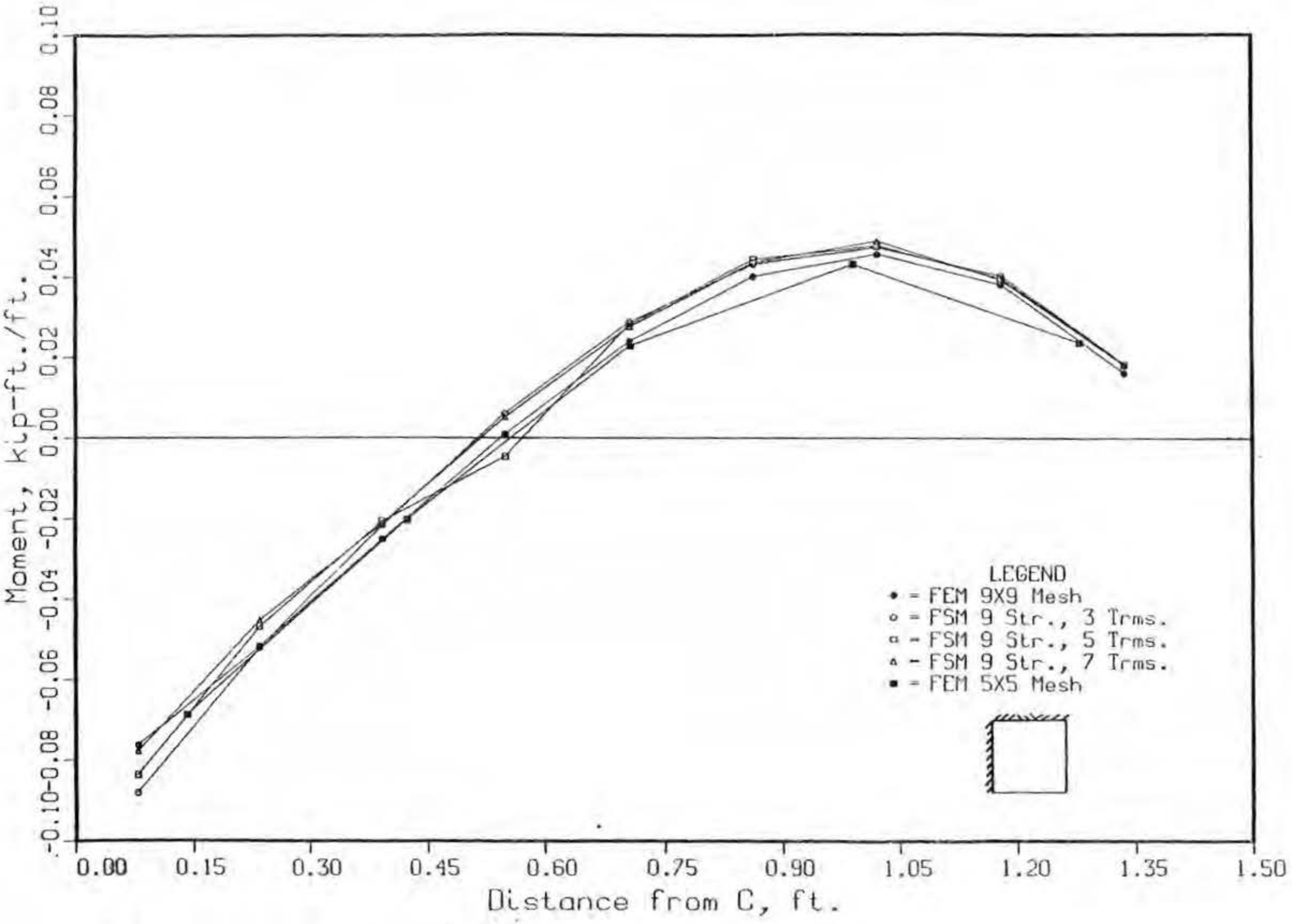

Fig. 6.7 Moment-X along G-C

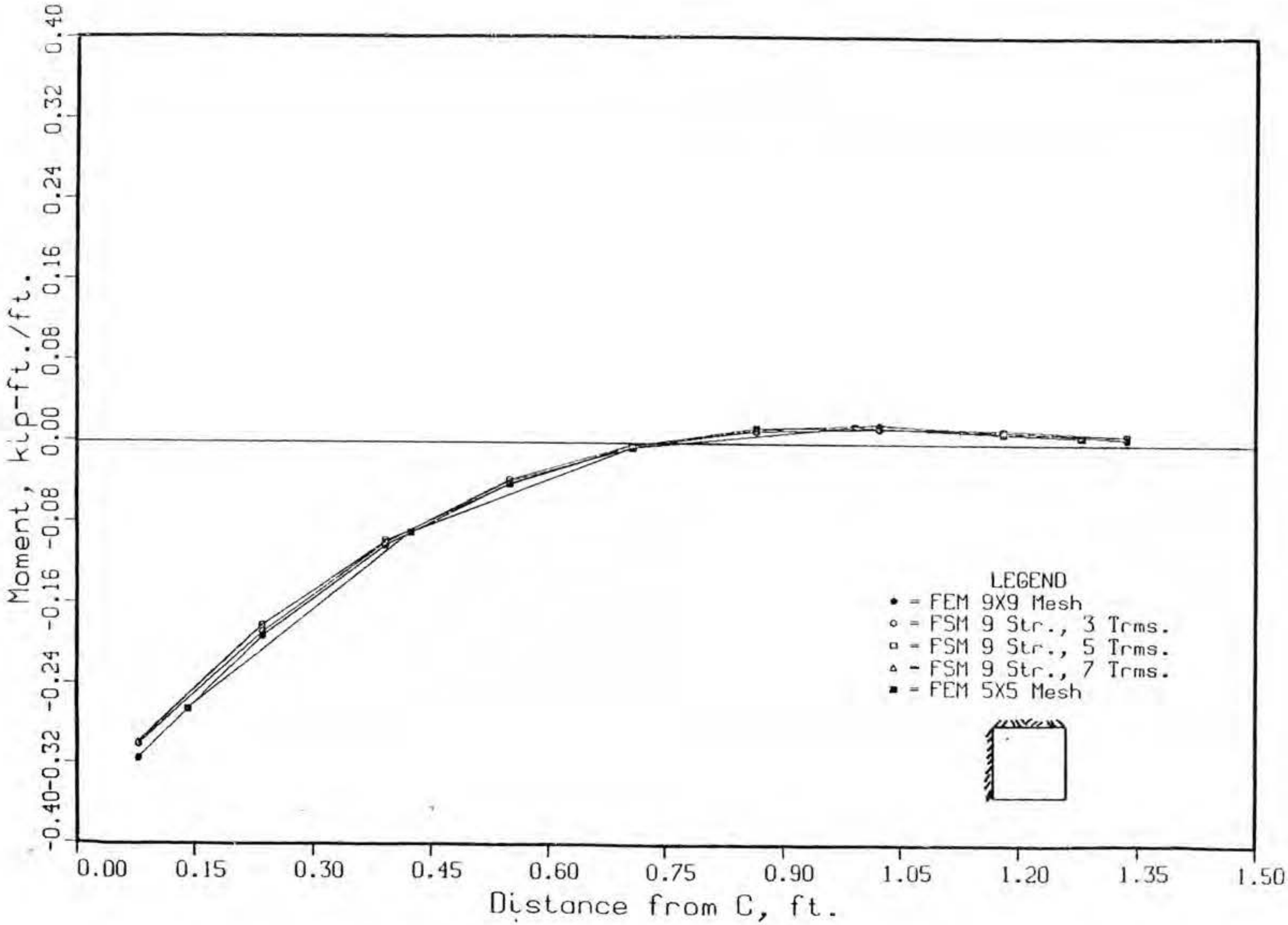

Fig. 6.8 Moment-Y along G-C

6.2.5. Column supported plate

The plate shown in Figure 6.1b was analyzed for a uniform unit load. The deflections are given in Figures 6.9-6.11 and the moments in Figures 6.12-6.15. The maximum deflection calculated by the two methods differed by five percent and the maximum moments differed by six percent.

6.2.6. Beam oriented along the strip

The plate shown in Figure 6.1c has a beam oriented longitudinal strip direction. As illustrated in Figures 6.16-6.22 the 9,7 FSM and 9x9 FEM methods compare quite well with deflections differing by less than one half of one percent and the maximum values being identical (to four significant digits in the output). Moments differed by less than three percent while the computed maximum moments are also the same to four significant digits.

6.2.7. Rotational spring

A rotational spring was placed at E as shown in Figure 6.1d. The stiffness of the spring was moderate (K_x = 1.0 kip), decreasing the deflection at E 10.6 percent from the unsupported case described in section 6.2.4. The finite element and finite strip model compared very well as illustrated in Figures 6.23-6.29.

6.2.8. Beam oriented transverse to the strips

The plate shown in Figure 6.1e has a beam oriented transverse to the strip located near the center of the plate. As shown in Figures 6.30-6.36 the FEM and FSM compare favorably with the maximum deflection within 1.25 percent and the maximum moment differed by approximately six percent.

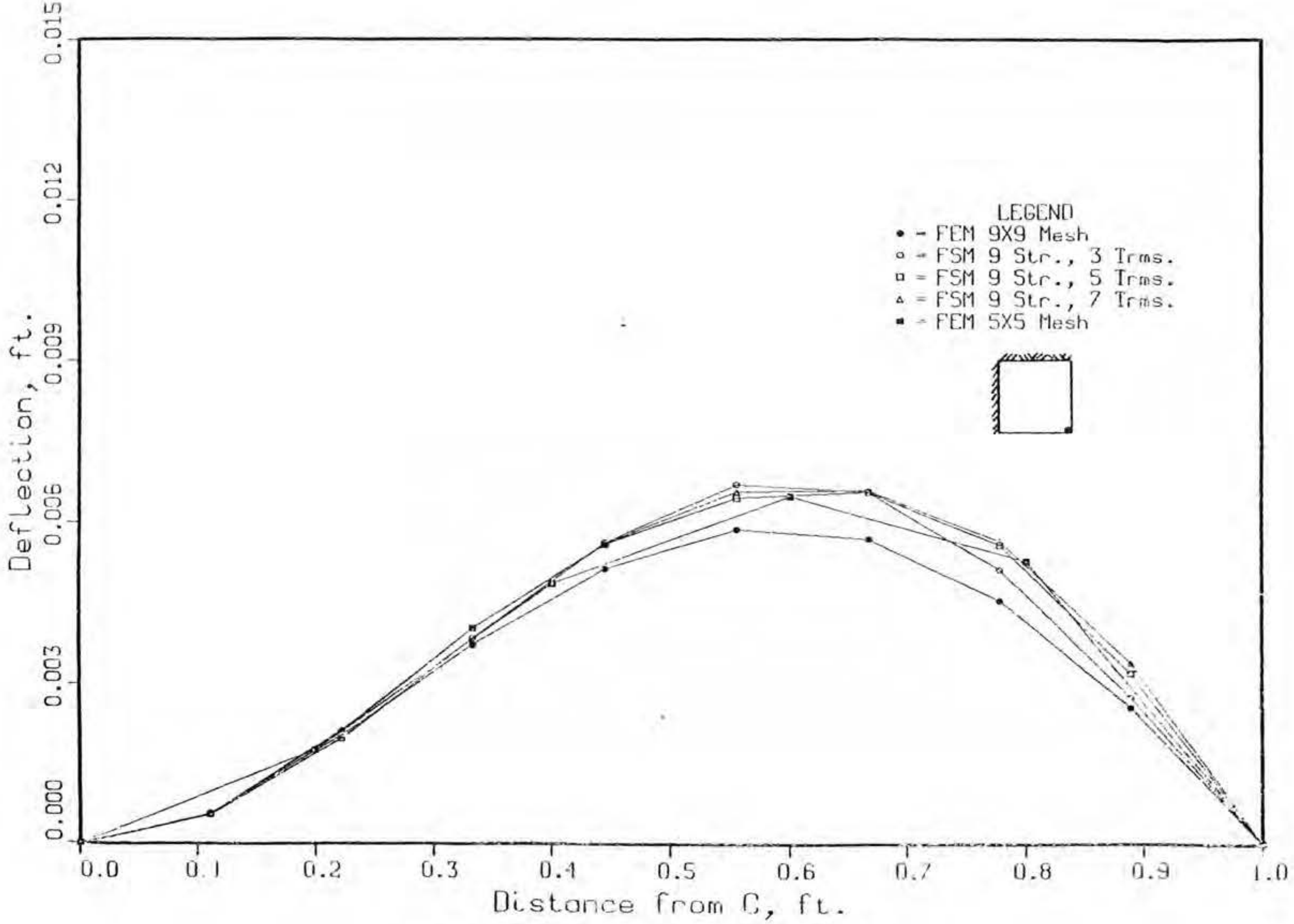

Fig. 6.9 Deflection along C-E

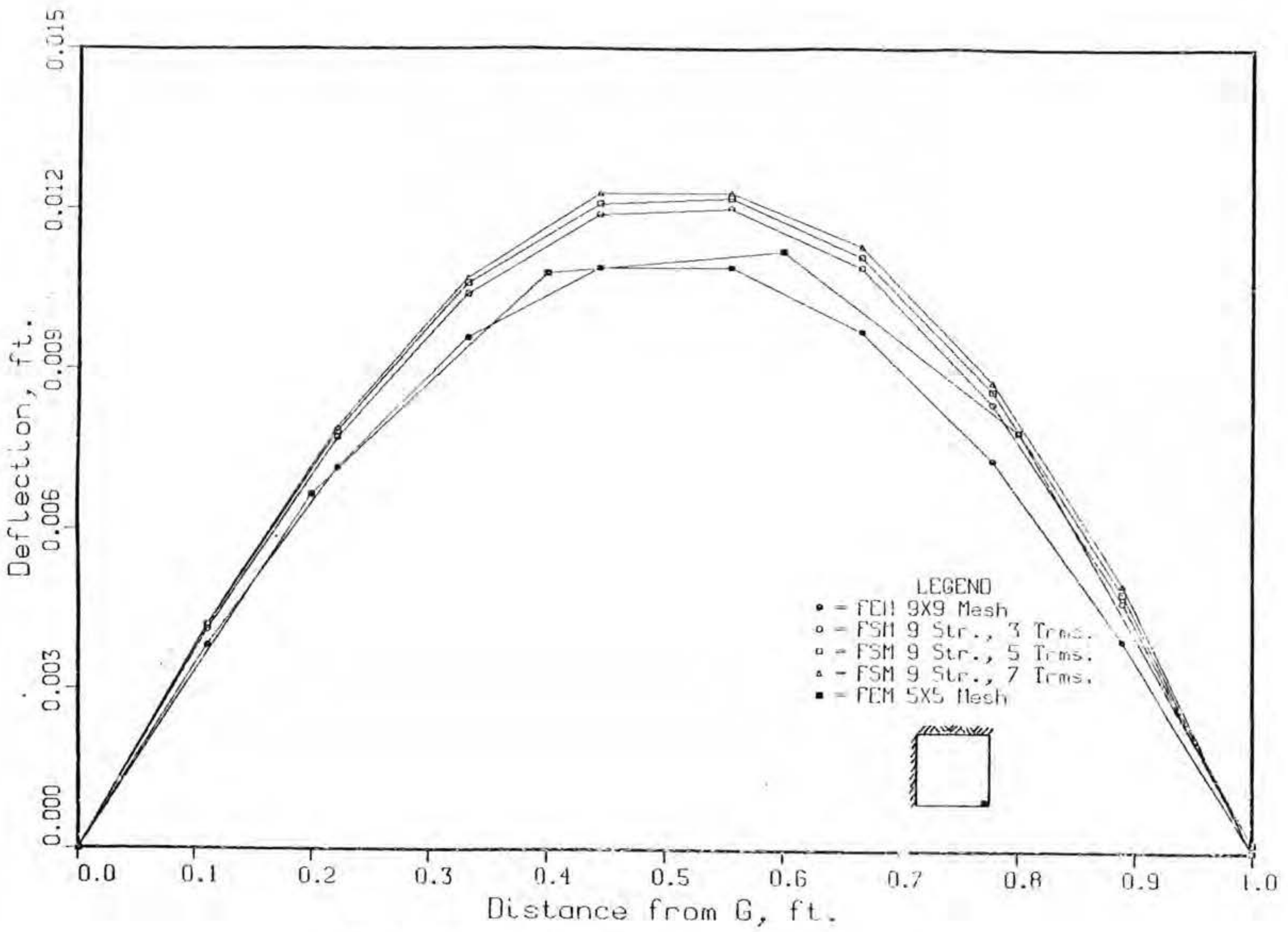

Fig. 6.10 Deflection along G-E

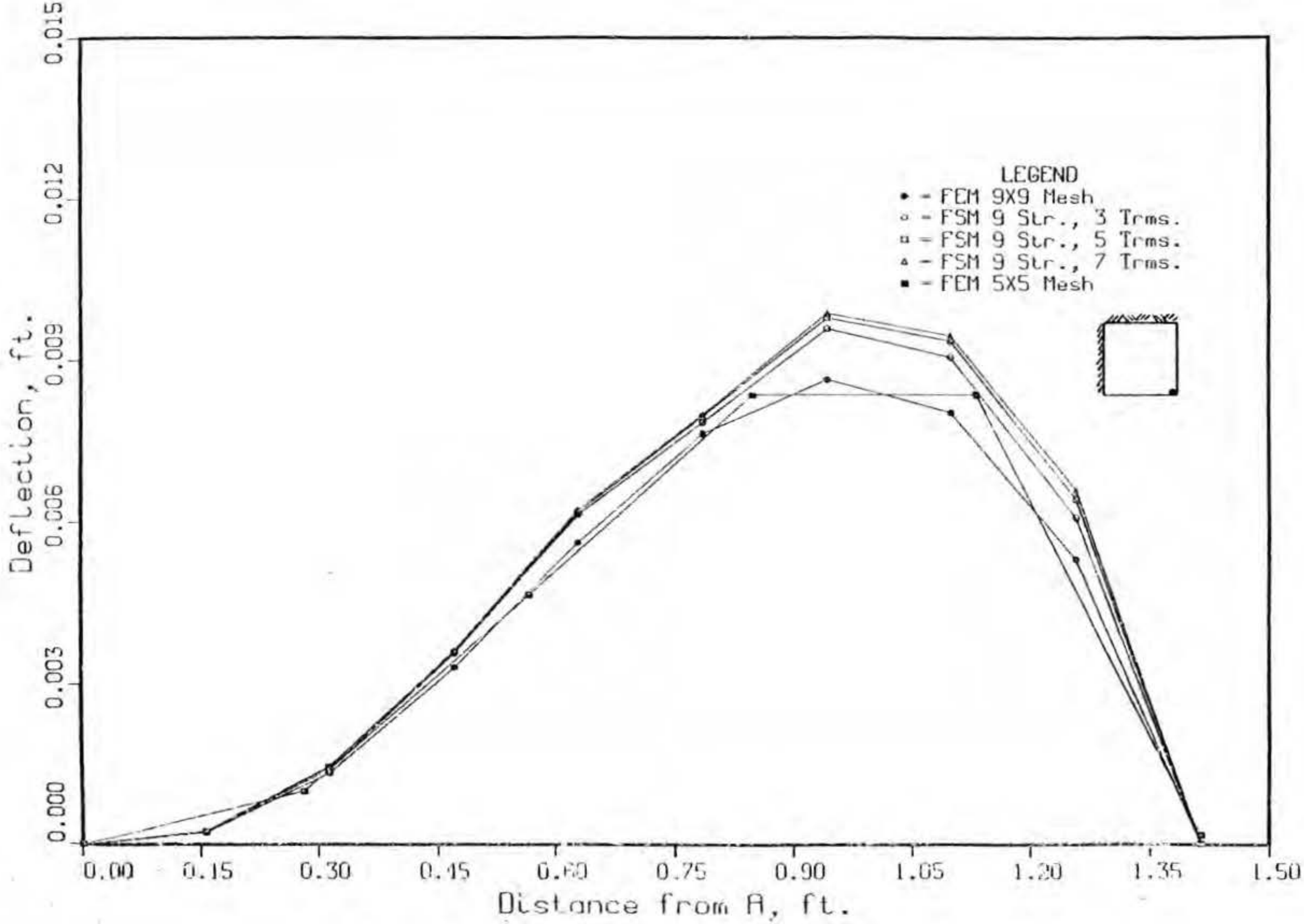

Fig. 6.11 Deflection along A-E

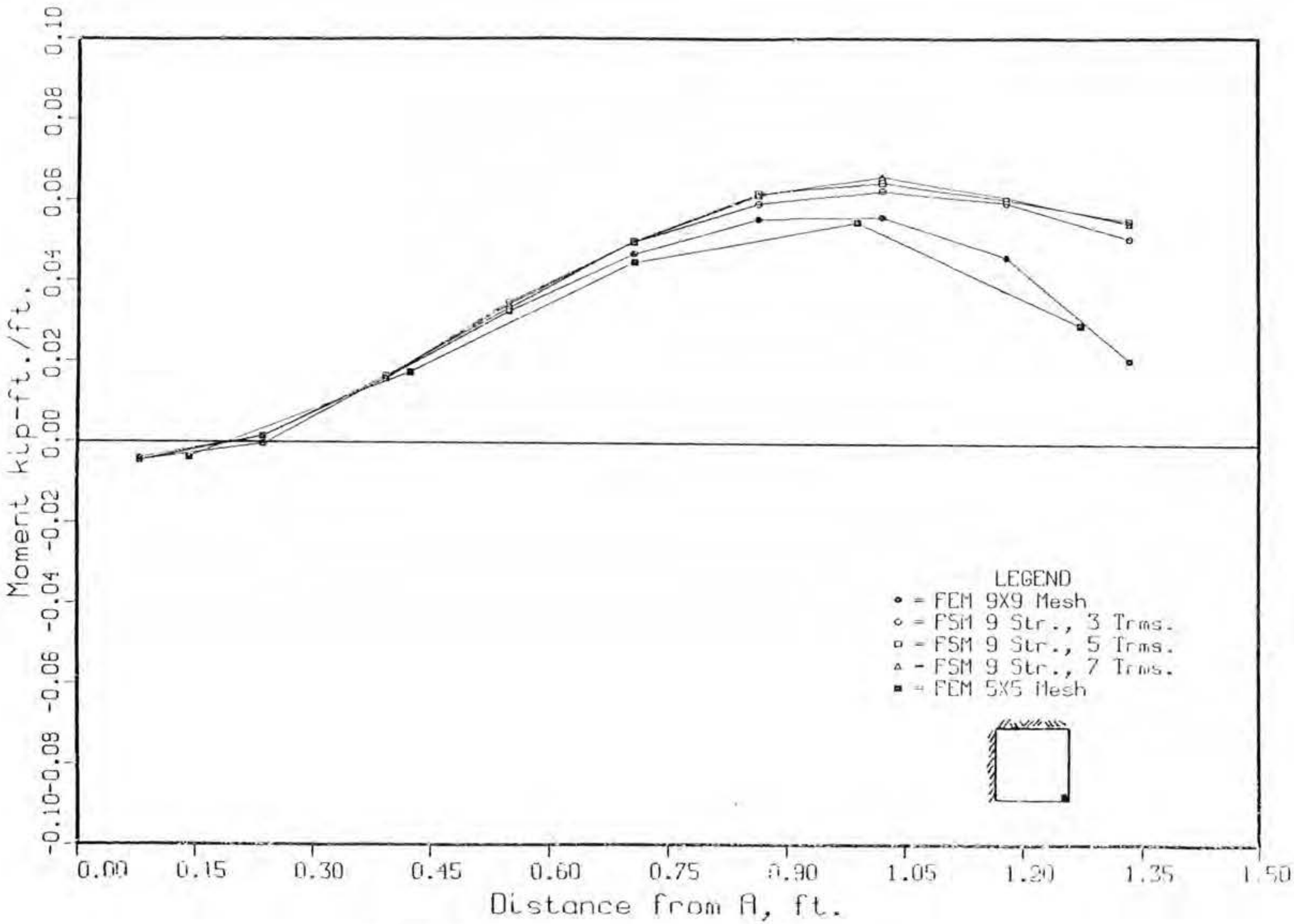

Fig. 6.12 Moment-X along A-E

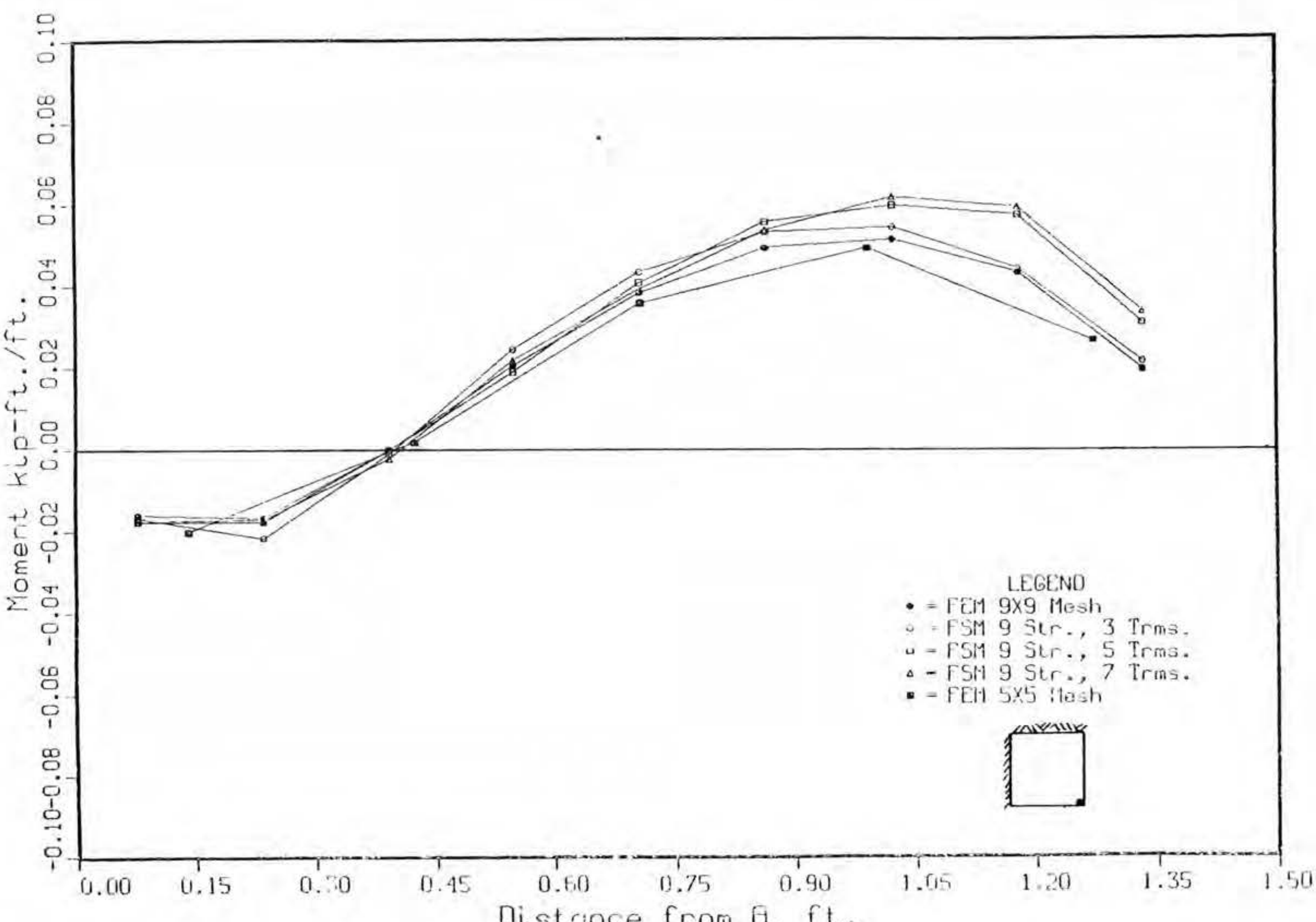

Fig. 6.13 Moment-Y along A-E

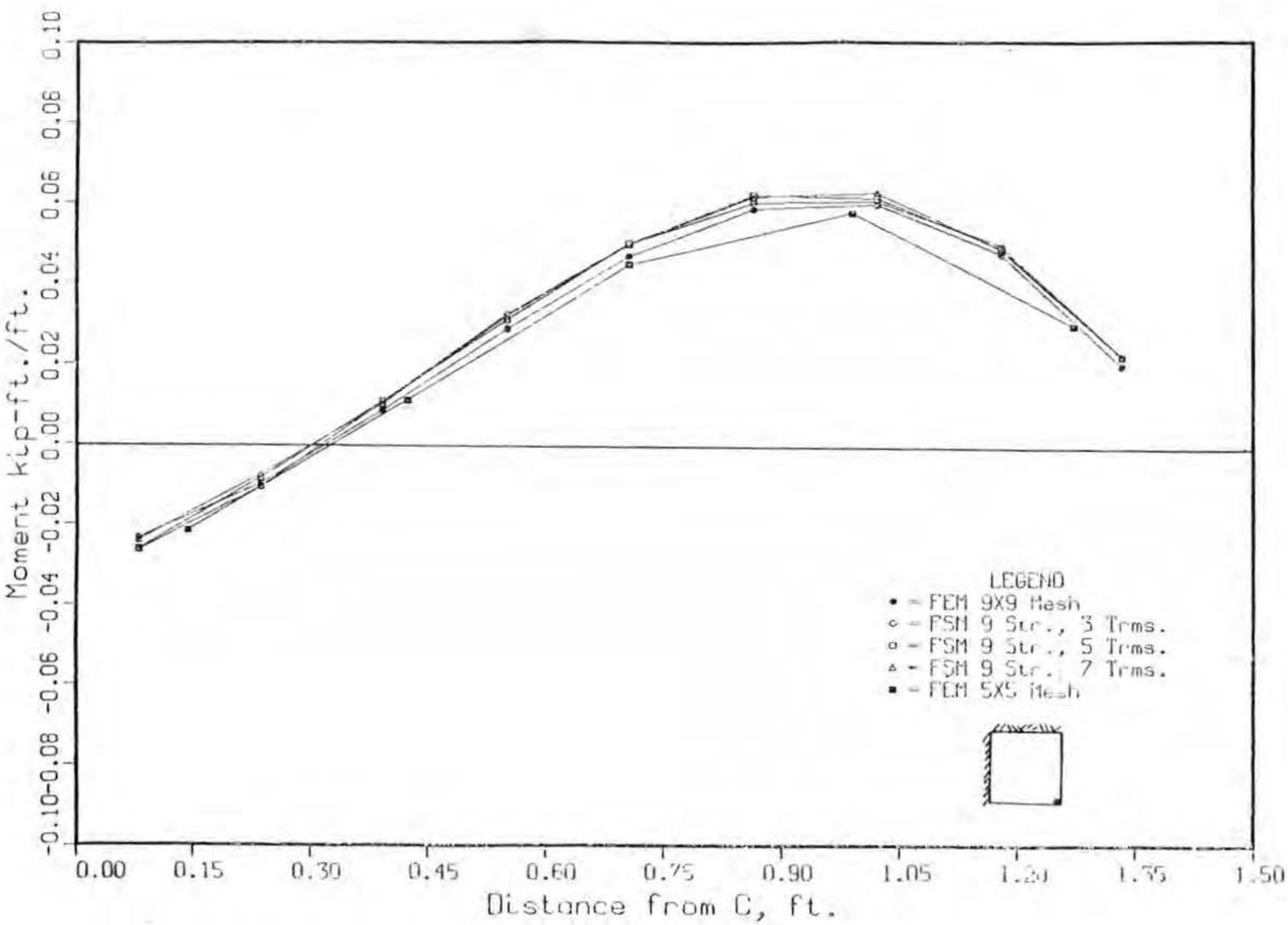

Fig. 6.14 Moment along C-G

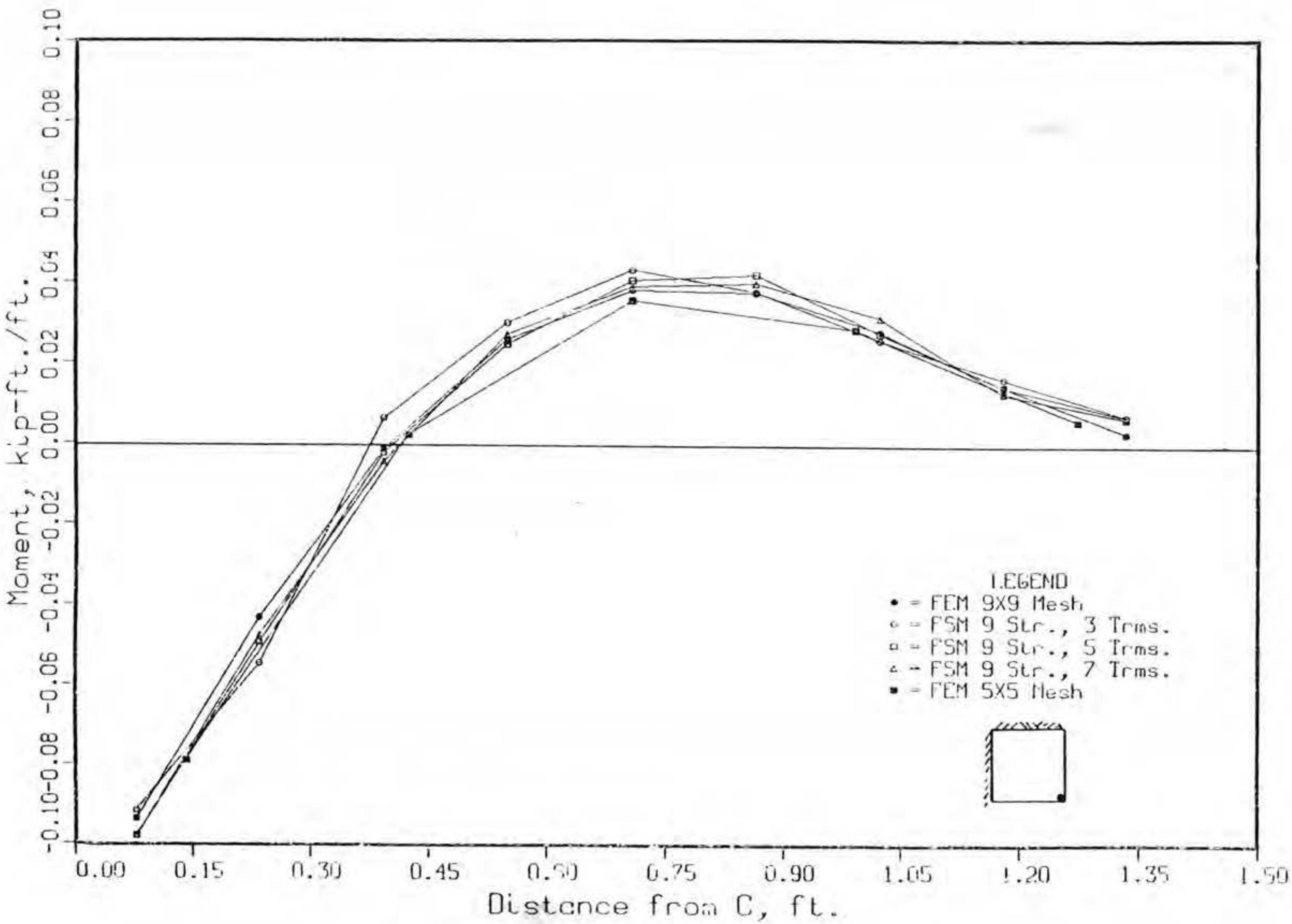

Fig. 6.15 Moment-Y along C-G

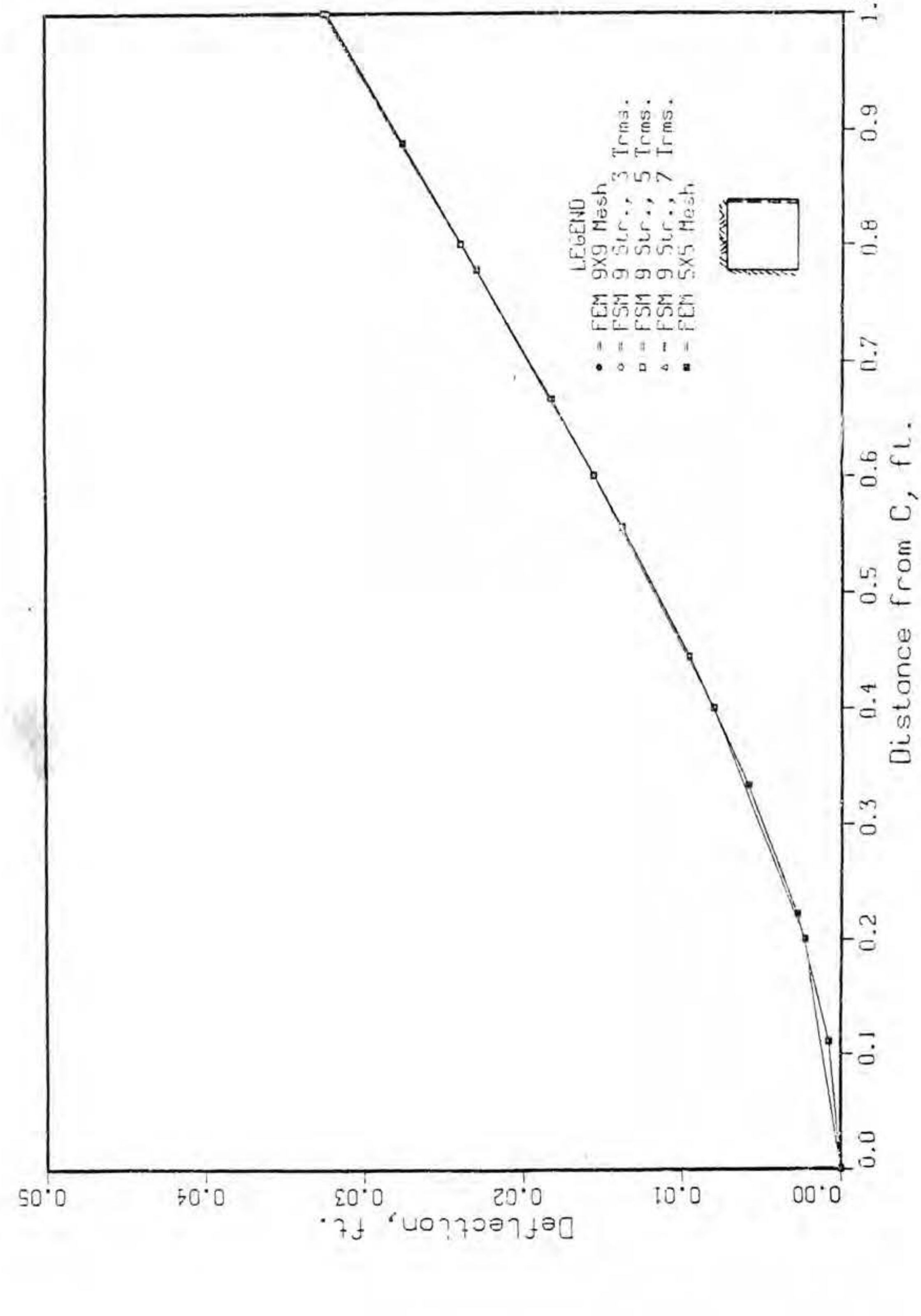

Fig. 6.16 Deflection along C-E

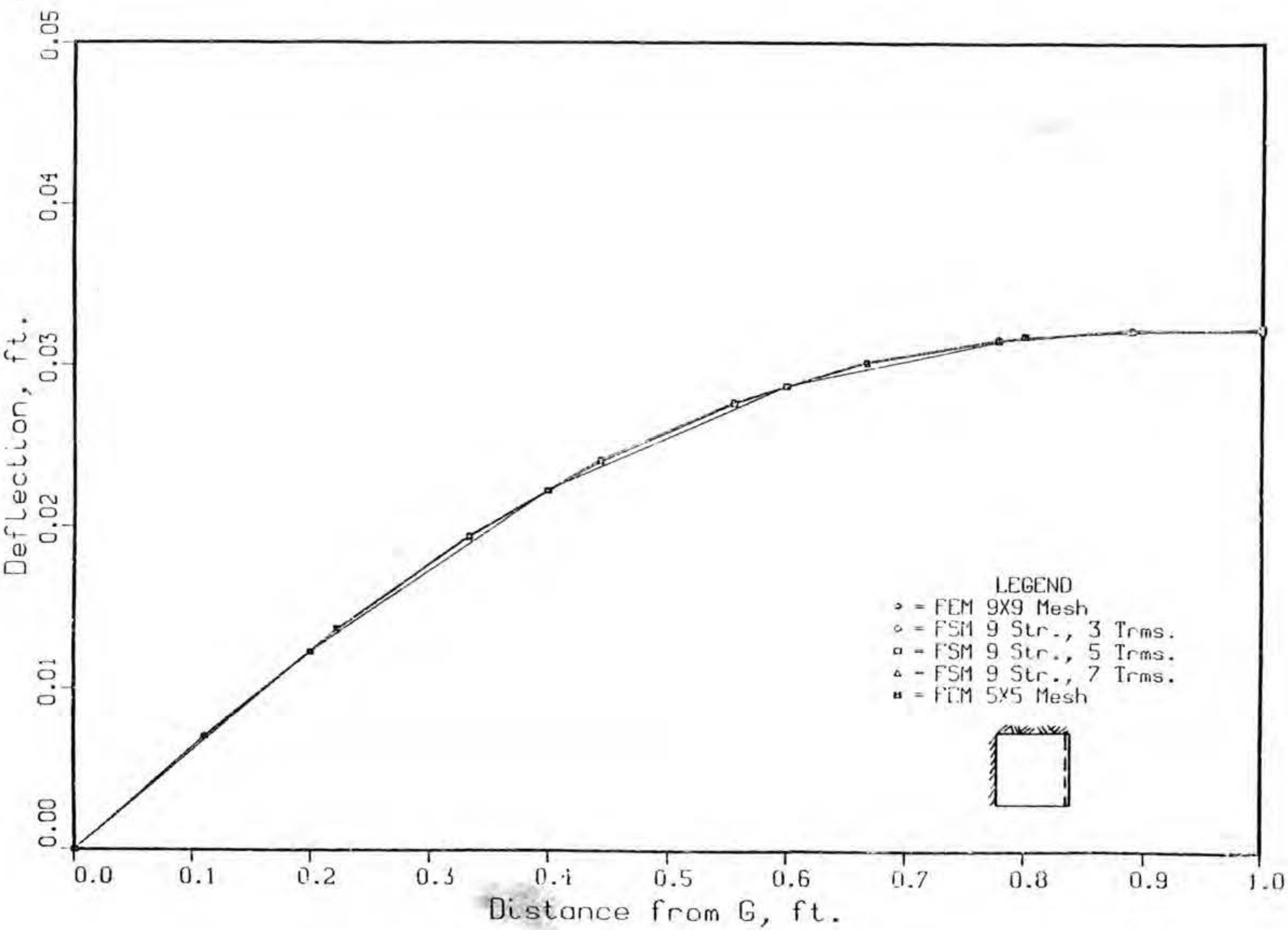

Fig. 6.17 Deflection along G-E

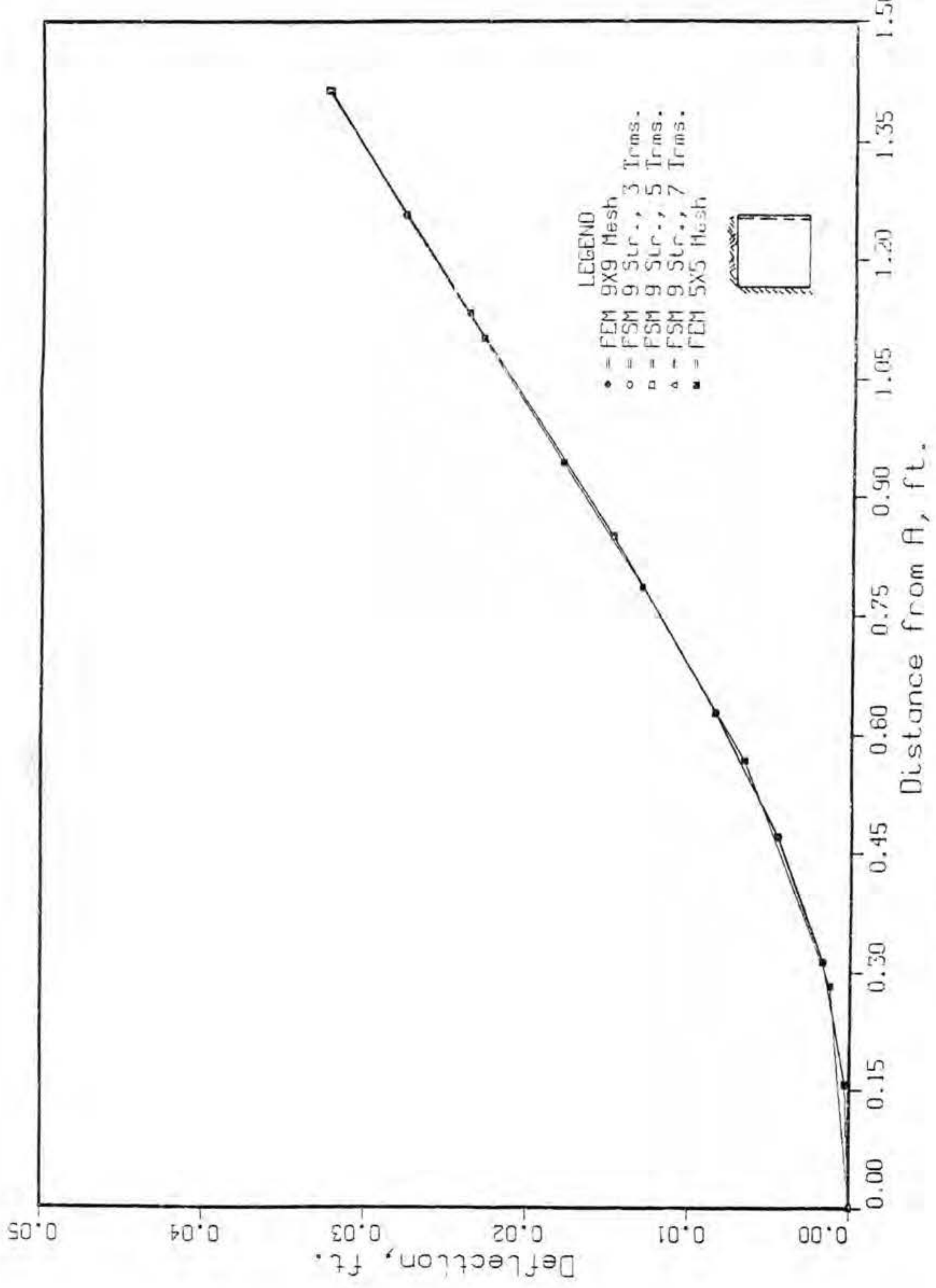

Fig. 6.18 Deflection along A-E

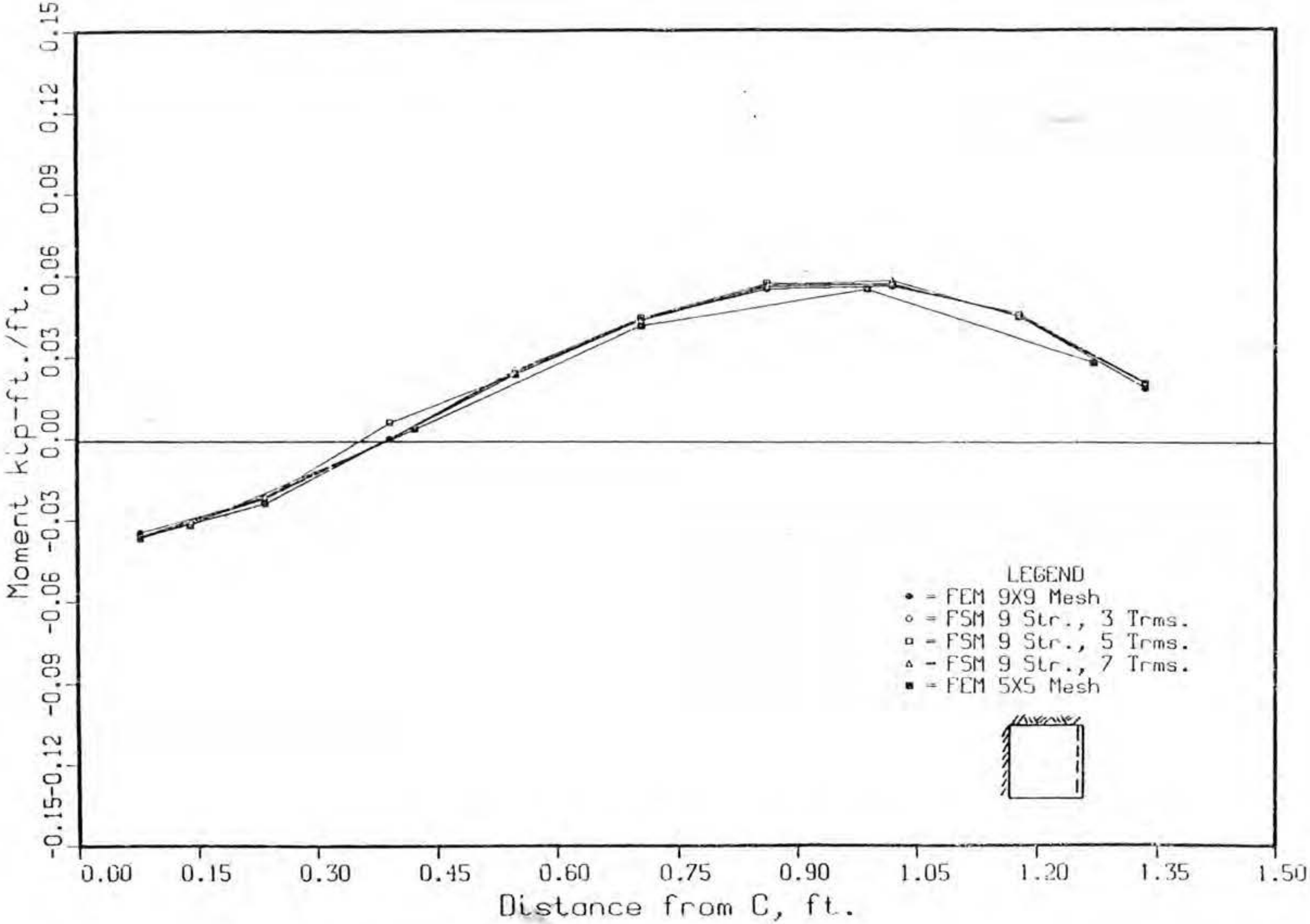

Fig. 6.19 Moment-X along G-C

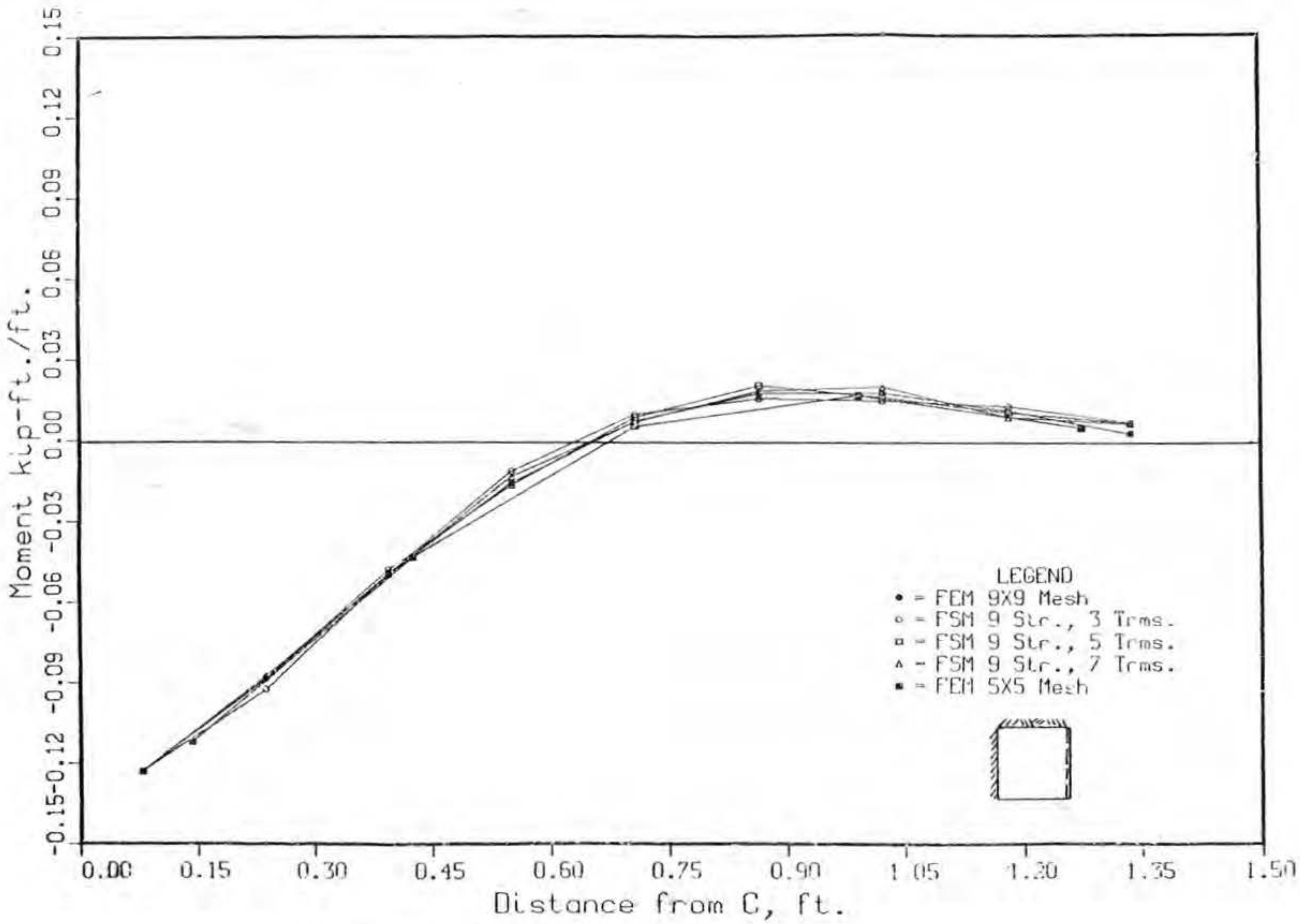

Fig. 6.20 Moment-Y along G-C

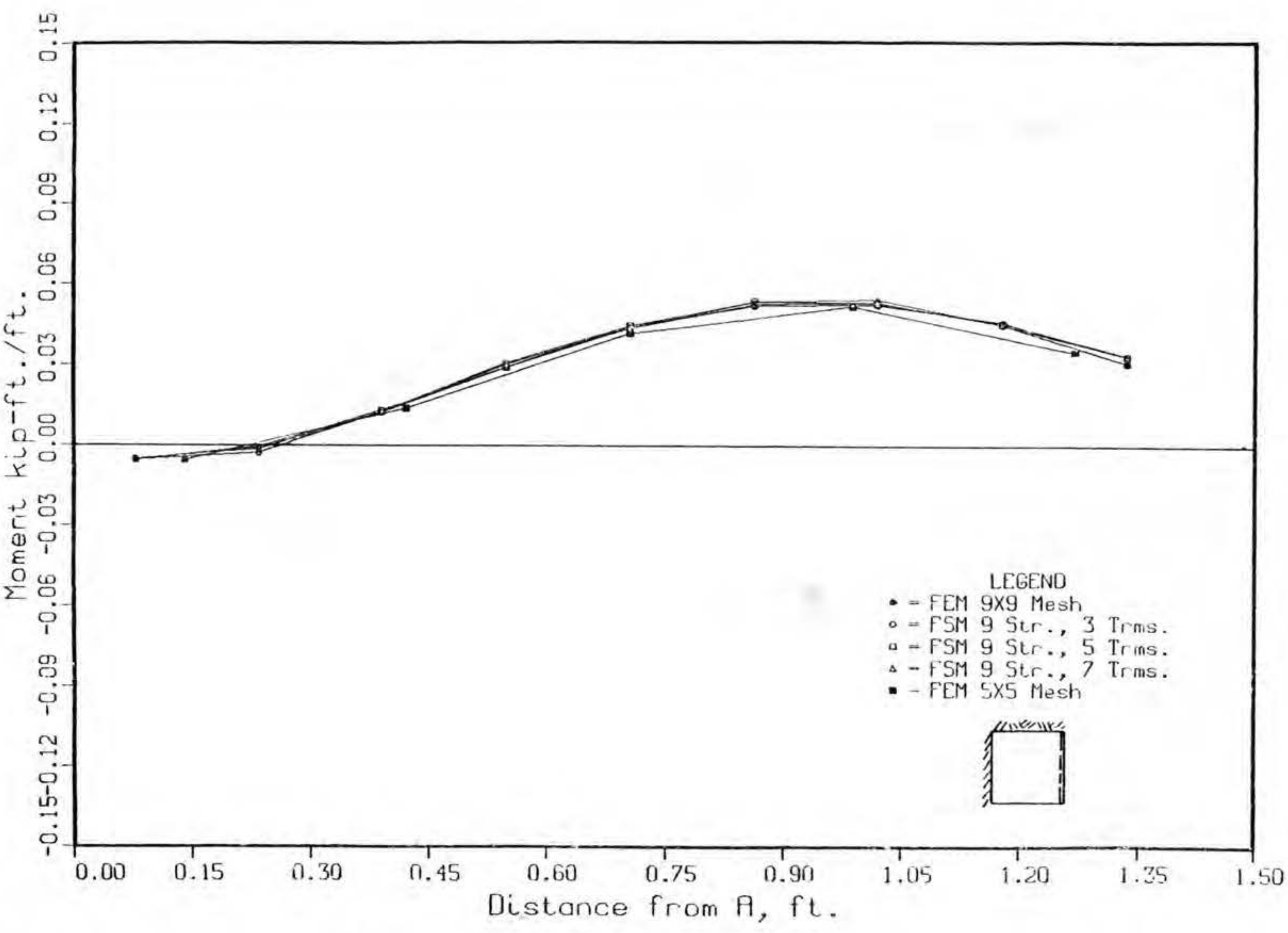

Fig. 6.21 Moment-X along A-E

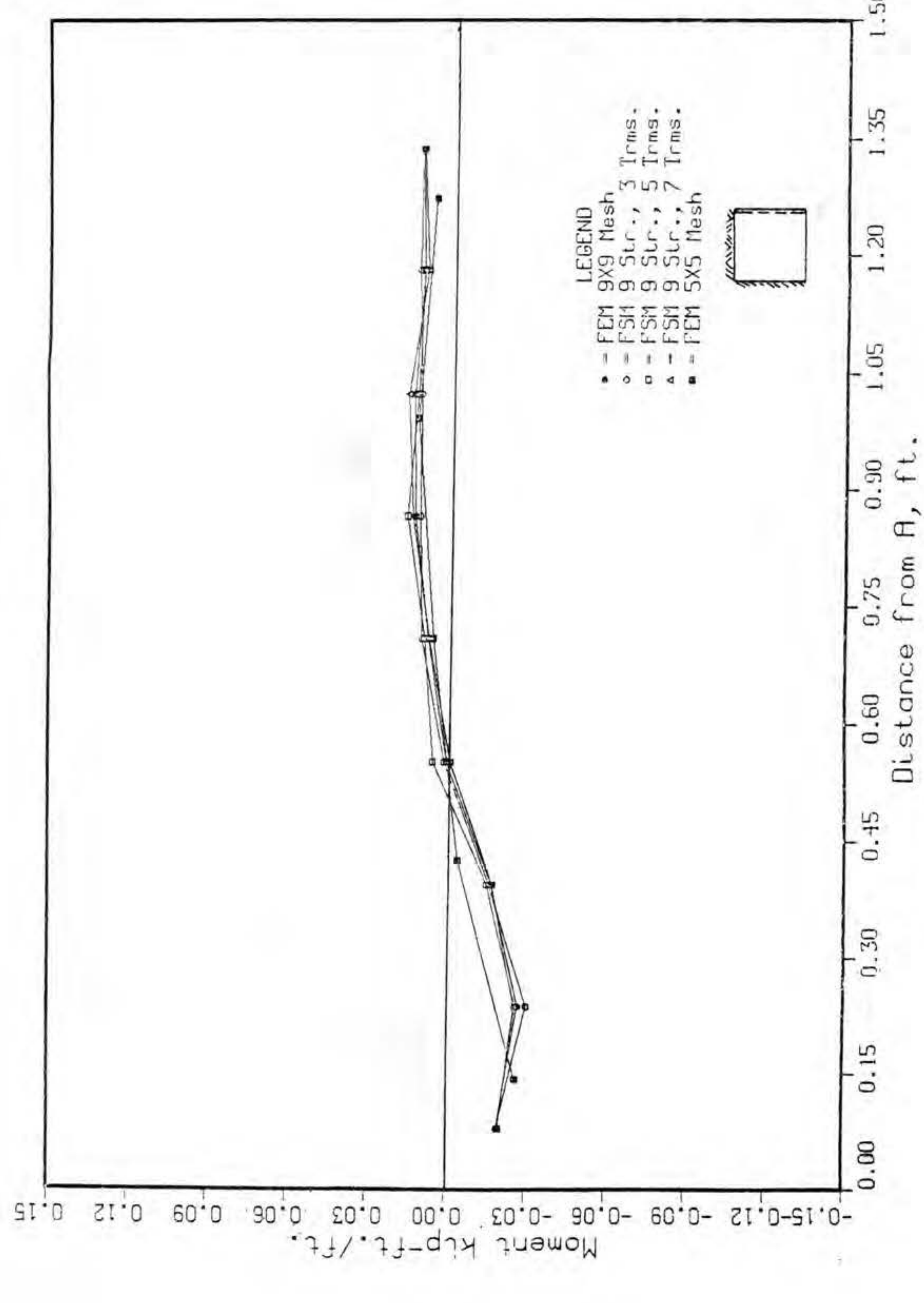

Fig. 6.22 Moment-Y along A-E

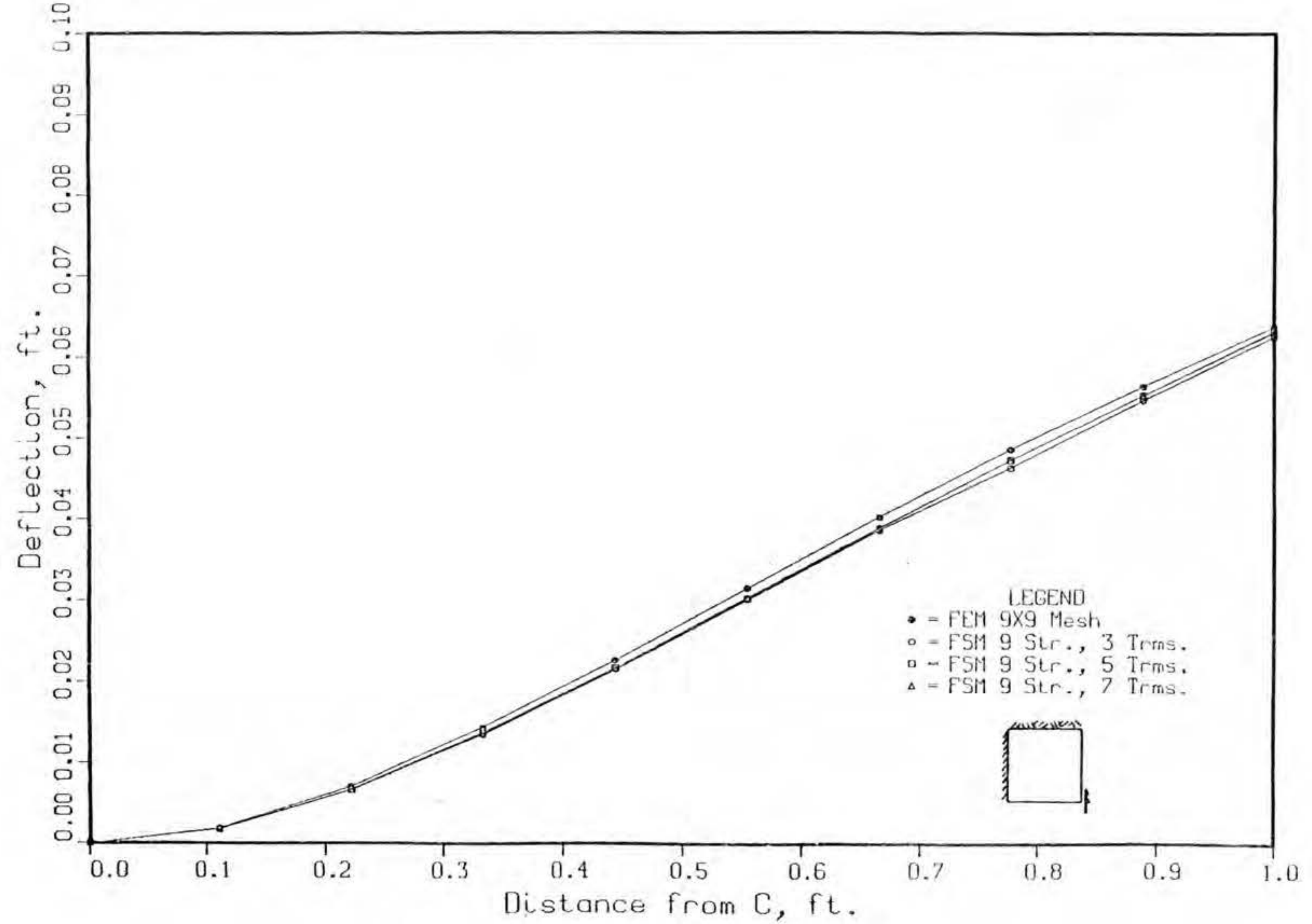

Fig. 6.23 Deflection along C-E

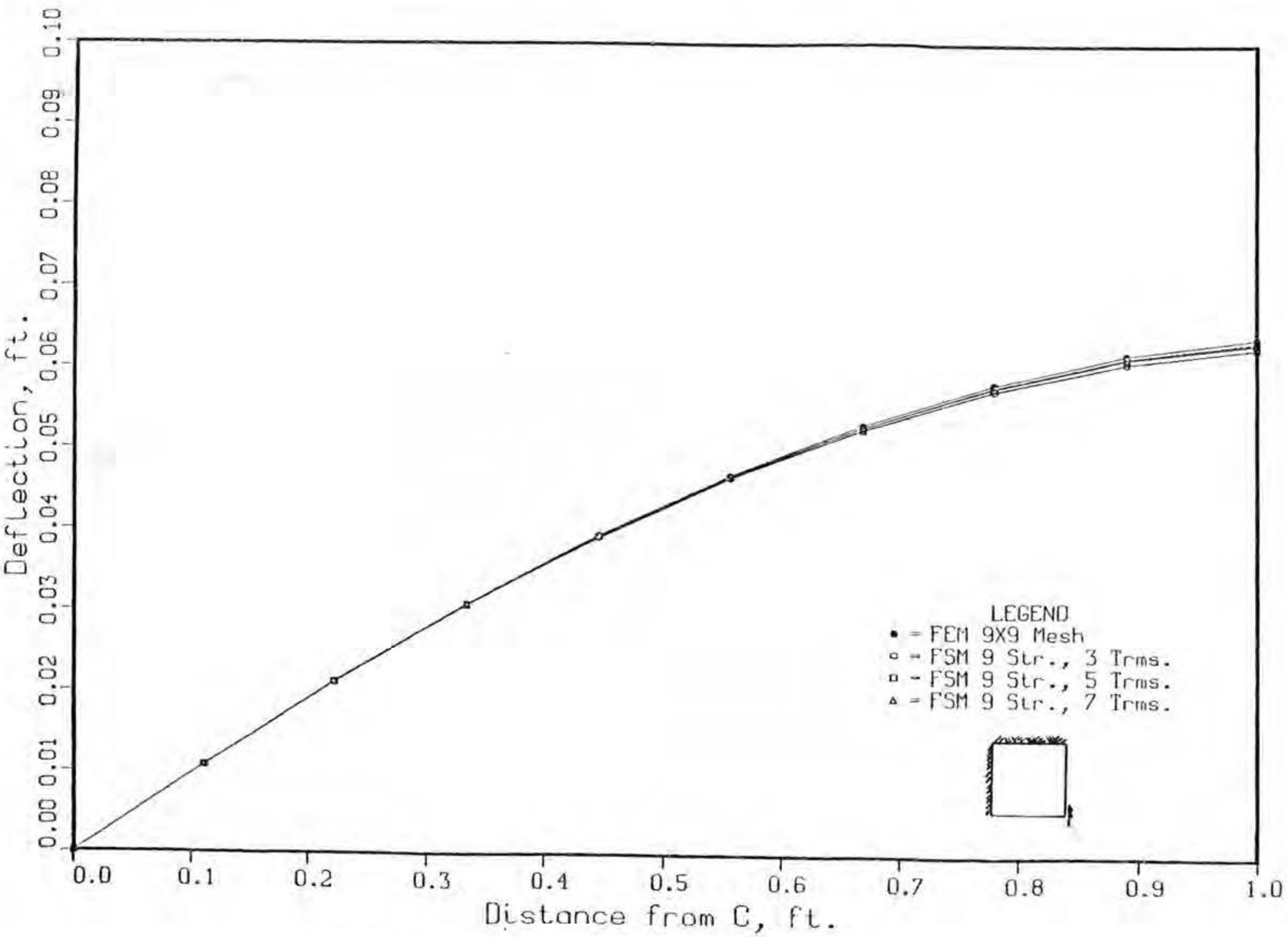

Fig. 6.24 Deflection along G-E

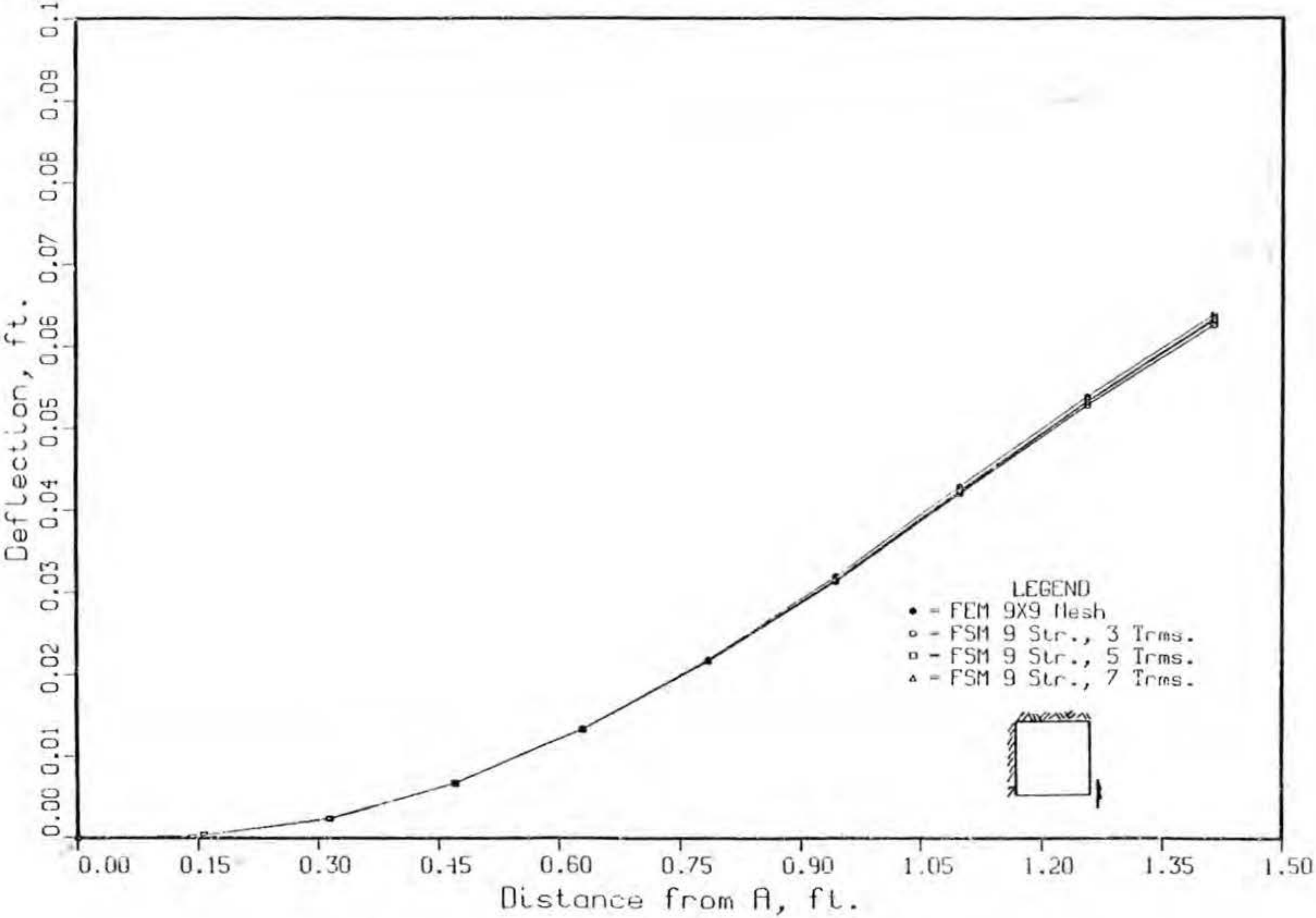

Fig. 6.25 Deflection along A-E

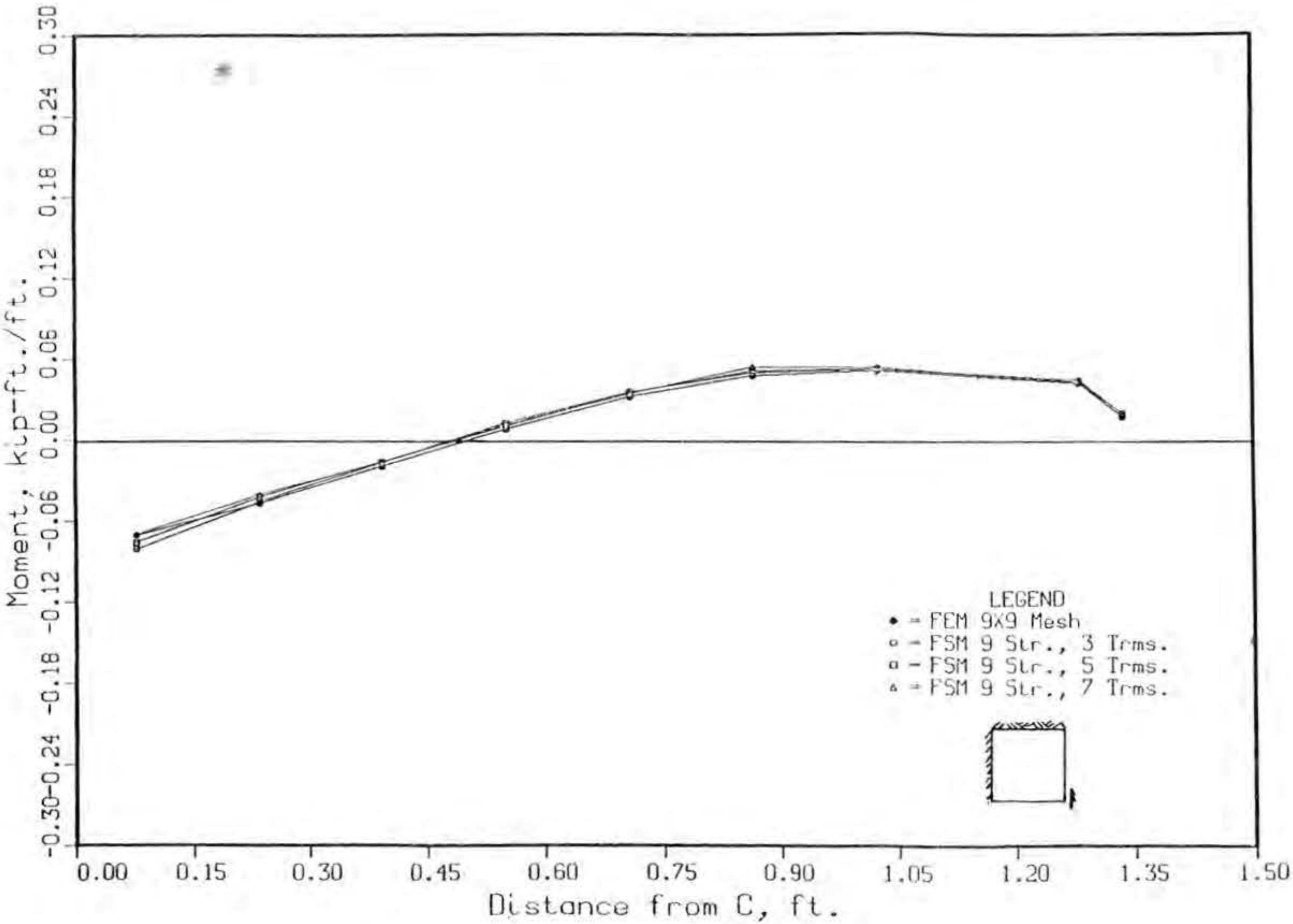

Fig. 6.26 Moment-X along C-G

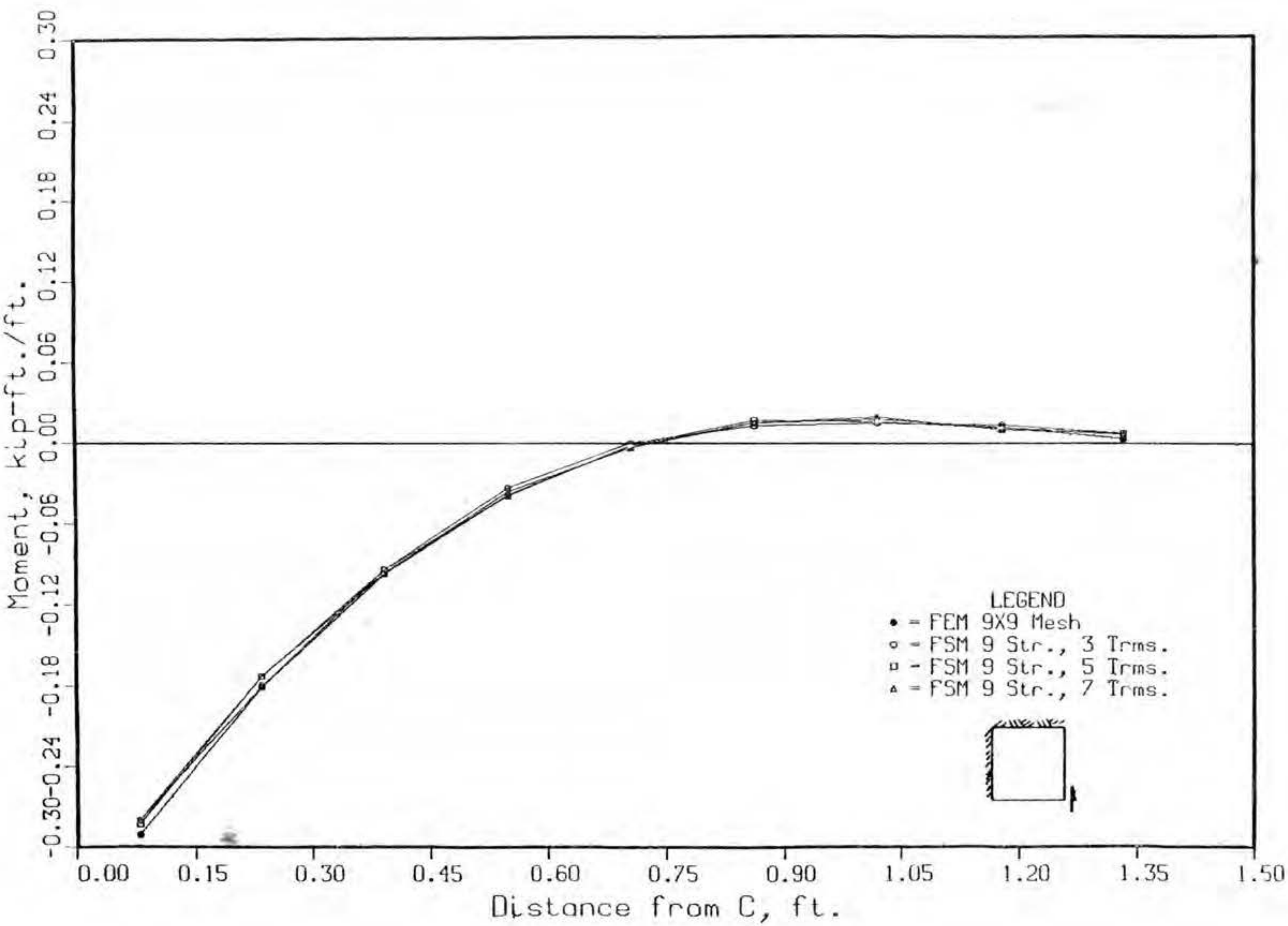

Fig. 6.27 Moment-Y along C-G

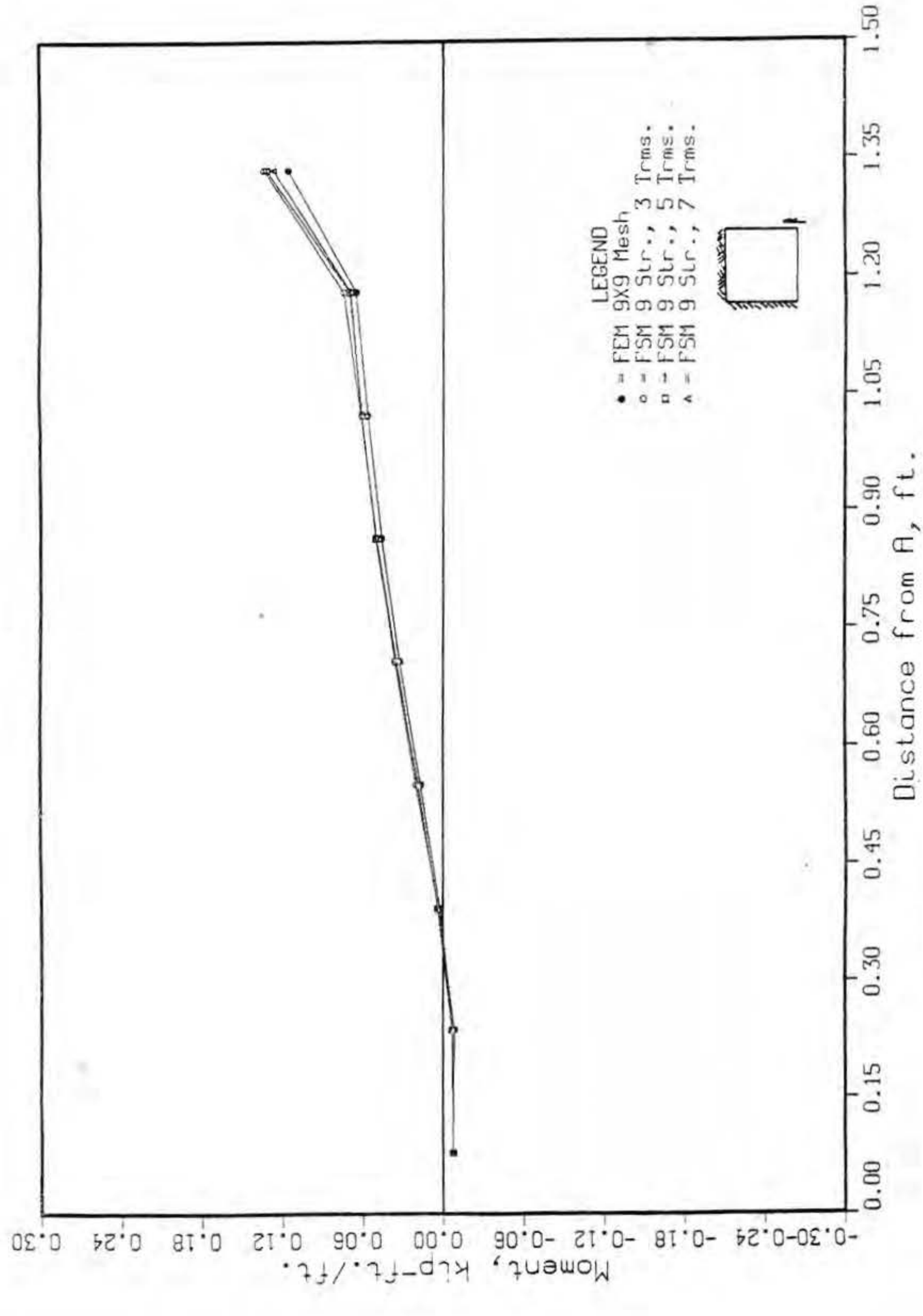

Fig. 6.28 Moment-X along A-E

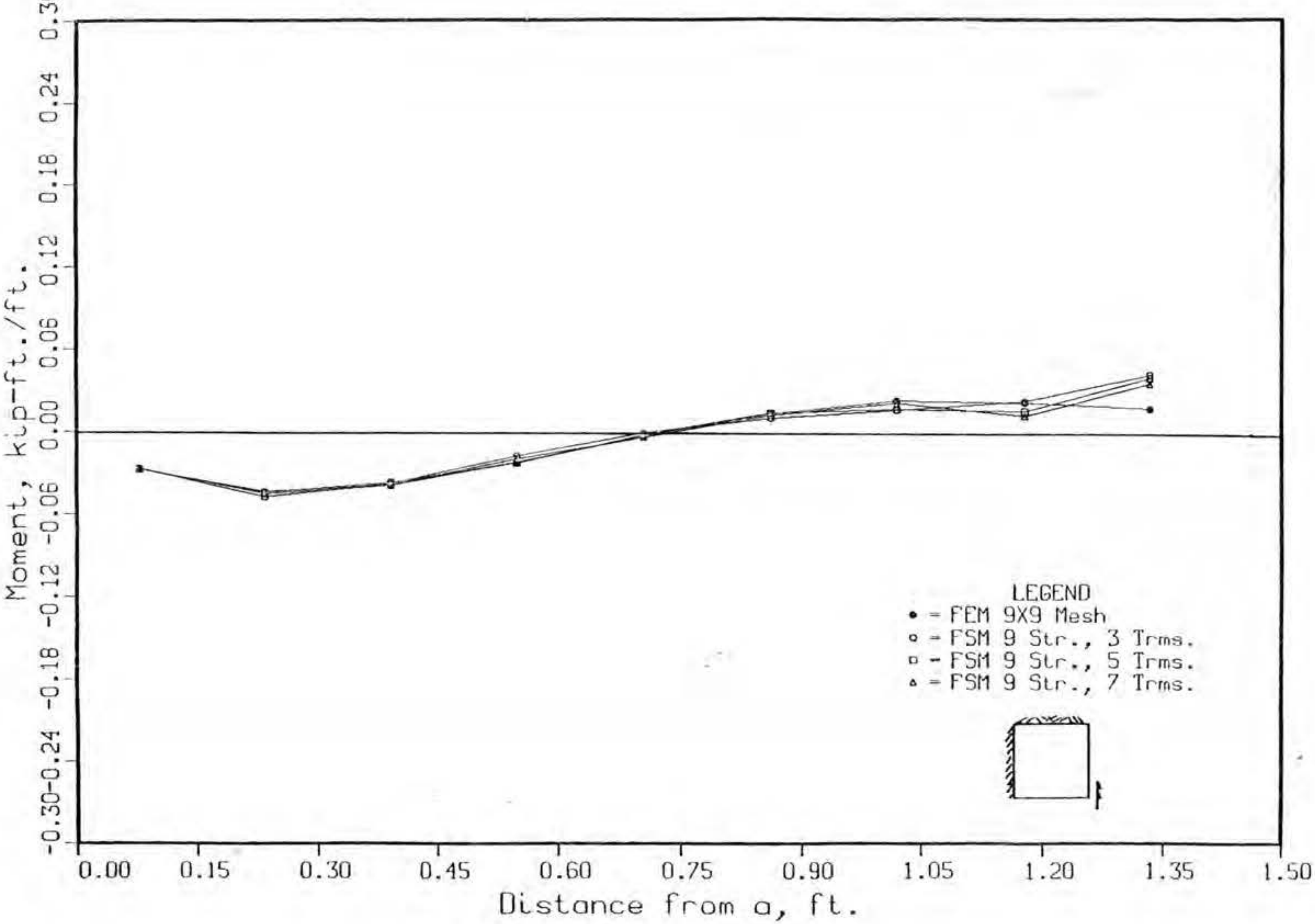

Fig. 6.29 Moment-Y along A-E

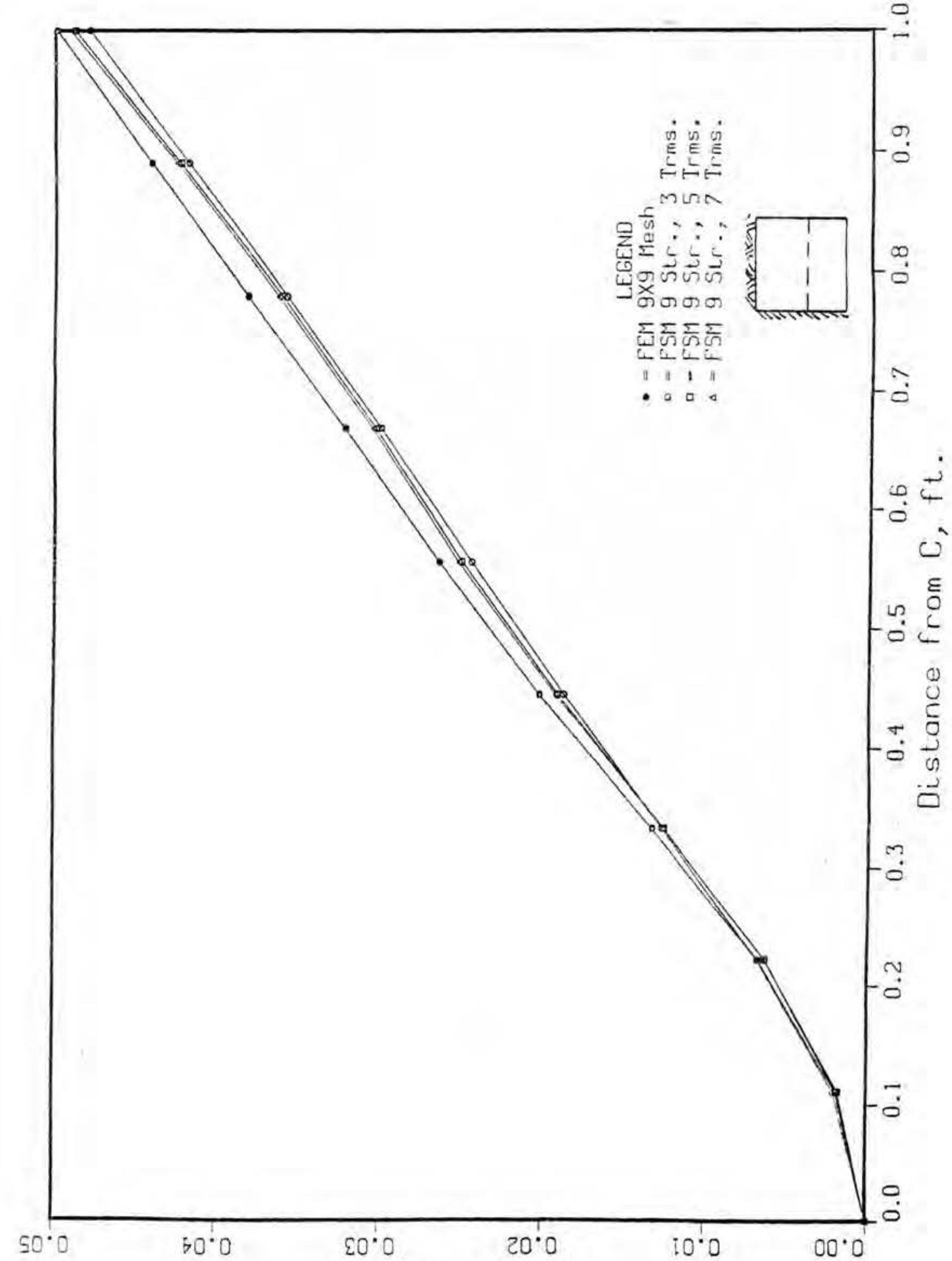

Fig. 6.30 Deflection along C-E

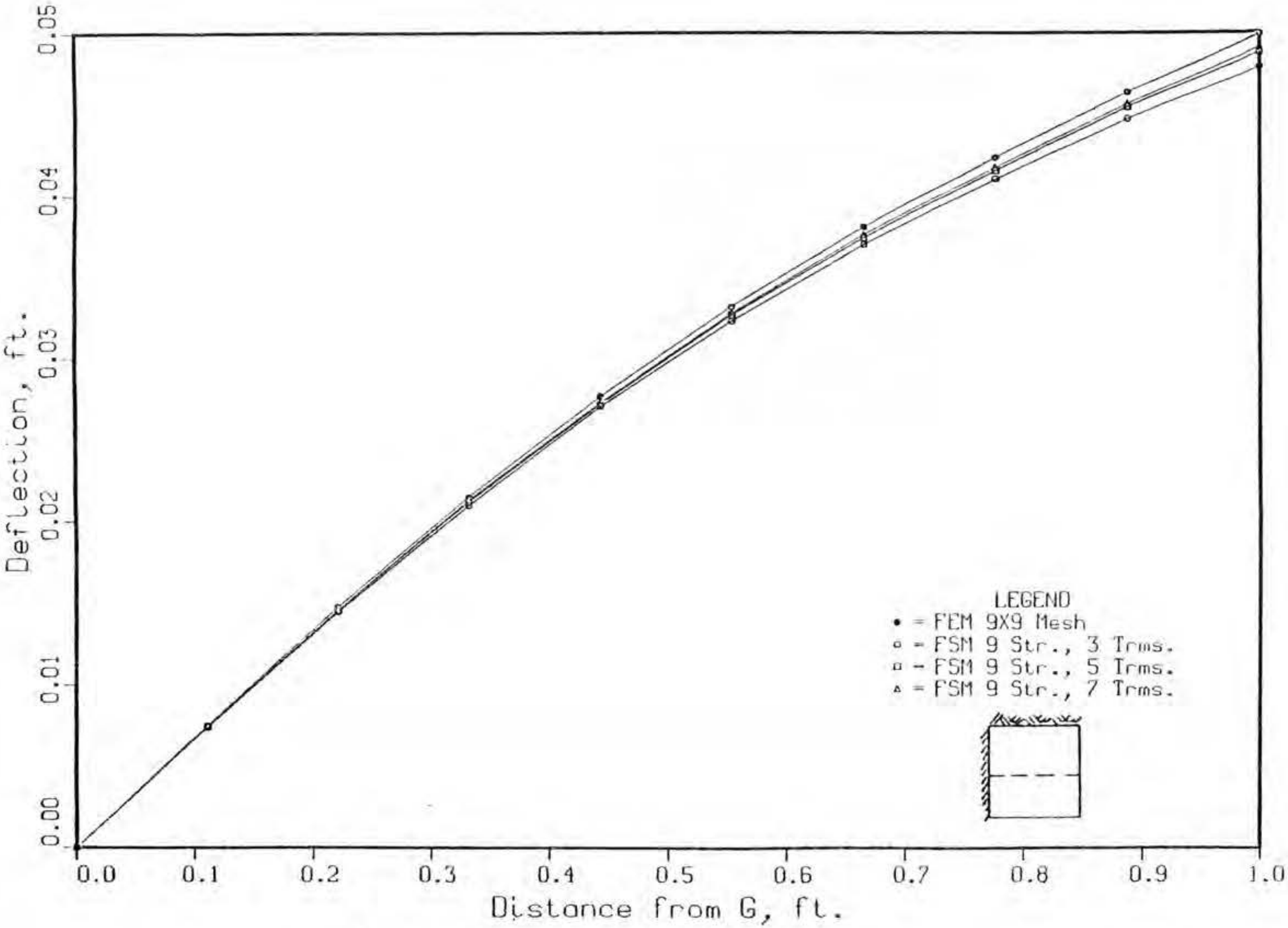

Fig. 6.31 Deflection along G-E

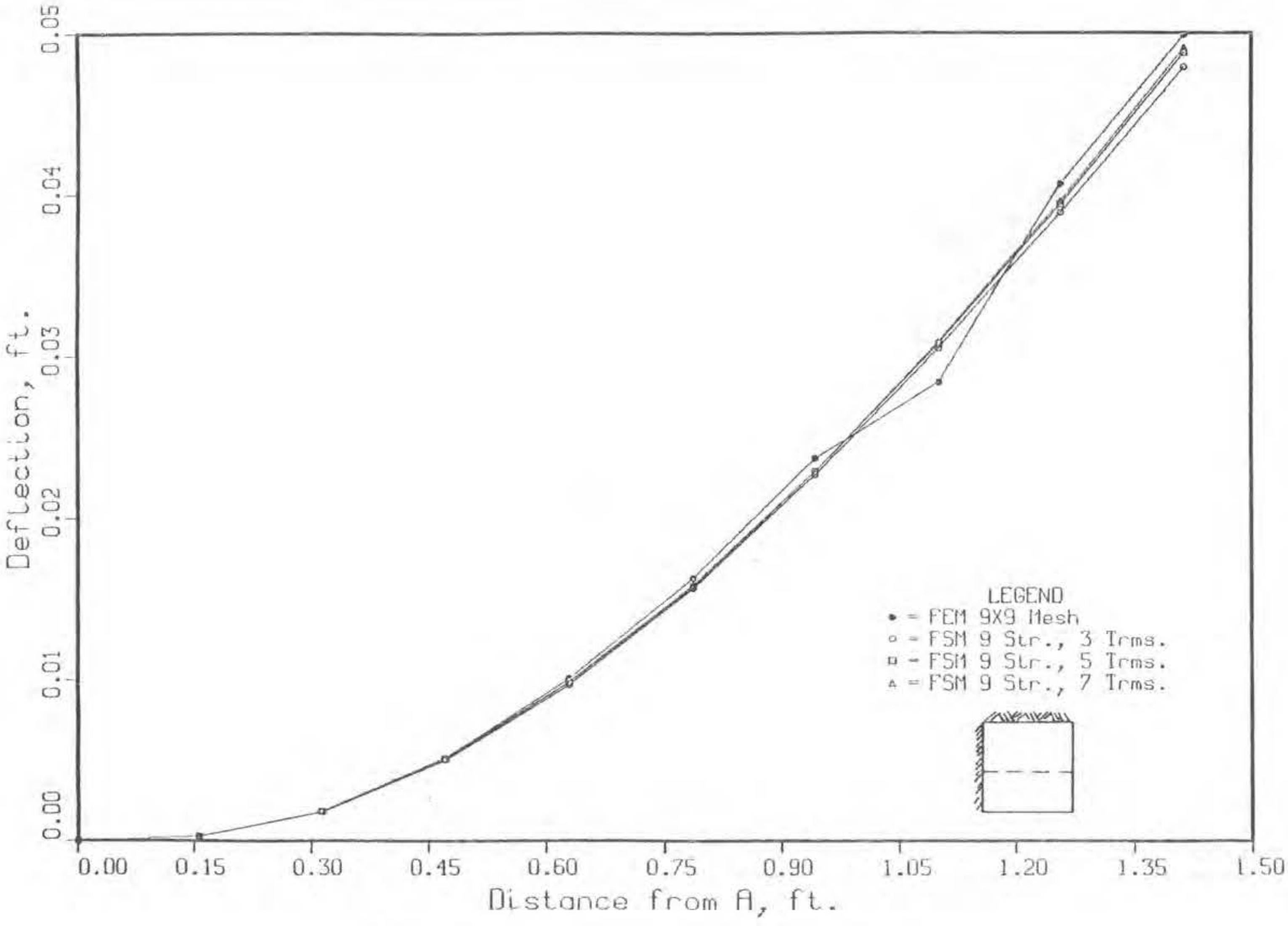

Fig. 6.32 Deflection along A-E

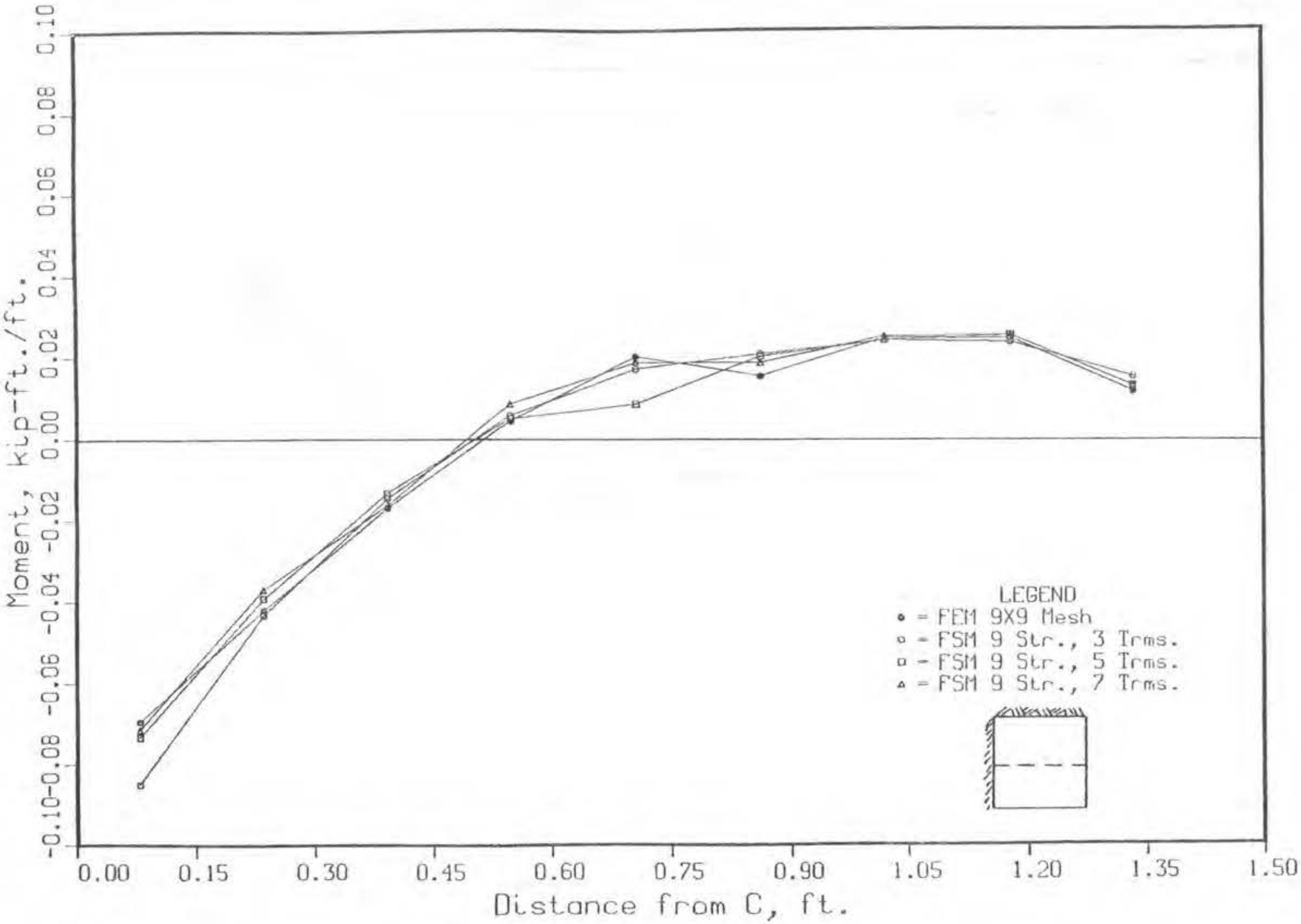

Fig. 6.33 Moment-X along C-G

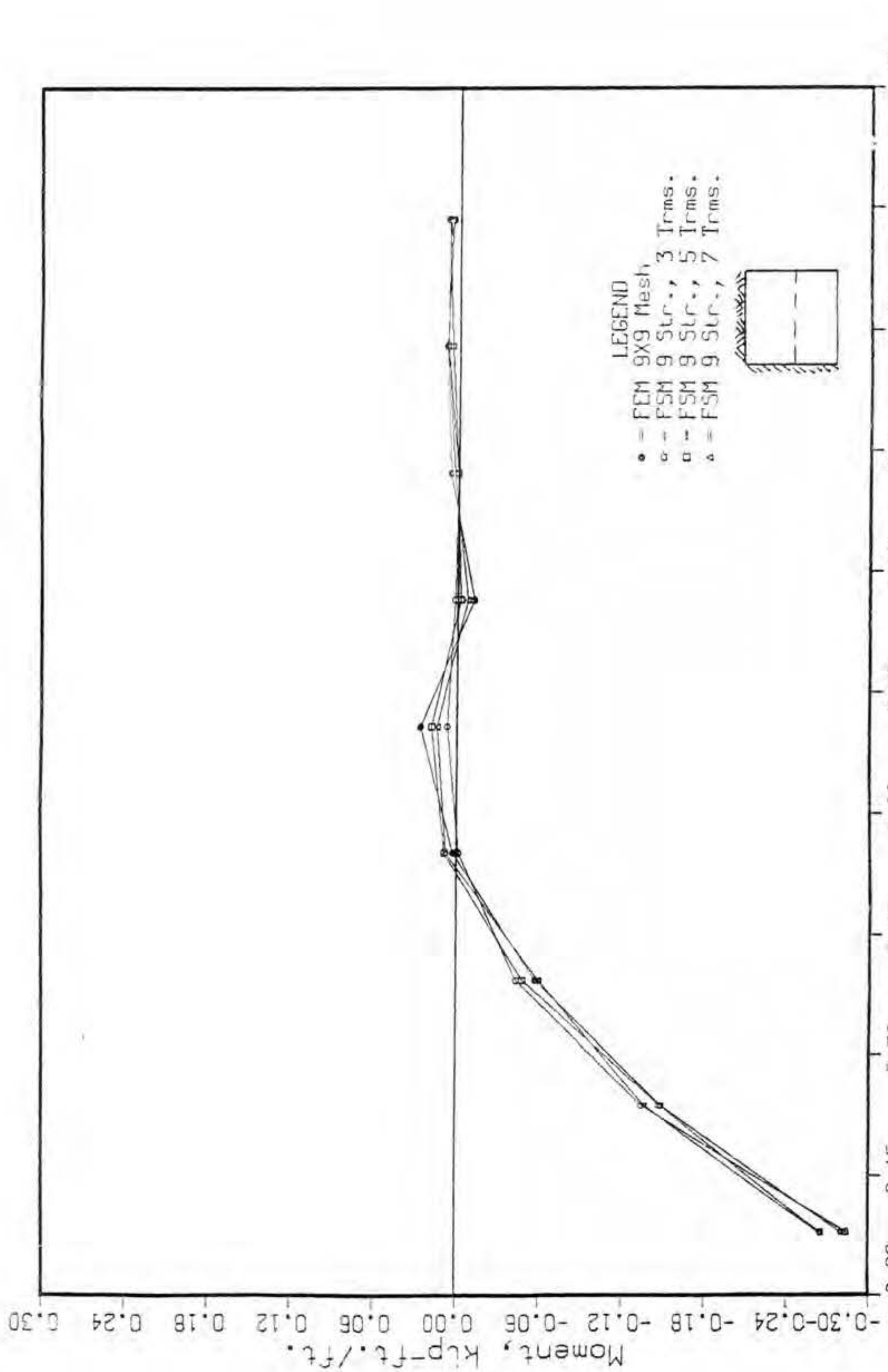

Fig. 6.34 Moment-Y along C-G

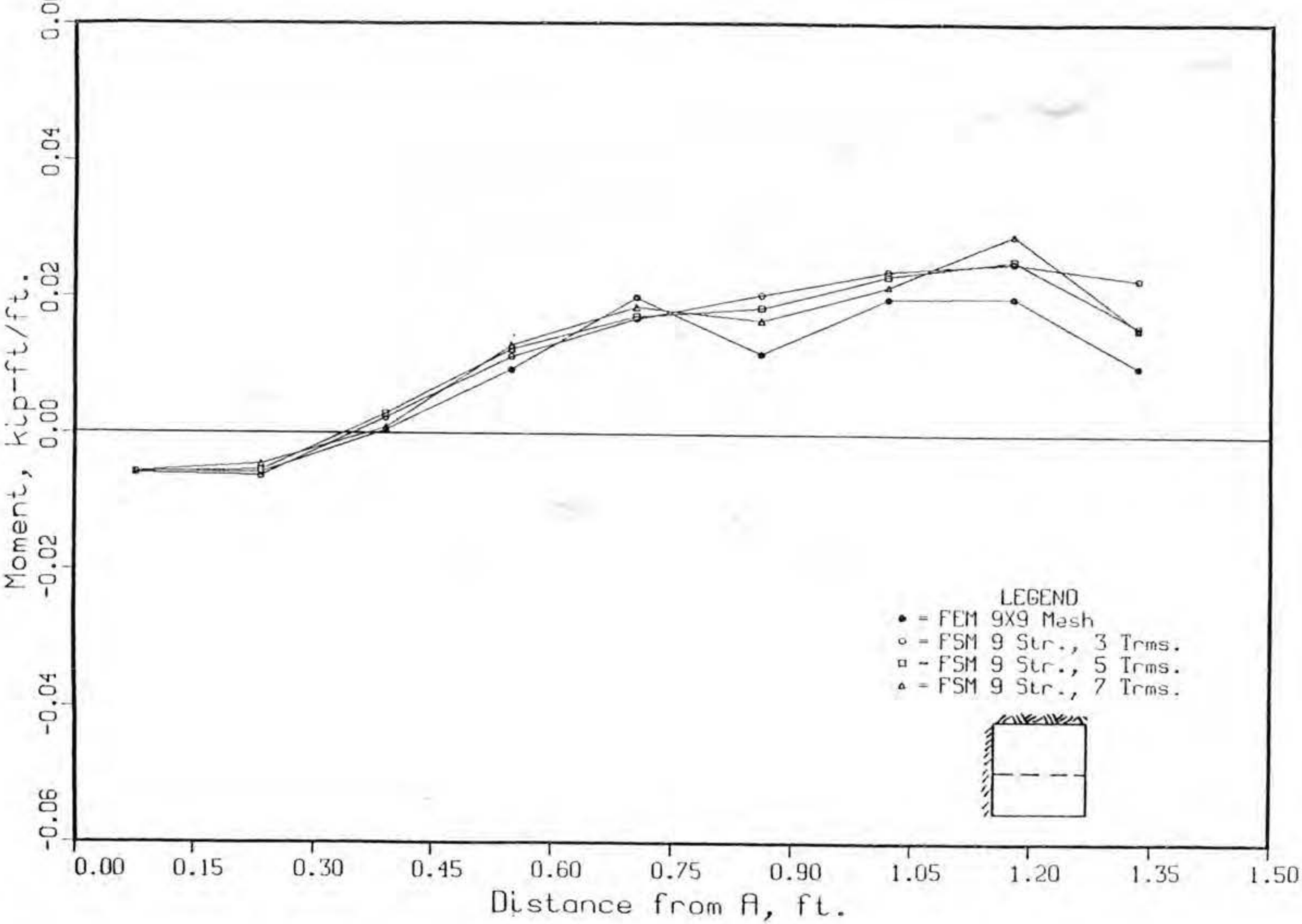

Fig. 6.35 Moment-X along A-E

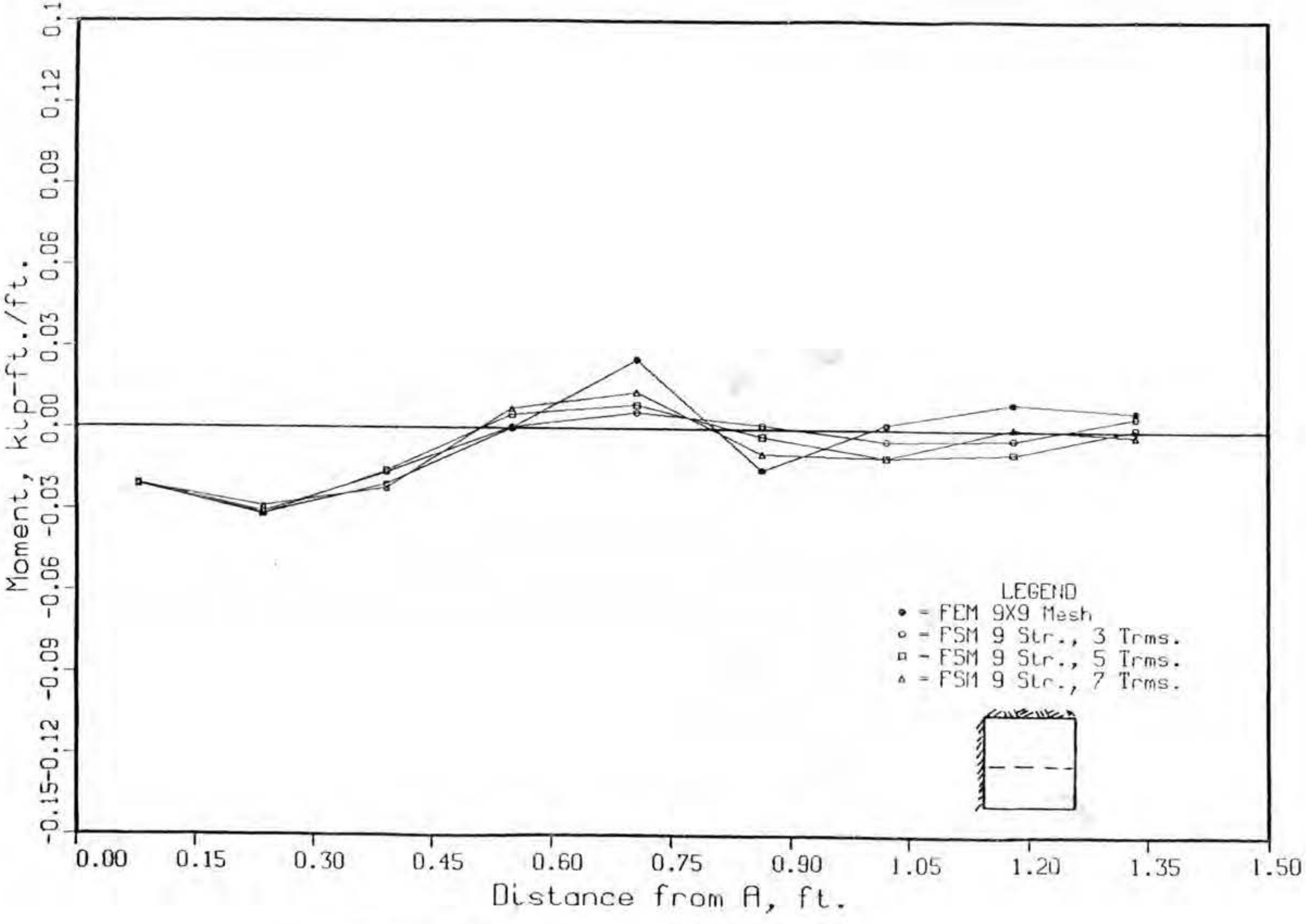

Fig. 6.36 Moment-Y along A-E

6.2.9. Comprehensive single panel example

A single panel plate which incorporated the important features of the compound strip method is shown in Figure 6.1f. The system has beams with flexural and torsional rigidities. One beam is oriented parallel and the other is transverse to the strip. A pinned column of 10000 k/ft located at the intersection of the free adjacent edges. The deflections are given in Figures 6.37-6.39 and the moments are given in Figures 6.40 and 6.41. The FSM and FEM compared favorably for deflection and moment with the different in the maximums of less than three percent.

6.3. Continuous Plate System

The application of compound strip model to a multipanel plate system is illustrated with the analysis of the system shown in Figure 6.42. This plate was first analyzed by Maugh and Pan (40) using a flexibility approach to invoke compatibility along the edge of each plate. Later Gutkowski (16,17) studied this system and used it to compare the FEM with his finite panel method (FPM) and the rigorous solution given by Maugh and Pan. The system is composed of fifteen pinned supported panels with varying aspect ratios. The entire system is uniformly loaded thus symmetry techniques have been employed. Two mesh layouts were used and are shown in Figure 6.43. Note, a quarter of the plate was modeled. Three strip models were used and are shown in Figure 6.44.

Deflection along A-A, B-B, and C-C and moments along B-B and C-C are reported giving a representative overview of the systems' behavior and equitable comparison of the methods. The deflections are given in Figures 6.45-6.47. The strip models compared quite well with the 10 x

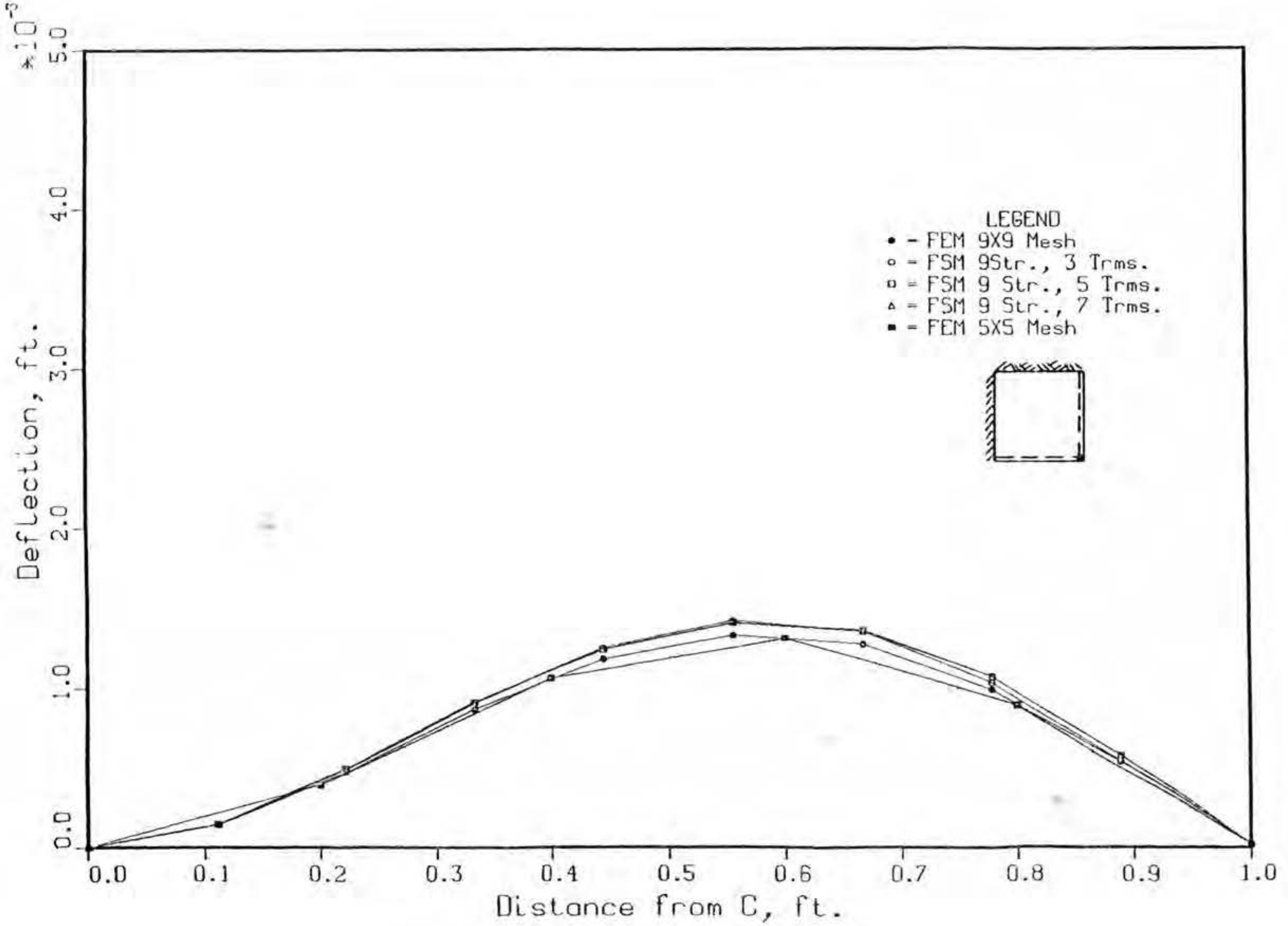

Fig. 6.37 Deflection along C-E

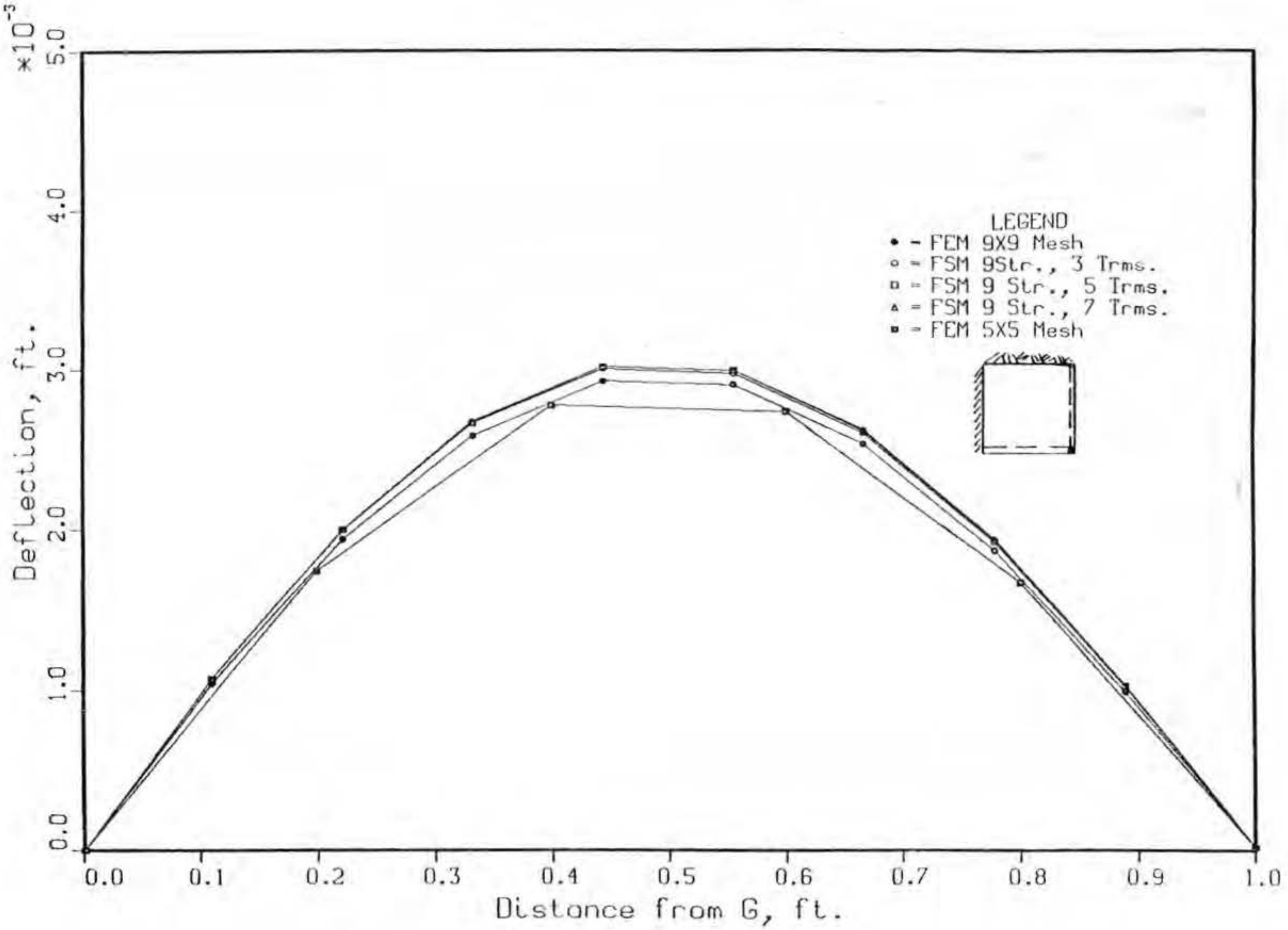

Fig. 6.38 Deflection along G-E

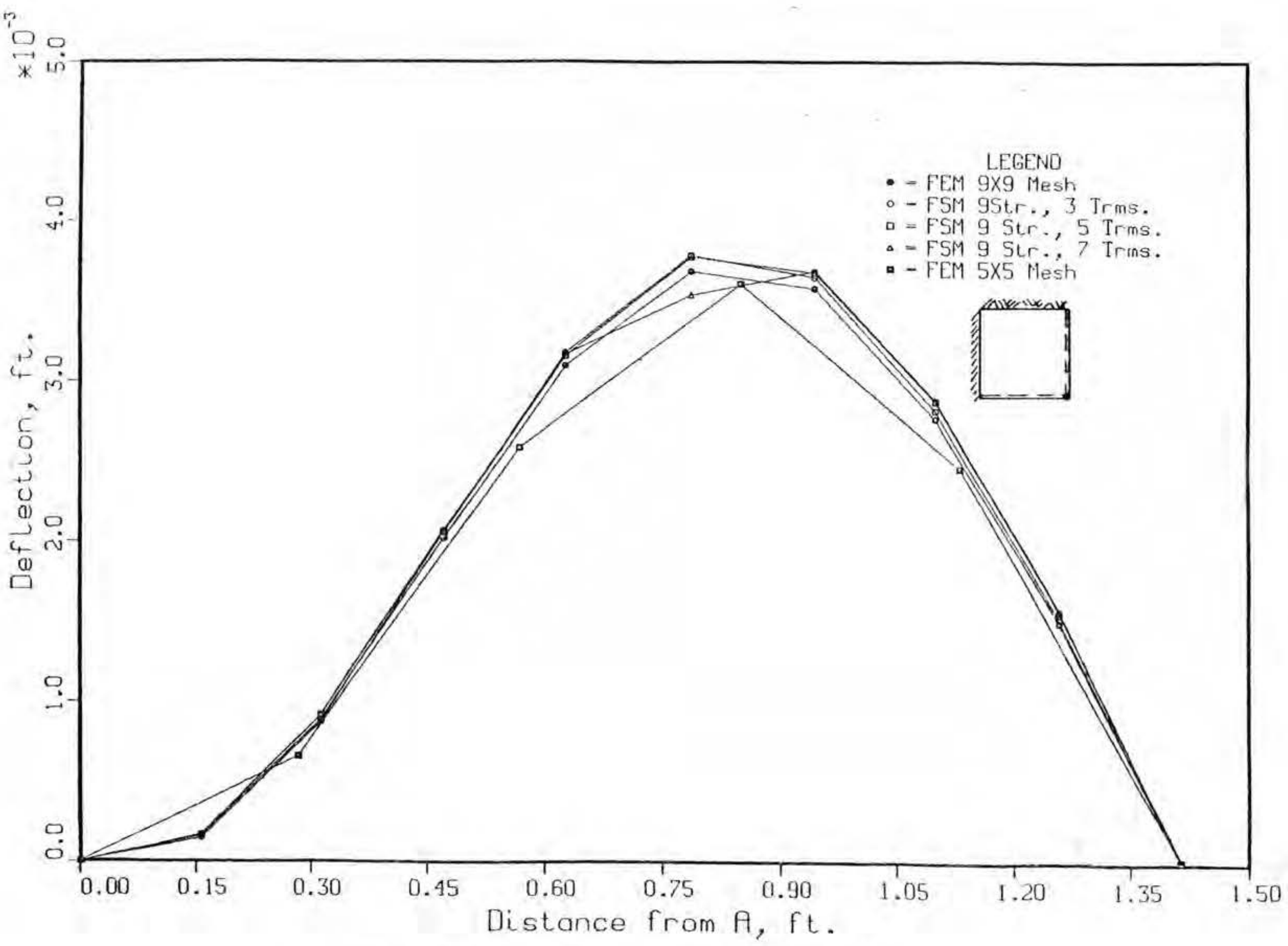

Fig. 6.39 Deflection along A-E

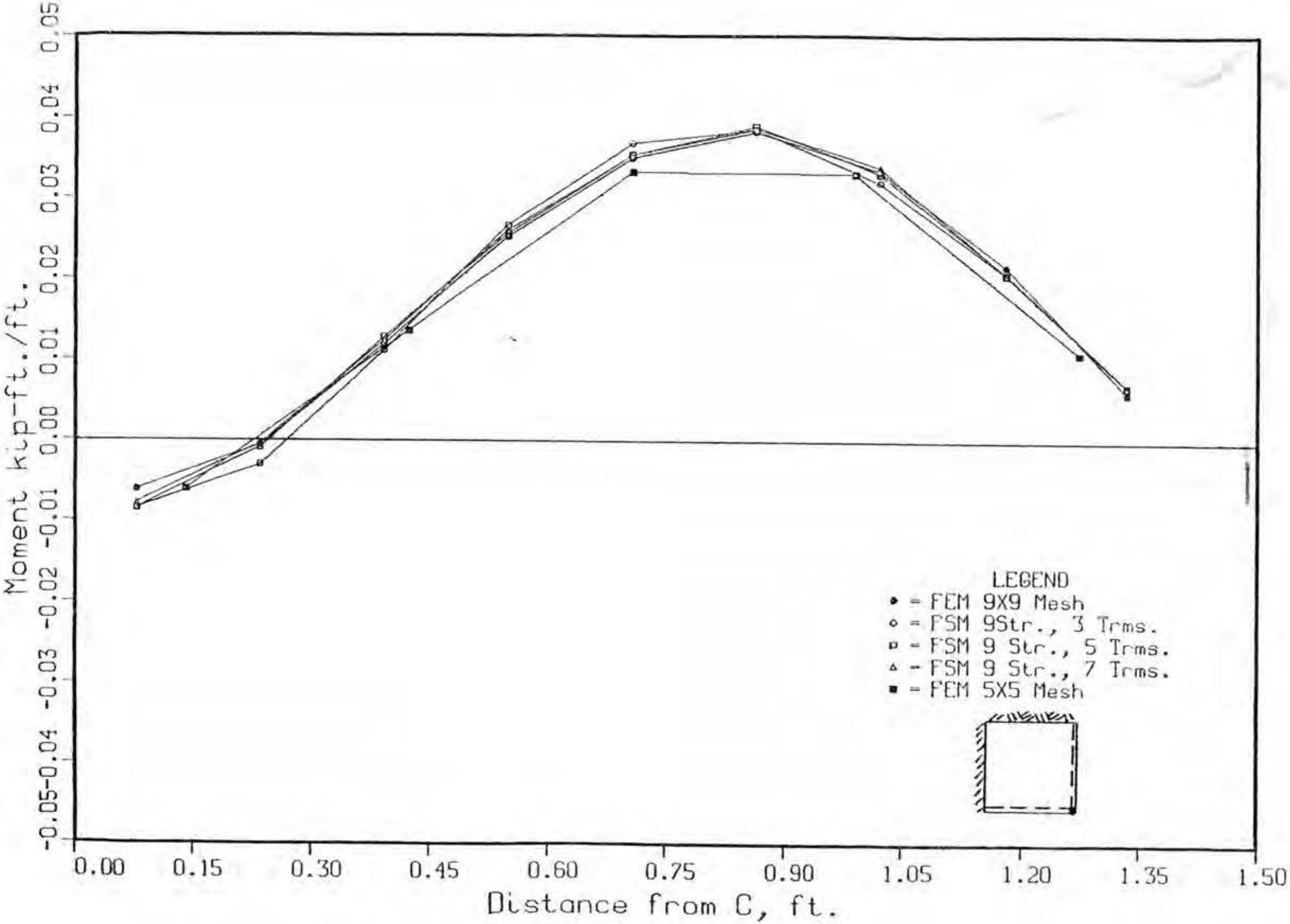

Fig. 6.40 Moment-X along C-G

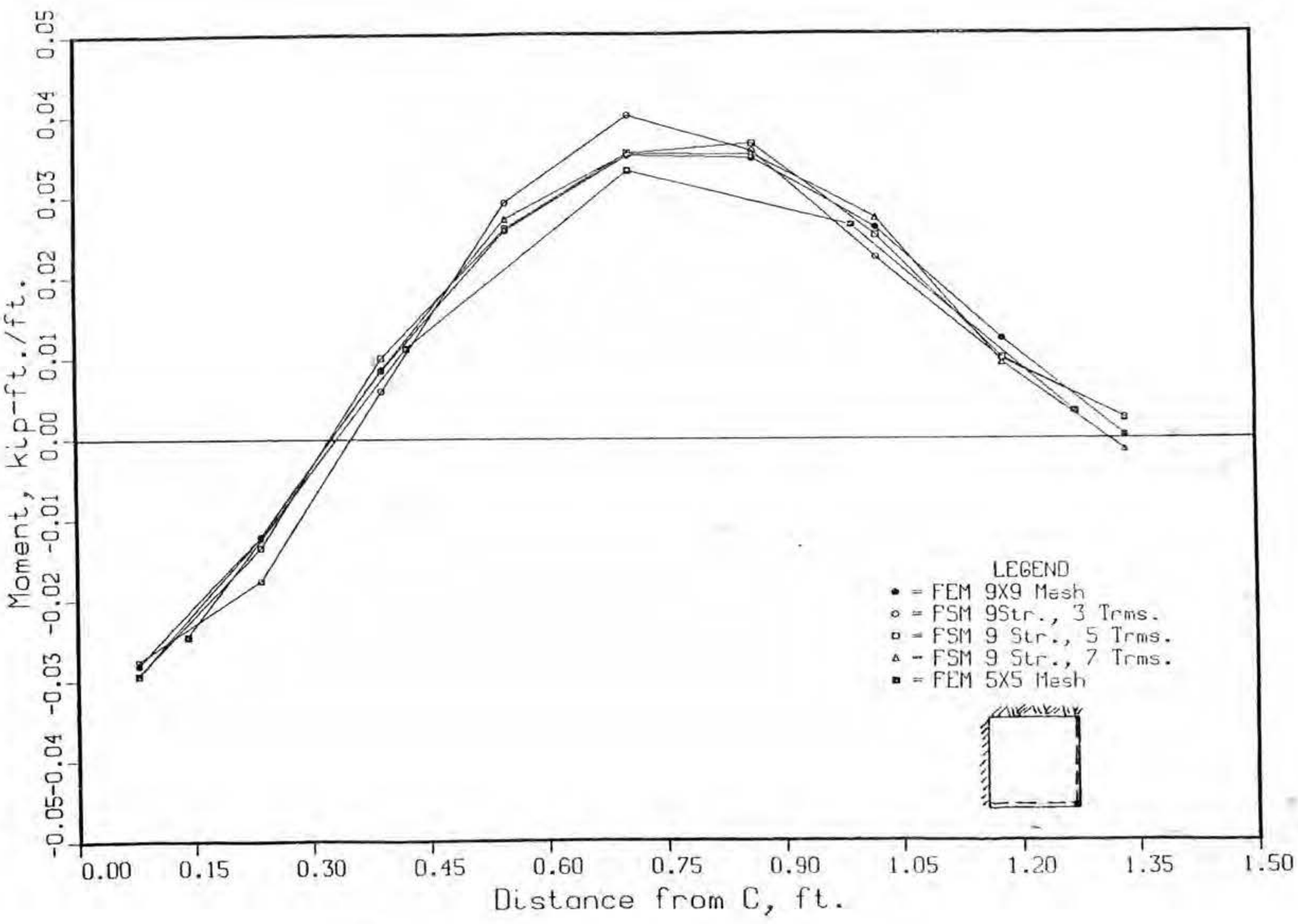

Fig. 6.41 Moment-Y along C-G

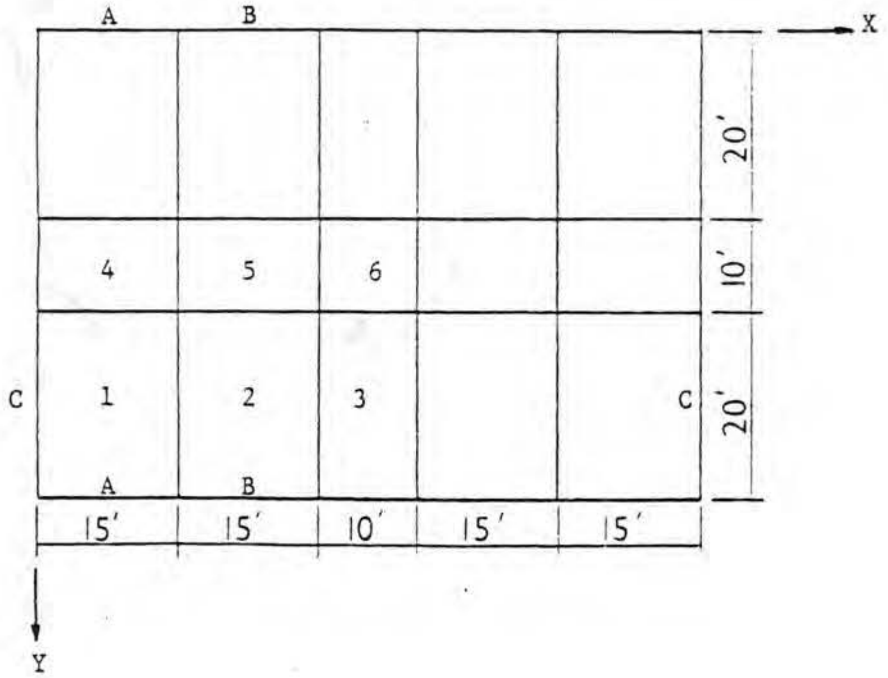

All lines represent pinned supports
Uniform load = 1.0 ksf.
Isotropic material
Numbers are for reference
A-A: X=7.5 ft.
B-B: X=22.5 ft.
C-C: Y=40.0 ft.

Figure 6.42 Continuous Plate System

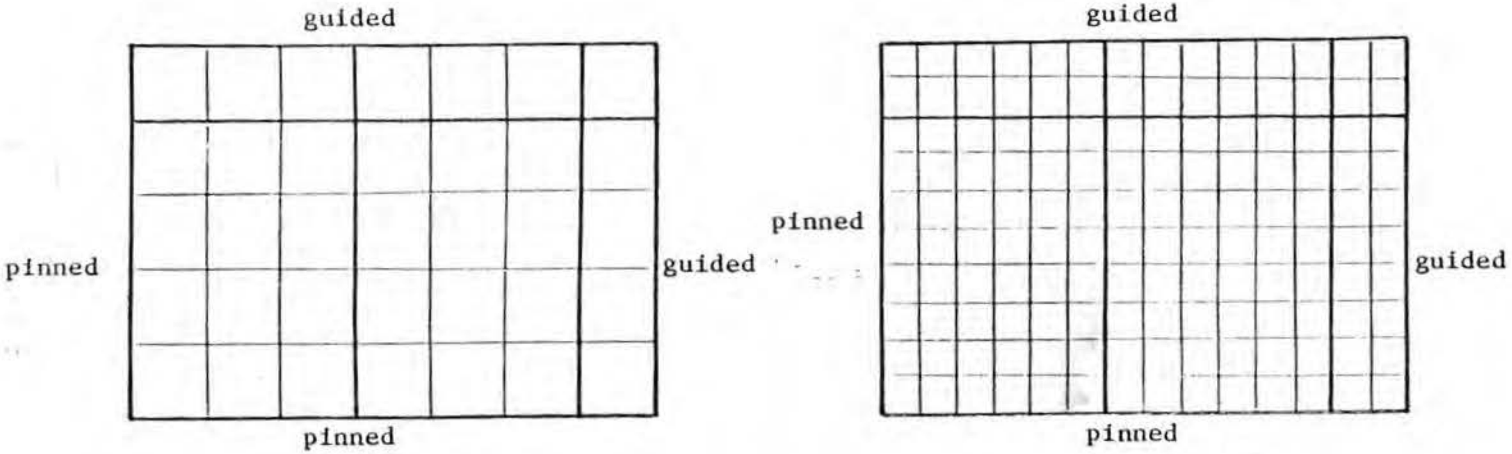

(a) 5X7 Mesh

(b) 10X14 Mesh

Figure 6.43 SAP IV Mesh Layouts for the Continuous Plate System

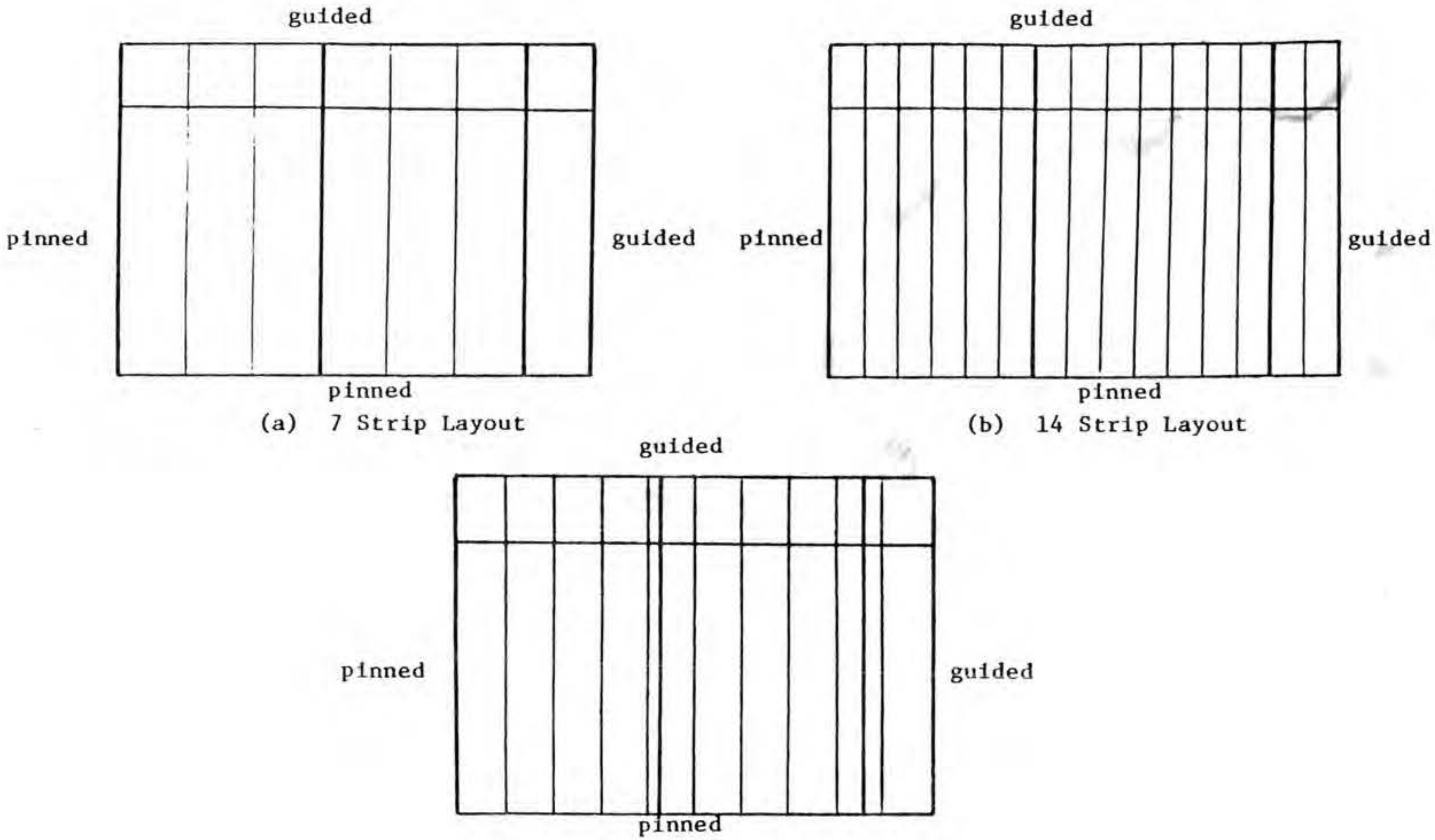

(a) 7 Strip Layout

(b) 14 Strip Layout

(c) 10 Strip Layout

Figure 6.44 Strip Layout for the Continuous Plate System

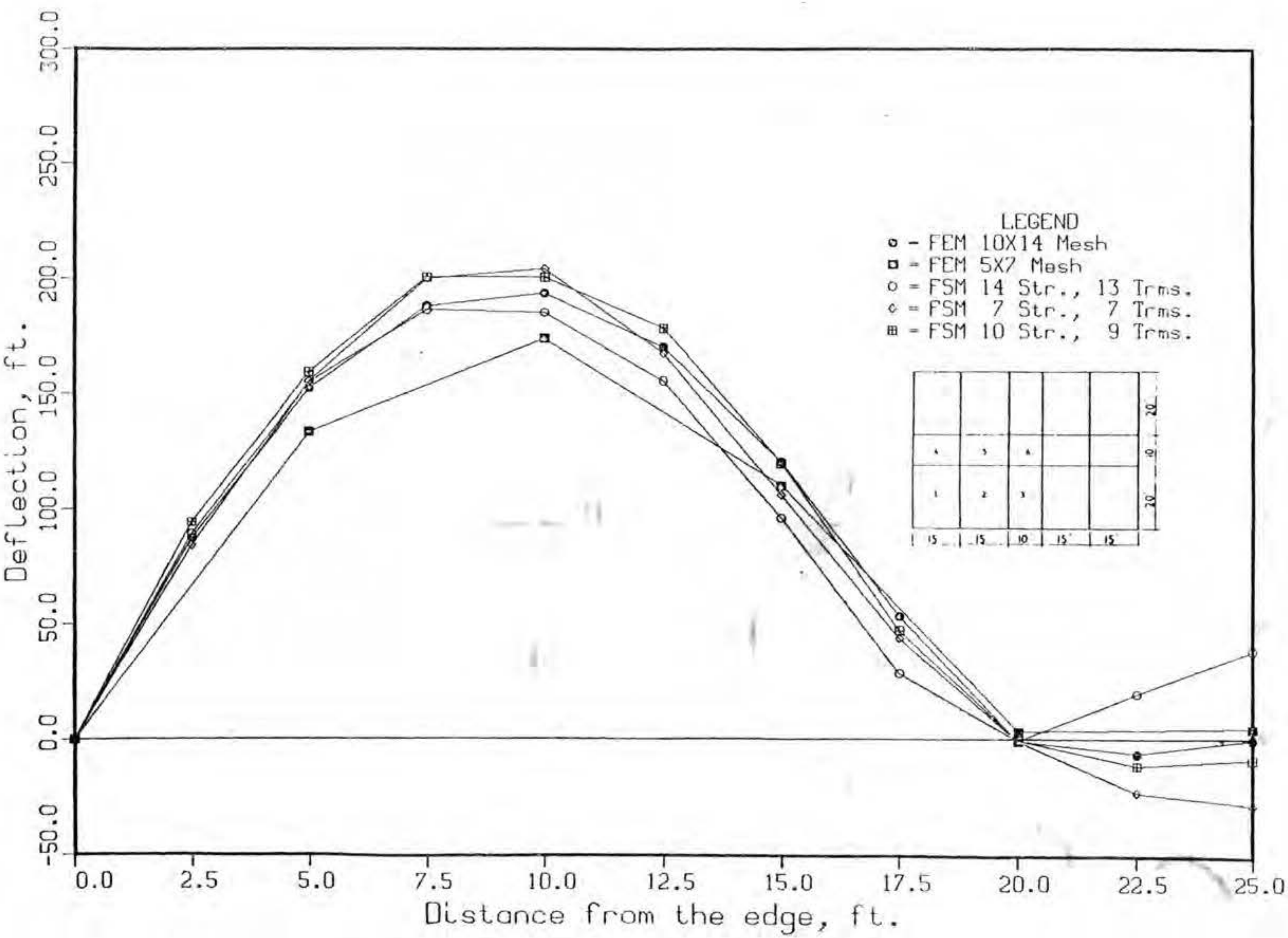

Fig. 6.45 Deflection along A-A

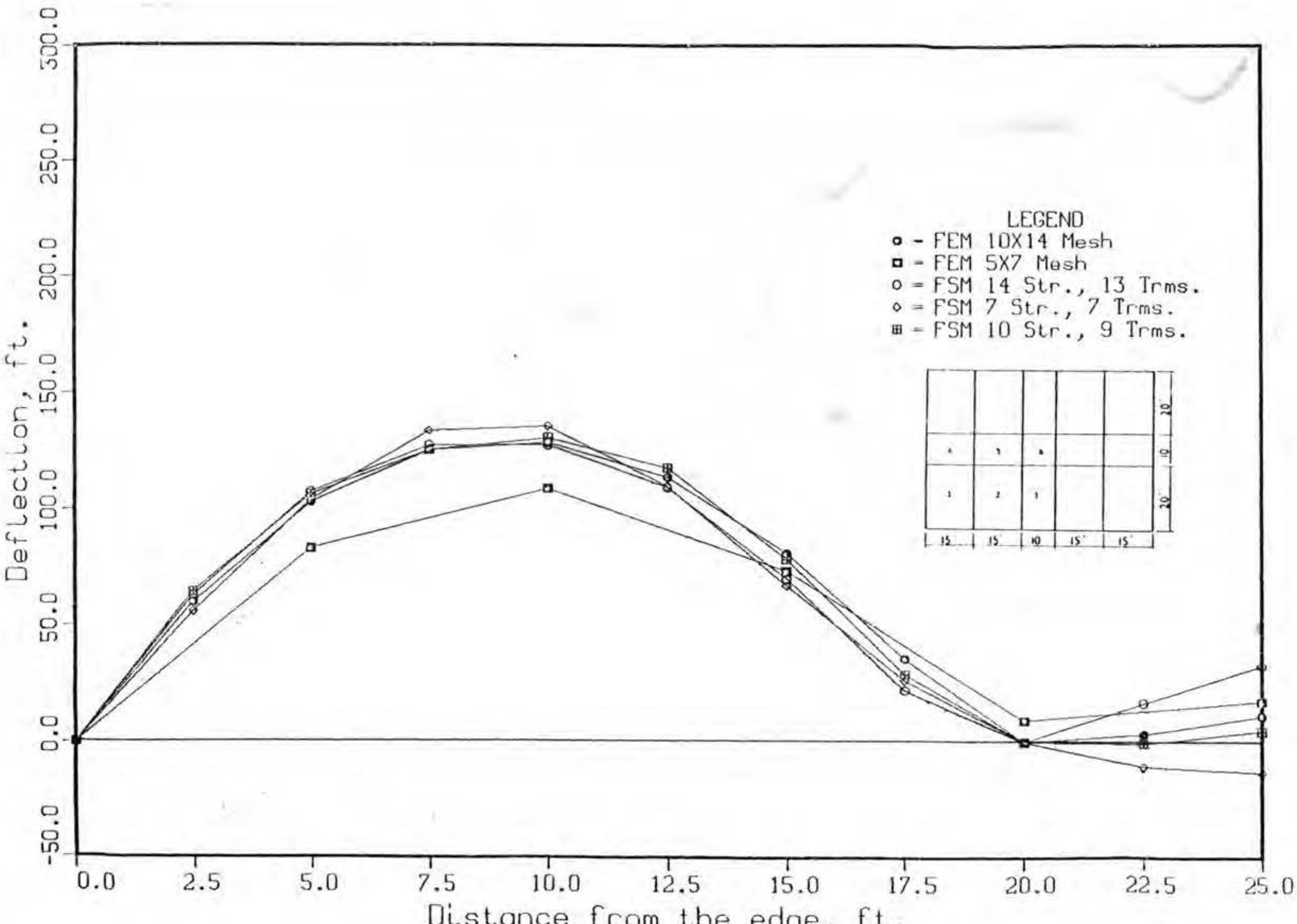

Fig. 6.46 Deflection along B-B

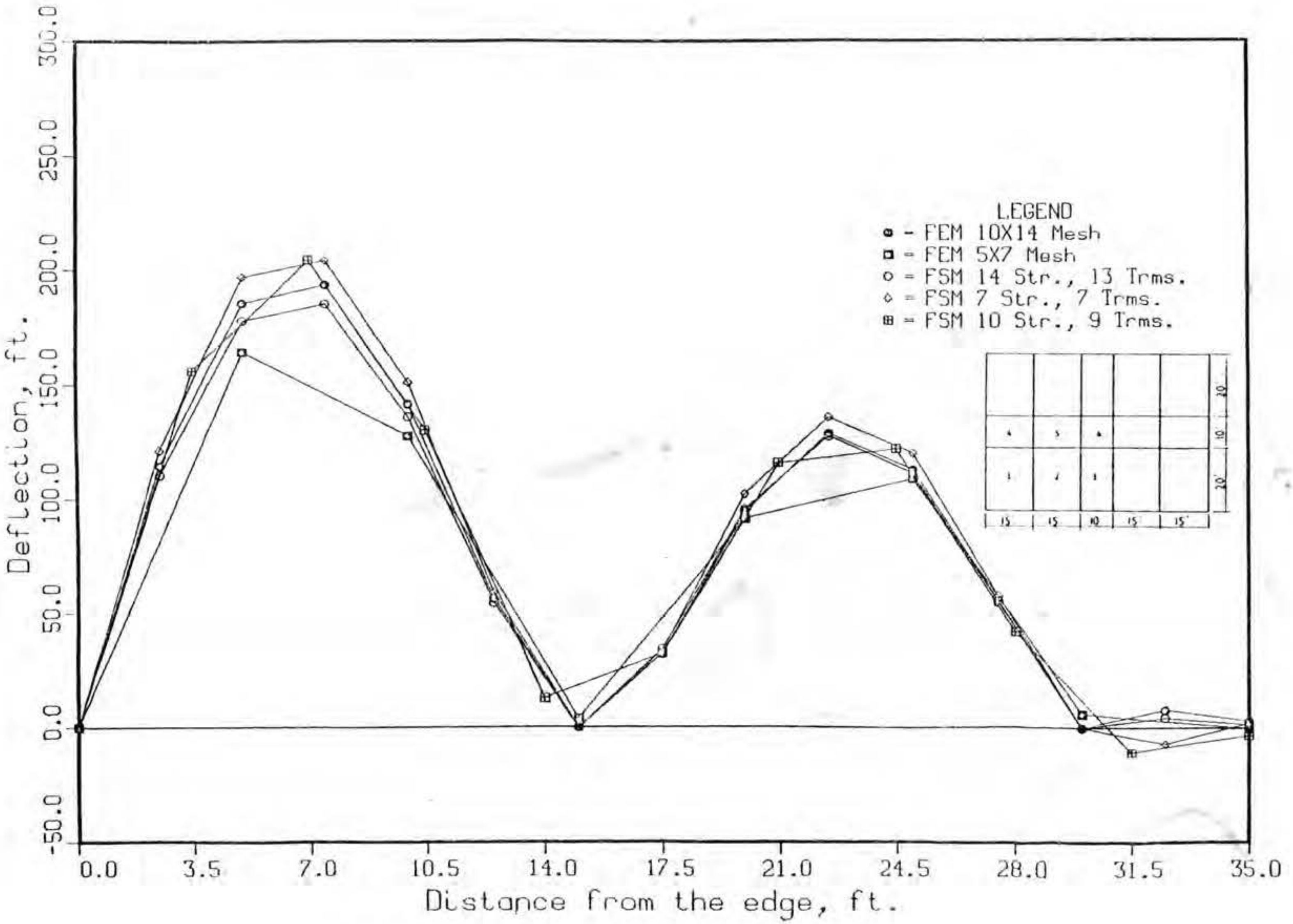

Fig. 6.47 Deflection along C-C

14 mesh with a difference in the maximum deflections of two percent. The moments compared favorably as illustrated in Figures 6.48-6.51 and the maximum negative moment calculated by the FSM (14 strip, 13 terms) differed from the value reported by Maugh and Pan by 11 percent. The moments at this location were not readily available from the finite element model. The maximum positive moment occurs near the middle of the corner panel. The FSM gave a moment in the x-direction of 9.71 k-ft/ft and the moment given by Maugh and Pan is 9.34 k-ft/ft and the 10 x 14 SAP IV mesh gave 9.78 k-ft/ft Gutkowski reported 9.64 k-ft/ft with the FPM. The percent difference for the FSM, FEM and the FPM are 4.0, 4.7, and 3.2, respectively (relative to the Maugh and Pan value). The corresponding moments for the moment in the y-direction using the FSM, FEM, FPM and the Maugh and Pan rigorous method are 4.37, 4.37, 4.37, and 4.27 with percent difference for the FSM, FEM, and the FPM of 2.3 percent.

6.4. Rate of Convergence

The system shown in Figure 6.42 was analyzed as an orthotropic plate by Gutkowski (18) using the FPM and the Melosh rectangular element using four mesh layouts. The plate has orthotropic material properties of D_x, D_y, D_1, and D_{xy} of 6.0, 3.0, 4.0, and 1.0 k in., respectively. A uniform load of 1.0 ksi was applied and one quarter of the plate was modeled due to symmetry. The quarter system mesh layouts were 10x7, 10x14, 15x14, and 15x28 where the first number is the number of elements in the y-direction. These mesh sizes correspond to 158, 354, 544, and 1146 degrees-of-freedom, respectively. Herein a comparison was made between these results and the developed compound strip model.

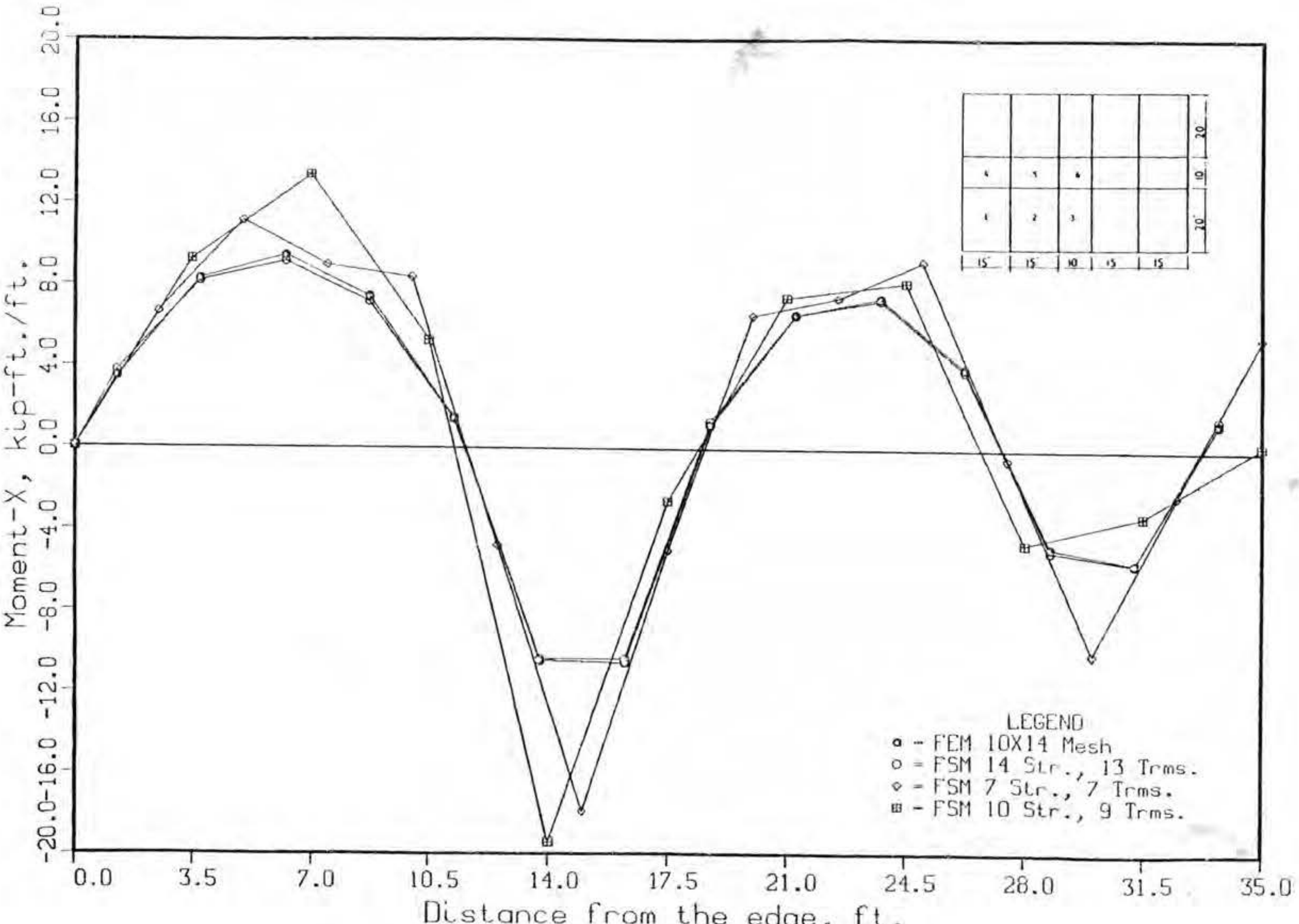

Fig. 6.48 Moment-X along C-C

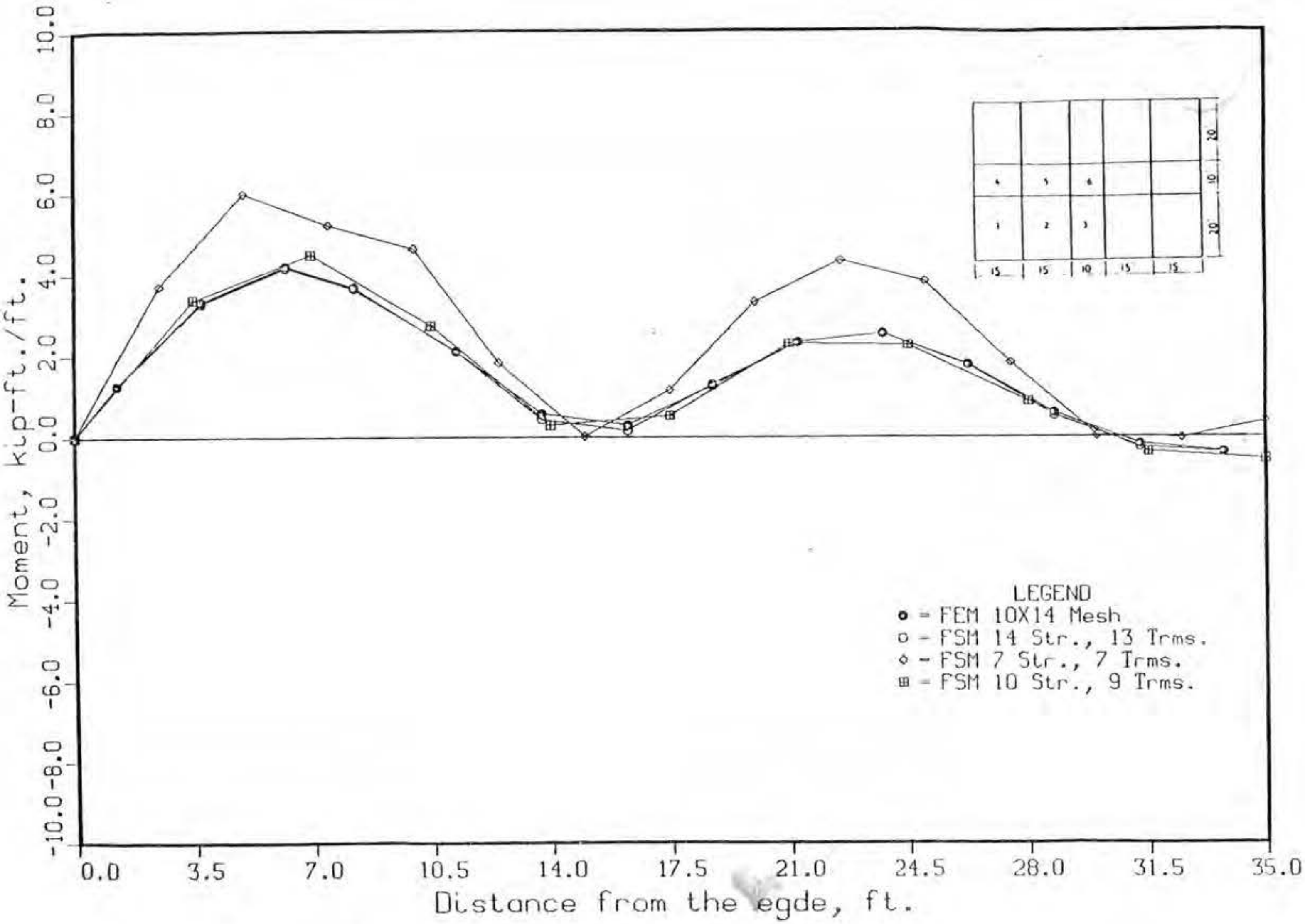

Fig. 6.49 Moment-Y along C-C

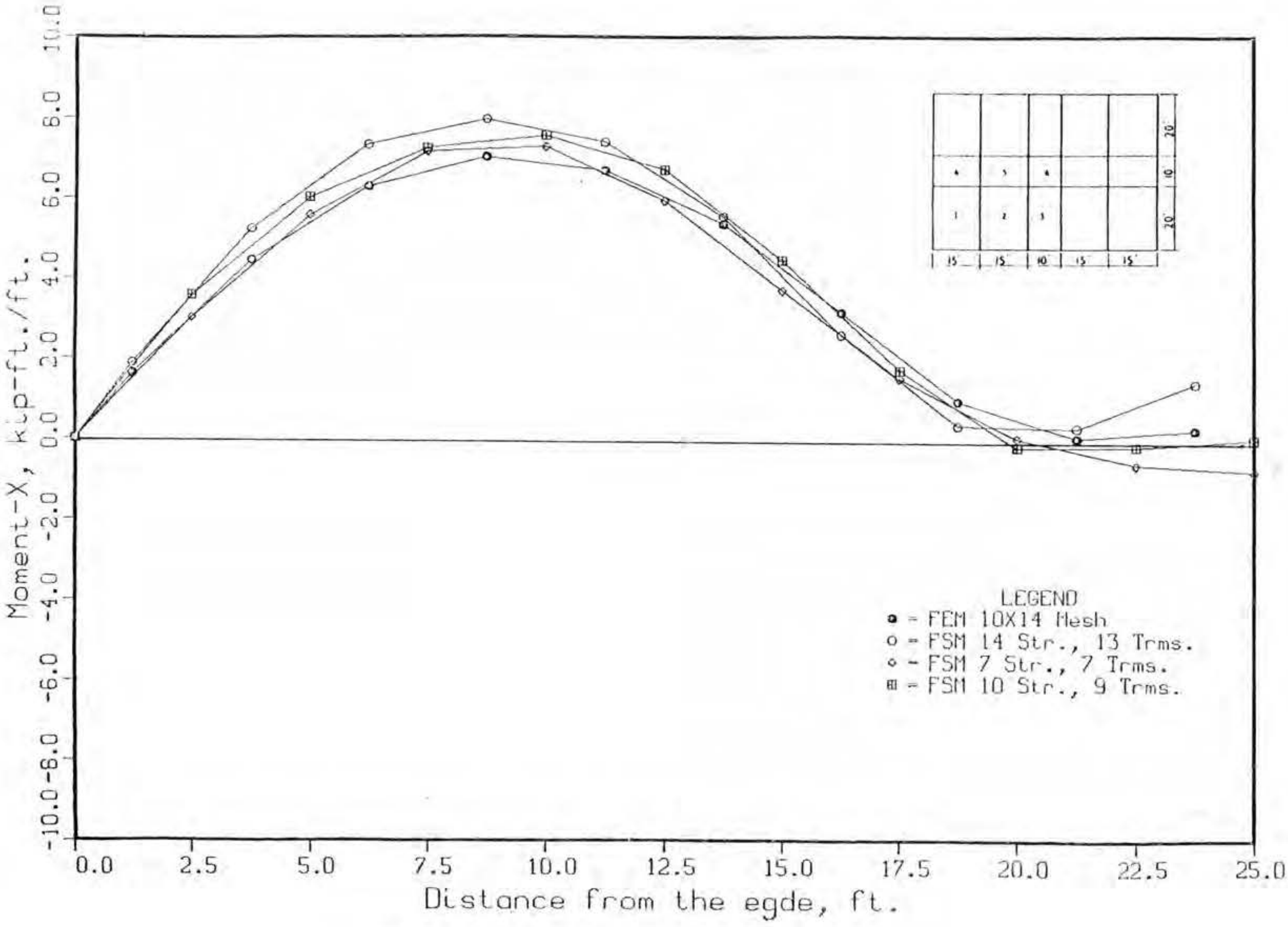

Fig. 6.50 Moment-X along B-B

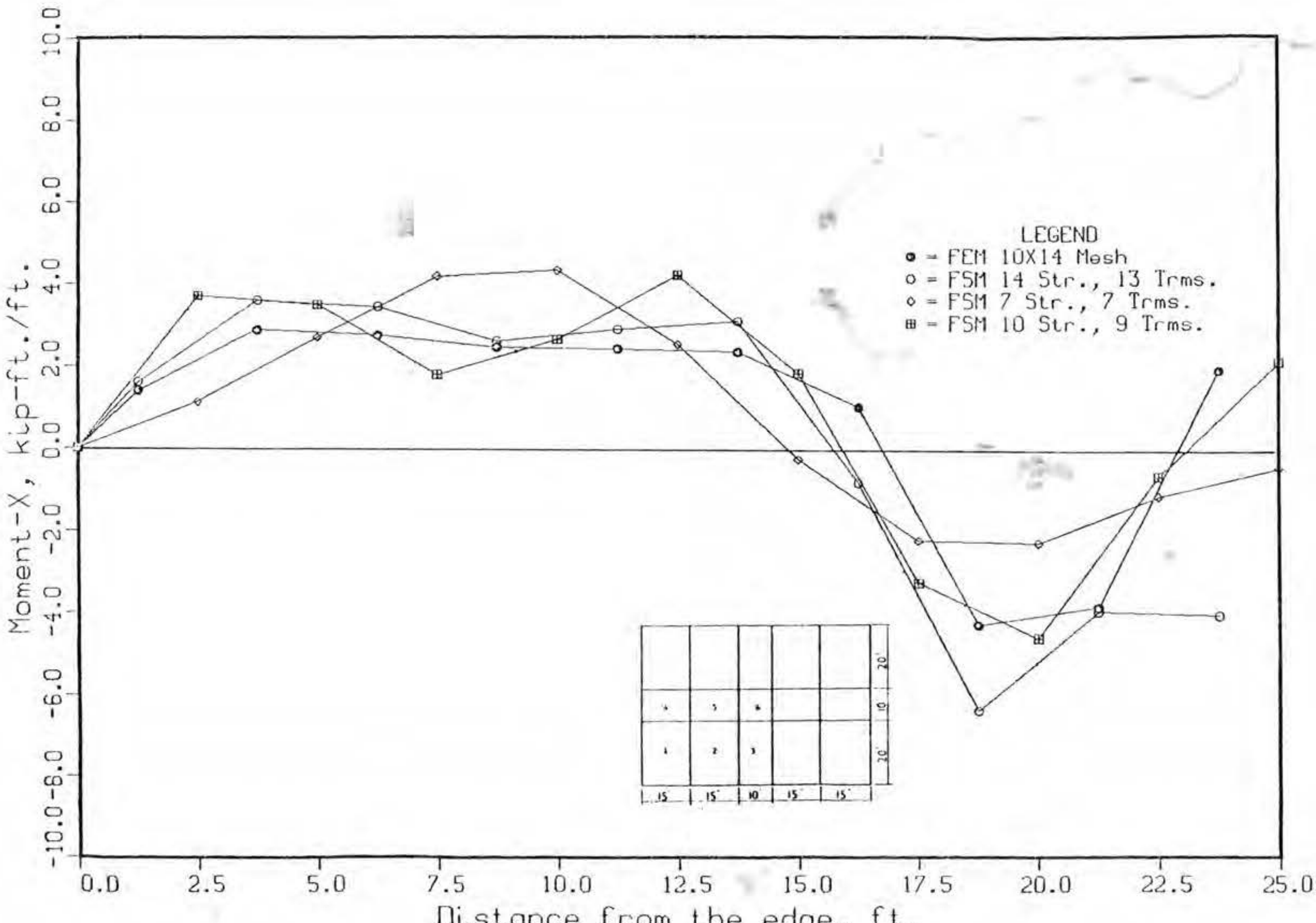

Fig. 6.51 Moment-Y along B-B

The finite strip models employed are those shown earlier in Figure 6.44 and the 28 strip model shown in Figure 6.52. The number of harmonics considered was varied for each model up to a maximum of 23 (12 non-zero) for the 28 strip model.

The deflections at the center of each panel are given in Table 6.1 and the moments are given in Table 6.2. The midedge moments are reported in Table 6.3. The degrees-of-freedom are stated for each analysis for comparison of computational effort.

The relative rates of convergence are shown in a series of figures showing the absolute value of percent difference between the 15x28 finite element model and the finite strip results. The convergence rate for deflection at the middle of panel no. 2 is shown in Figure 6.53. Convergence characteristics for the other large panels (1, 2, and 3) are similar. The FSM shows a much faster convergence rate with respect to the number of degrees-of-freedom for mid-panel deflections than the FEM. For example, for approximately a 1.5 percent difference the FSM requires approximately 120 degrees-of-freedom while the FEM requires about 450, thus an apparent computational savings. In the small panels (4, 5, and 6), where the deflections are much smaller, the FEM converges more rapidly than the FSM.

The relative rate of convergence of the moment in the y-direction at the center of panel no. 1 is shown in Figure 6.54. The convergence characteristics of the other mid-panel moments are similar for the larger panels. The FSM exhibits a faster convergence rate than the FEM for these actions as illustrated in Figure 6.54. Similar to deflection, the FEM converges more rapidly for the mid-panel moment of the smaller

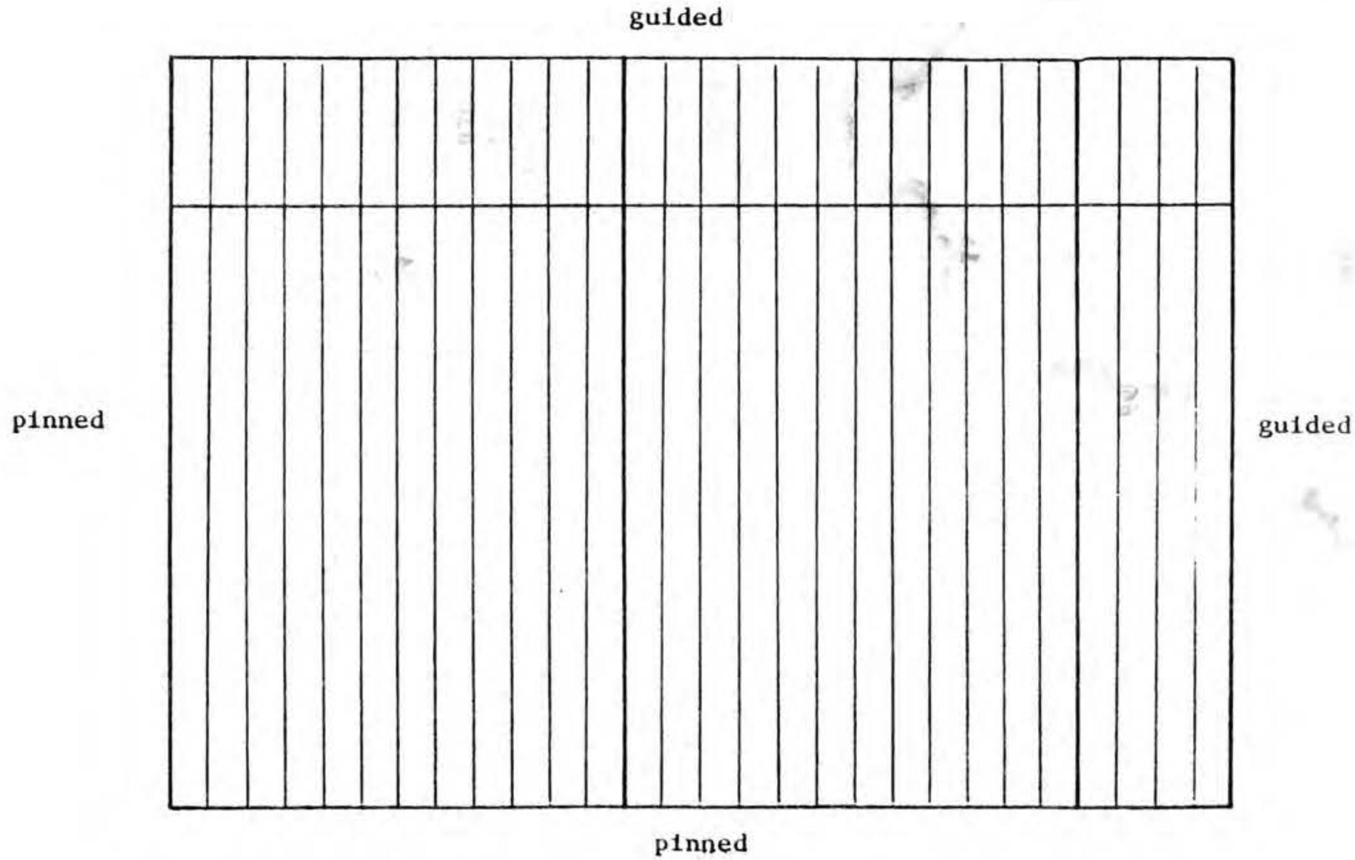

Figure 6.52 28 Strip Layout for the Continuous Plate System

Table 6.1. Deflection at the Center of the Panels.

METHOD	DOF	DEFLECTIONS, IN. W1	W2	W3	W4	W5	W6
FEM 10X14	354	0.2781	0.1804	-0.0062	0.0353	0.0435	0.0270
FEM 15X14	544	0.2639	0.1788	-0.0061	0.0320	0.0422	0.0259
FEM 15X28	1146	0.2763	0.1766	-0.0058	0.0321	0.0406	0.0250
FPM	-	0.2782	0.1788	-0.0047	0.0331	0.0397	0.0239
FSM 7,3	32	0.2663	0.1711	-0.0015	-0.0770	-0.0495	0.0004
FSM 7,5	48	0.2662	0.1713	-0.0015	-0.0542	-0.0311	0.0042
FSM 7,7	64	0.2828	0.1836	0.0010	-0.0285	-0.0107	0.0091
FSM 7,9	80	0.2744	0.1747	-0.0043	0.0107	0.0224	0.0200
FSM 7,11	96	0.2713	0.1716	-0.0058	0.0251	0.0340	0.0230
FSM 7,13	112	0.2751	0.1748	-0.0043	0.0305	0.0386	0.0248
FSM 7,15	128	0.2750	0.1748	-0.0043	0.0302	0.0383	0.0246
FSM 10,7	88	0.2829	0.1827	-0.0022	-0.0284	-0.0103	0.0091
FSM 10,9	110	0.2745	0.1738	0.0071	0.0108	0.0227	0.0192
FSM 10,11	132	0.2714	0.1707	-0.0086	0.0251	0.0342	0.0219
FSM 10,13	154	0.2752	0.1738	-0.0072	0.0306	0.0388	0.0236
FSM 10,15	176	0.2752	0.1738	-0.0072	0.0303	0.0385	0.0230
FSM 14,9	150	0.2756	0.1765	-0.0043	0.0106	0.0225	0.0197
FSM 14,11	180	0.2725	0.1733	-0.0058	0.0250	0.0445	0.0227
FSM 14,13	210	0.2762	0.1765	-0.0044	0.0304	0.0387	0.0245
FSM 14,15	240	0.2762	0.1765	-0.0044	0.0302	0.0385	0.0242
FSM 28,7	232	0.2849	0.1885	0.0049	-0.0256	0.0028	0.0182
FSM 28,15	464	0.2771	0.1795	-0.0004	0.0333	0.0464	0.0334
FSM 28,23	696	0.2777	0.1798	-0.0005	0.0325	0.0454	0.0322

Table 6.2. Moment at the Center of the Panels.

METHOD	DOF	MOMENT, K-IN./IN. MX1	MY1	MX2	MY2	MX3	MY3
FEM 10X7	158	1733	1182	1335	905	541	355
FEM 10X14	354	1931	1320	1498	1016	301	196
FEM 15X14	544	1918	1312	1487	1010	302	196
FEM 15X28	1146	1882	1288	1430	972	243	157
FPM	-	1865	1277	1409	958	222	142
FSM 7,3	32	1804	1243	1350	926	657	438
FSM 7,5	48	1804	1243	1350	926	657	438
FSM 7,7	64	2070	1437	1569	1084	787	527
FSM 7,9	80	1764	1210	1288	877	546	358
FSM 7,11	96	1603	1090	1146	772	459	296
FSM 7,13	112	1770	1214	1296	883	573	378
FSM 7,15	28	1770	1214	1296	883	573	377
FSM 10,7	88	2185	1513	1631	1126	562	376
FSM 10,9	110	1880	1287	1346	915	373	243
FSM 10,11	132	1719	1167	1204	810	301	191
FSM 10,13	154	1886	1292	1355	923	393	258
FSM 10,15	176	1886	1292	1355	923	393	258
FSM 14,9	150	1903	1303	1452	987	294	190
FSM 14,11	180	1742	1182	1309	881	224	139
FSM 14,13	210	1910	1308	1461	994	314	206
FSM 14,15	240	1910	1307	1461	994	312	204
FSM 28,7	232	2171	1504	1696	1170	407	274
FSM 28,15	464	1871	1282	1420	966	253	165
FSM 28,23	696	1871	1281	1419	965	248	161

Table 6.2. Moment at the Center of the Panels (Continued).

METHOD	DOF	MOMENT, K-IN/IN. MX4	MY4	MX5	MY5	MX6	MY6
FEM 10X7	158	763	554	806	579	869	596
FEM 10X14	354	720	530	791	575	645	447
FEM 15X14	544	659	485	734	533	616	427
FEM 15X28	1146	640	470	710	516	567	394
FPM	-	596	438	662	481	529	366
FSM 7,3	32	842	600	-597	-423	124	84.5
FSM 7,5	48	-580	-412	-368	-259	-19.2	-10.5
FSM 7,7	64	-250	-174	-86.1	-57.7	193	134
FSM 7,9	80	357	266	455	334	113	82.7
FSM 7,11	96	664	491	719	526	813	563
FSM 7,13	112	846	625	882	646	932	647
FSM 7,15	128	828	612	865	633	911	633
FSM 10,7	88	-267	-186	-89.6	-59.9	161	113
FSM 10,9	110	348	260	462	338	521	362
FSM 10,11	132	658	487	729	532	655	456
FSM 10,13	154	841	622	893	653	753	526
FSM 10,15	176	823	609	875	641	738	515
FSM 14,9	150	344	257	451	331	484	338
FSM 14,11	180	655	485	723	529	610	427
FSM 14,13	210	815	620	888	650	704	495
FSM 14,15	240	820	607	870	637	689	484
FSM 28,7	232	-265	-185	-97	-70	158	106
FSM 28,15	464	824	609	876	642	667	469
FSM 28,23	696	473	347	560	404	478	329

Table 6.3. Midedge Moments

		MOMENT, K-IN./IN.						
METHOD	DOF	M12	M23	M45	M56	M41	M52	M63
FEM 10X7	158	-2674	-1460	-638	-667	-1130	-923	-351
FEM 10X14	354	-2959	-1682	-876	-904	-1269	-1050	-356
FEM 15X14	544	-2935	-1669	-842	-867	-1336	-1117	-416
FEM 15X28	1146	-3008	-1723	-940	-953	-1315	-1088	-395
FPM	-	-3120	-1812	-917	-956	-1422	-1196	-463
FSM 10,9	110	-2324	-1072	-396	-360	-571	-436	-89.
FSM 10,11	132	-2278	-1035	-547	-462	-735	-570	-126
FSM 10,13	154	-2333	-1076	-618	-513	-803	-628	-151
FSM 10,15	176	-2333	-1076	-610	-151	-803	-628	-507
FSM 14,11	180	-2818	-1569	-734	-771	-738	-576	-138
FSM 14,13	210	-2892	-1639	-815	-844	-806	-634	-162
FSM 14,15	240	-2892	-1639	-815	-844	-806	-634	-163
FSM 28,7	232	-3233	-1943	-265	-90.	-279	191	-101
FSM 28,15	464	-2982	-1709	-908	-940	-805	-632	-159
FSM 28,23	696	-2981	-1706	-877	-883	-1011	-813	-249

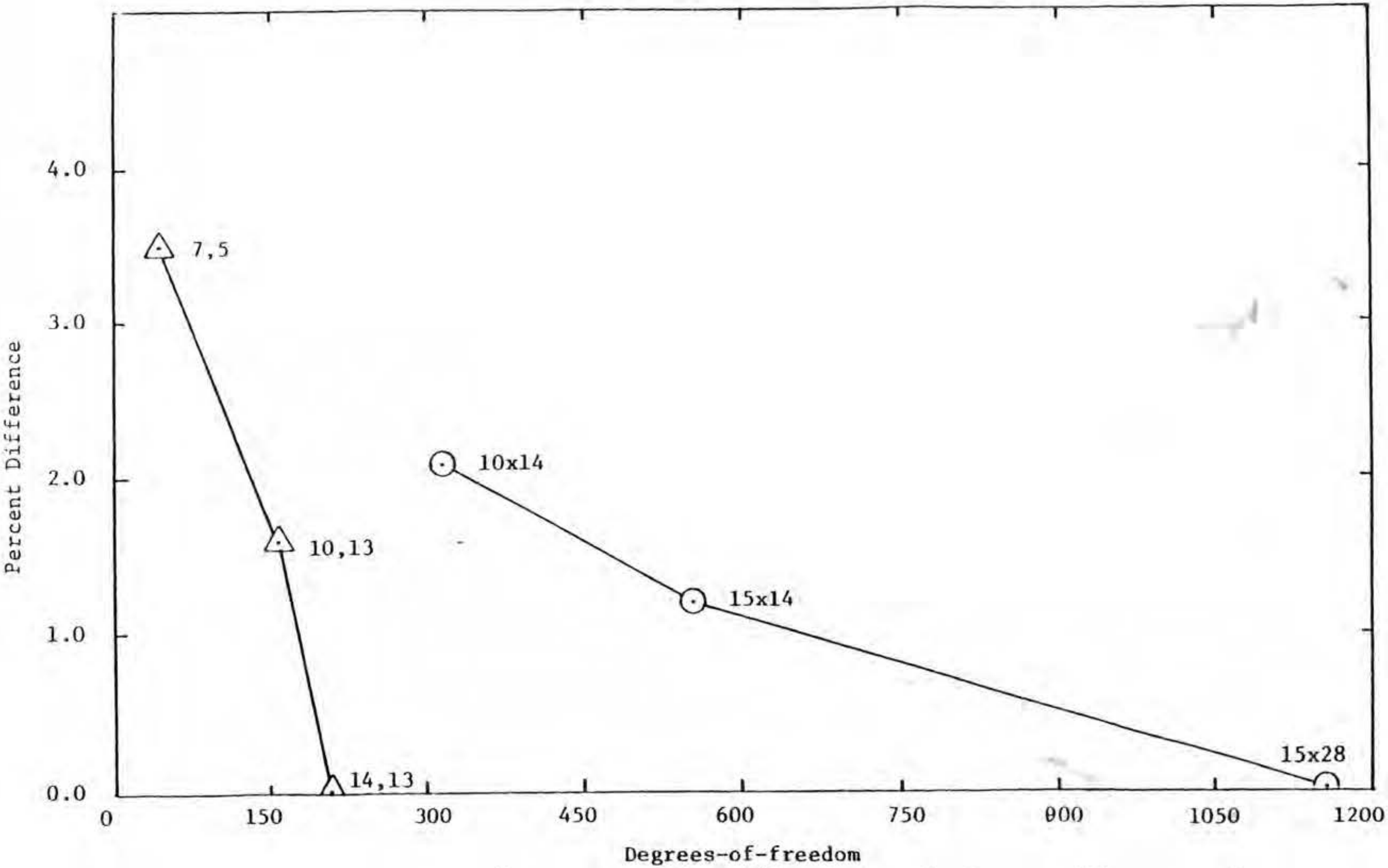

Figure 6.53 Rate of Convergence for Deflection at the Center of Panel No. 2

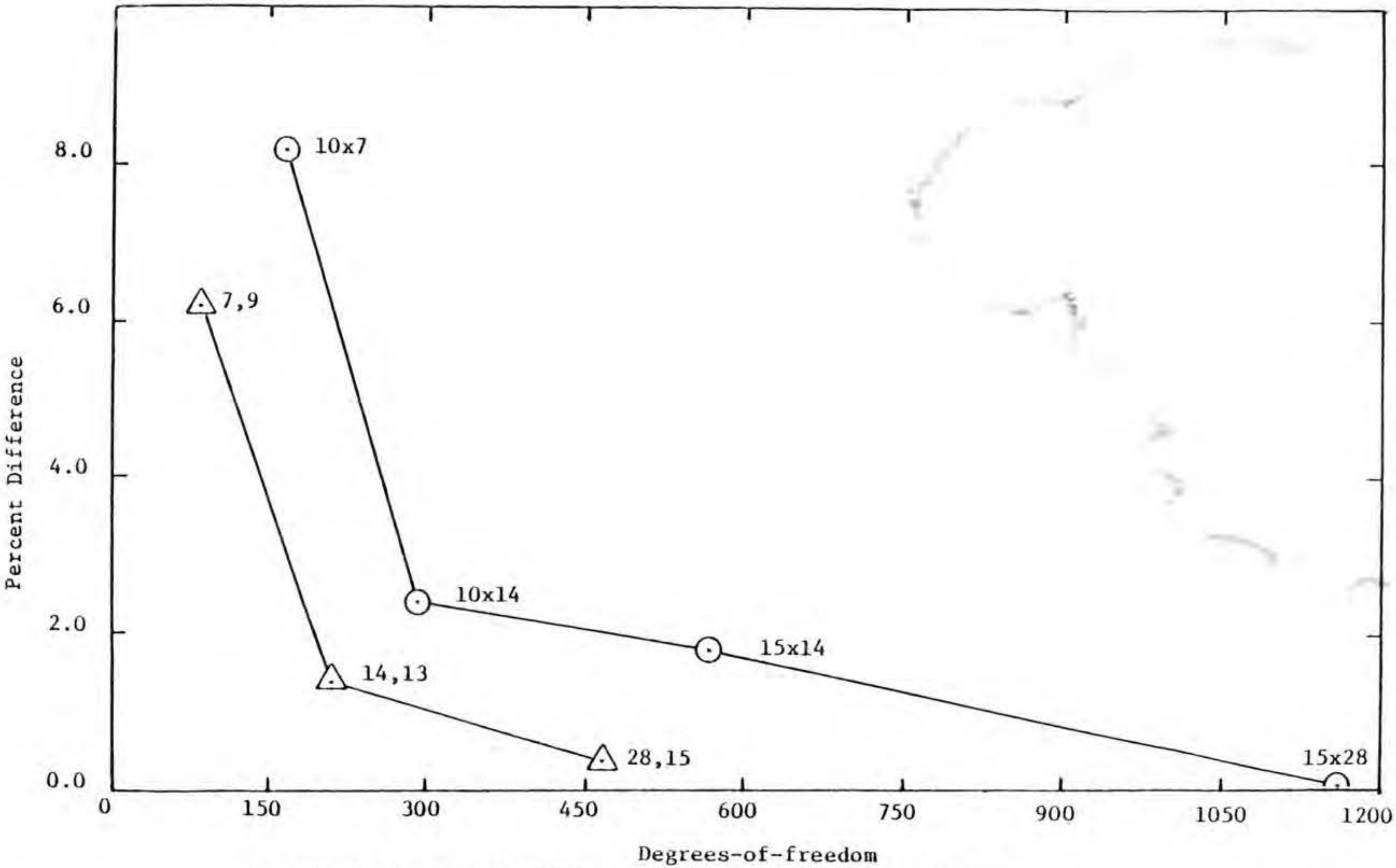

Figure 6.54 Rate of Convergence for Moment-Y, Panel No. 1

panels. The relative rate of convergence for these moments varies depending on the panel and action under consideration.

The relative rate of convergence of the midedge moments vary throughout the system. The convergence characteristics of the midedge moment between panels no. 1 and no. 2, M_{12}, is shown in Figure 6.55. The convergence rate of the two methods are nearly the same for this action. This is typical in locations where the midedge moments are larger; M_{12}, M_{23}. For edges where the moments are smaller, usually adjacent to the smaller panels, the FEM exhibits a convergence rate favorable to the FSM as illustrated in Table 6.3.

Based on the numerous example problems investigated and those presented, the following summary is made:

1. The convergence rate for maximum deflection in a plate is faster for FSM than the FEM.
2. The rate of convergence for the maximum midpanel moments is favorable for the FSM.
3. For relatively smaller panels, the FEM exhibits a favorable convergence rate for midpanel moments.
4. The convergence rate for the maximum midedge moment is nearly the same for the two methods. Where the midedge moments are small, typically in the smaller panels of a system, the FEM is favorable.
5. In general, where actions or deflections are large (relative to the system) the FSM has favorable convergence characteristics.

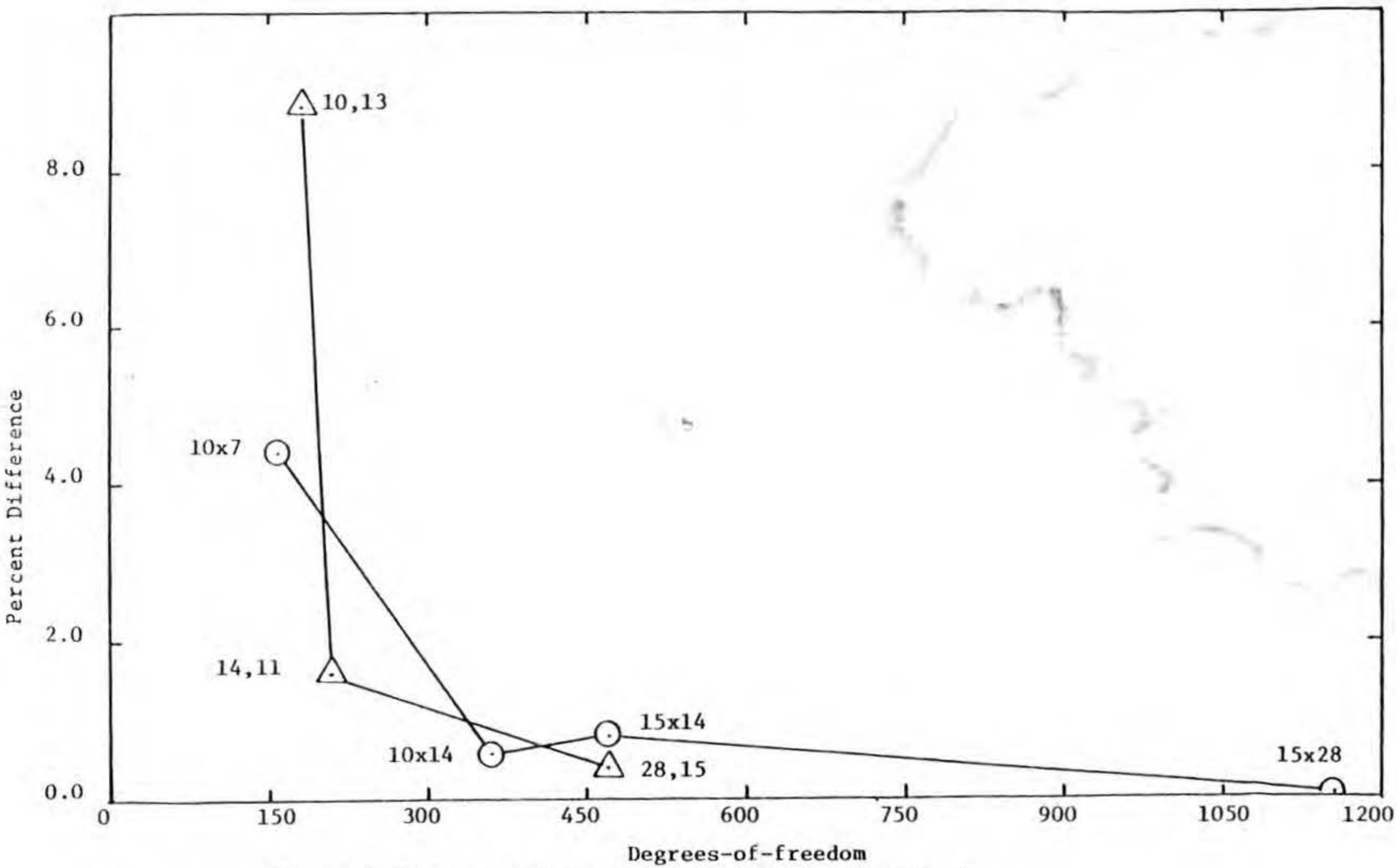

Figure 6.55 Rate of Convergence for Midedge Moment, M_{12}

6.5. Summary

Several illustrative examples have been presented in this chapter. Throughout, the compound strip model compared very well with the more established FEM. The continuous plate system illustrated the capability of the compound strip to accurately model multipanel plate systems which are commonplace in engineering practice. The convergence rate varies with quantities of interest and location, but generally the FSM is particularly well suited to determine maximum deflection and moment.

In addition, over two hundred plate systems have been successfully analyzed with the compound strip method as part of this research. Examples include many problems found in (reference 2), plane grids, continuous beams, and numerous other systems. Some of these will be presented in future published papers. The compound strip methodology compared favorably with rigorous and/or FEM solutions in all cases.

CHAPTER VII

7. SUMMARY, CONCLUSIONS, AND FUTURE RESEARCH

7.1. Summary

A finite strip method was developed for the analysis of linear elastic flat plate systems which are continuous over deflecting supports. The approach presented incorporates the effect of the support elements in a direct stiffness methodology. The stiffness contribution of the support elements have been derived and are given in the form of strip matrices which are directly added to the plate strip stiffness matrix at the element level. The combination of the plate and support elements is termed the "compound strip."

The validity of the compound strip method was demonstrated in several illustrative problems. The FSM and FEM compared favorably for displacement and moment.

The rate of convergence of the compound strip was studied for a continuous multipanel system. The FSM was found to be more computationally efficient than the FEM when maximum values for moment or deflection are required. The FEM exhibited favorable convergence characteristics in locations where the magnitudes of displacement and moment are relatively small.

7.2. Conclusions

The following conclusions can be drawn from this research in this manuscript.

1. The FSM requires minimal input data. For example, the systems modeled required less than 30 lines of data.
2. The interpretation of output is straightforward. Actions and displacements may be calculated along any line or at point in the systems.
3. The stiffness matrices of the support elements add directly to the conventional strip stiffness matrix creating the compound element. The conventional assembly procedures may be used, thus only minor code modifications must be made in existing codes to incorporate the compound strip elements.
4. Single and multipanel plate systems can be accurately modeled with the compound strip method.
5. Support elements with large stiffness can be used to model rigid supports.
6. The compound strip analysis requires a single solution where, by contrast, flexibility techniques require repetitive analyses.
7. The system of equations usually has a narrow bandwidth. Further the bandwidth is only a function of the number of harmonics considered and is independent of the number of strips or nodal lines.
8. Maximum deflections and moments may be calculated with less computational effort (fewer degrees-of-freedoms) than both the FEM used in this study.
9. Small deflections and moments in the systems are calculated more efficiently with the FEM employed.

7.3. Future Research

The scope of the study presented herein was limited to plate bending. By incorporating in-plane effects, this fundamental concept can be employed to model more complex continuous systems such as folded plates, box girders, and slab-girder bridges and floors. Compound strip concepts could also be applied to create mass matrices for the support elements allowing dynamic analysis of folded plate systems continuous over flexible supports.

REFERENCES

1. Szilard, R., Theory and Analysis of Plates-Classical and Numerical Methods, Prentice-Hall, 1974.

2. Timoshenko, S., and Woinowsky-Krieger, S., Theory of Plates and Shells, Second edition, McGraw Hill, 1971.

3. Ugural, A. C., Stresses in Plates and Shells, McGraw-Hill, 1981.

4. Zienkiewicz, O.C., The Finite Element Method in Engineering Science, Third Edition, McGraw-Hill, 1977.

5. Cheung, Y. K., "The Finite Strip Method in the Analysis of Elastic Plates with Two Opposite Supported Ends," Proc. Inst. Civ. Engr., Vol. 40, 1968.

6. Cheung, Y. K., "Finite Strip Method Analysis of Elastic Slabs," Jour. of the Engr. Mech. Div., ASCE, Vol. 94, No. EM6, Dec. 1968.

7. Powell, G. H., and Ogden, D. W., "Analysis of Orthotropic Steel Plate Bridge Decks," Journal of the Structural Division, ACSE, Vol. 95, ST5, July 1968.

8. Cheung, Y. K., "Folded Plate Structures by the Finite Strip Method," Journal of the Structural Division, ASCE, Vol. 95, ST12, Dec. 1969.

9. Scordelis, A. C., and DesFries, A., "Direct Stiffness Solution for Folded Plates," Journal of the Structural Division, ASCE, Vol. 90, No. ST4, Aug. 1964.

10. Cheung, Y. K., "Orthotropic Right Bridges by the Finite Strip Method," Publ. SP 26, Amer. Conc. Inst., Detroit, Mich., 1969.

11. Cheung, Y. K., "Analysis of Box Girders Bridges by the Finite Strip Method," SP 26, Amer. Conc. Inst., Detroit, Mich. 1969.

12. Cheung, M. S. and Cheung, Y. K., "Analysis of Curved Box Girder Bridges by the Finite Strip Method," Proc. Int'l. Assoc. Bridge and Str. Engr., 31-I, 1971.

13. Cheung, Y. K., "The Analysis of Cyclindrical Orthotropic Curved Bridge Decks," Proc. Int'l. Assoc. Bridge and Str. Engr., 29-II, 1969.

14. Coull, A., and Das, P. C., "Analysis of Curved Bridge Decks," Proc. Inst. Civ. Engr., Vol. 37, May 1967.

15. Cheung, M. S., Cheung, Y. K., and Ghali, A., "Analysis of Slab and Girder Bridges by the Finite Strip Method," Build. Sci., Vol. 5, 1970.

16. Gutkowski, R. M., "The Finite Panel Method for the Elastic Analysis of Continuous Rectangular Plate Systems," dissertation presented to the University of Wisconsin (Madison), in 1974, in partial fulfillment of the requirements for the degree of Doctor of Philosophy.

17. Gutkowski, R. M. and Wang, C. K., "Continuous Plate Analysis by Finite Panel Method," Journal of the Structural Division, ASCE, Vol. 102, No. ST3, Proc. Paper 12002, March 1976, pp. 629-643.

18. Gutkowski, R. M., "Finite Panel analysis of Orthotropic Plate Systems," Journal of the Structural Division, ASCE, Vol. 103, No. ST11, Proc. Paper 13371, Nov. 1977, pp. 2211-2224.

19. Cheung, Y. K., "Flexural Vibrations of Rectangular and Other Polygonal Plates," Jour. of the Engr. Mech. Div., ASCE, Vol. 97, EM2, Apr. 1971.

20. Cheung, Y. K., and Cheung, M. S., "Free Vibration of Curved and Straight Beam-Slab or Box Girder Bridges," Proc. Int'l. Assoc. Bridge and Str. Engr., 32-II, 1972.

21. Cheung, M. S., and Cheung, Y. K., "Static and Dynamic Behaviour of Rectangular Plates Using Higher Order Finite Strips," Build. Sci., Vol. 7, 1972.

22. Wu, C. I., and Cheung, Y. K., "Frequency Analysis of Rectangular Plates Continuous in One or Two Directions," Earthquake Engr. and Str. Dyn., Vol. 3, 1974.

23. Delcourt, C., and Cheung, Y. K., "Finite Strip Analysis of Continuous Folded Plates," Proc. Int'l. Assoc. Bridge and Str. Engrs., May 1978.

24. Beaufait, F. W., "Analysis of Continuous Folded Plates," Journal of the Structural Division, ASCE, Vol. 91, ST6, Dec. 1965.

25. Scordelis, A. C., and Lo, K. S., "Finite Segment Analysis of Folded Plates," Journal of the Structural Division, ASCE, Vol. 95, ST5, May 1969.

26. Cheung, M. S., and Chan, M. Y. T., "Analysis of Continuous Curved Box-Girder Bridges by the Finite Strip Method," ASCE, Preprint 3515, Boston, Apr. 1979.

27. Rao, P. S., and Rao, P. S., "Continuous Folded Plates," source unknown.

28. Smith, J. W., "Finite Strip Analysis of the Dynamic Response of Beam and Slab Highway Bridges," Earthquake Engr. and Str. Dyn., Vol. 1, 1973.

29. Cheung, Y. K., and Delcourt, C., "Buckling and Vibration of Thin Flat-Walled Structures Continuous Over Several Spans," Proc. Inst. Civ. Engrs., Part 2, Vol. 63, Mar. 1977.

30. Dawe, D. J., "Finite Strip Models for Vibration of Mindlin Plates," Jour. Sound Vibr., Vol. 59, 1978.

31. Smith, T. R. G., and Sridharan, S., "A Finite Strip Method for the Buckling of Plate Structures Under Arbitrary Loading," Jour. Mech. Sci., Vol. 20, 1978.

32. Petyt, M., "Finite Strip Analysis of Flat Skin-Stringer Structures," Jour. Sound Vibr., Vol. 54, 1977.

33. Cheung, Y. K., "Analysis of Simply Supported Thick, Layered Plates," Jour. of the Engr. Mech. Div., ASCE, Vol. 97, EM3, June 1971.

34. Mawenya, M. S., and Davies, J. D., "Finite Strip Analysis of Plate Bending Including Transverse Shear Effects," Build. Sci., Vol. 9, 1974.

35. Brown, T. G., and Ghali, A., "Finite Strip Analysis of Quadrilateral Plates in Bending," Journal of the Structural Division, ASCE, Tech. Note, Vol. 104, EM2, Apr. 1978.

36. Sisodiya, R. G., Ghali, A., and Cheung, Y. K., "Diaphragms in Single and Double-Cell Box Girder Bridges with Varying Angle of Skew," ACI Jour., July 1972.

37. Young, D., and Felgar, R. P., "Tables of Characteristic Functions Representing Normal Models of Vibrations of a Beam," Publication No. 4913, University of Texas, Austin, July 1949.

38. Felgar, R. P., "Formulas for Integrals Containing Characteristic Functions of Vibrating Beam," Circular 14, Bureau of Engineering Research, University of Texas, Austin, 1950.

39. Bathe, K., Wilson, E. L., and Peterson, F. E., "SAP IV, A Structural Analysis Program for Static and Dynamic Response of Linear Systems," Report No. EERC 73-11, University of California, Berkeley, 1974.

40. Maugh, L. C., and Pan, C. W., "Moments in Continuous Rectangular Slabs on Rigid Supports," ASCE Transactions, 1942, p. 1118.